2008

Chronic low-level Pb exposure during development alters proteins involved in energy metabolism in auditory neurons of the brainstem

John Prins
The University of Montana

Chronic low-level Pb exposure during development alters proteins involved in energy metabolism in auditory neurons of the brainstem

By

John Marcus Prins

B.S., California State University, San Bernardino, CA, 1998
M.S., Montana State University, Bozeman, MT, 2001

Dissertation

presented in partial fulfillment of the requirements
for the degree of

Doctor of Philosopy
in Pharmacology/Pharmaceutical Sciences

The University of Montana
Missoula, MT

Spring 2008

Approved by:

Dr. David A. Strobel, Dean
Graduate School

Diana I. Lurie, Chair
The Department of Biomedical and Pharmaceutical Sciences

Charles M. Thompson
The Department of Biomedical and Pharmaceutical Sciences

Darrell Jackson
The Department of Biomedical and Pharmaceutical Sciences

Michael Kavanaugh
The Department of Biomedical and Pharmaceutical Sciences

Edward Rubel
The Department of Otolaryngology-Head and Neck Surgery

Prins, John M., Phd., May 2008 Pharmacology/Pharmaceutical Sciences

Chronic low-level Pb exposure during development alters proteins involved in energy metabolism in auditory neurons of the brainstem

Chairperson: Dr. Diana Lurie

ABSTRACT

Low level lead (Pb) exposure is a risk factor for neurological dysfunction including ADHD. How Pb produces these behavioral deficits is unknown, but low-level exposure during development is associated with auditory temporal processing deficits, even though hearing remains normal. Pb disrupts cellular energy metabolism and efficient energy production is crucial for auditory neurons to maintain their high rates of synaptic activity. The voltage dependent ion channel (VDAC) is an ion channel involved in the regulation of mitochondrial physiology and is a critical component in controlling mitochondrial energy production. No studies to date have investigated the effect of Pb on VDAC, therefore the current series of studies examines the interactions between Pb and VDAC. In-vitro studies were used to delineate the effects of Pb on VDAC expression. Both differentiated SH-SY5Y cells and PC-12 cells exposed to 10 μM Pb for 48 h result in a significant decrease in VDAC expression. Exposure to 24 h of hypoxia fails to decrease VDAC expression, suggesting this is a specific effect of Pb. In addition, a corresponding decrease in cellular ATP that is correlated with decreased VDAC expression occurs with Pb. Real-time RT-PCR demonstrated a significant decrease in mRNA levels for VDAC1 isoform, suggesting that Pb decreases VDAC protein expression through decreased transcription. A proteomics approach was then used to confirm that Pb exposure during development results in changes in proteins involved in energy metabolism in auditory regions of the brainstem. CBA mice were exposed to 0 mM (control), 0.01 mM (low), or 2 mM (high) Pb acetate during development. At P21, the ventral brainstem region containing several auditory nuclei, including the Medial Nucleus of the Trapezoid Body, and the medial and lateral superior olivary nuclei, was separated from the total brainstem. Proteomic analysis (isolation and separation of proteins by 2D-PAGE; analysis by MALDI-MS) revealed that chronic Pb exposure alters the expression of proteins involved in the regulation of cellular energy metabolism including VDAC and creatine kinase B. Immunohistochemistry confirms that Pb exposure results in decreased expression of VDAC in auditory nuclei, supporting the hypothesis that Pb disrupts energy metabolism in auditory neurons.

ACKNOWLEDGMENTS

I owe a great deal of gratitude to the faculty, staff and fellow graduate students of the Department of Biomedical and Pharmaceutical Sciences for making my time here at the University of Montana a truly enjoyable and valuable educational experience.

Thank you to my dissertation advisor Dr. Diana Lurie, who has been a wonderful mentor not only by providing guidance for my dissertation project but for having confidence in my ability to complete the degree.

I truly appreciate the guidance and support given by my dissertation committee, Drs. Jackson, Thompson, Lurie, Kavanaugh, and Rubel, who have provided numerous invaluable suggestions over the course of this dissertation project.

Finally, I would like to thank my family and friends who endured this long process with me, always providing support and encouragement.

TABLE OF CONTENTS

LIST OF TABLES

LIST OF FIGURES

General Introduction

The extensive use of lead (Pb) in a wide variety of industrial processes and products has resulted in the widespread distribution of this toxic heavy metal throughout the environment. Environmental Pb can enter biological systems through ingestion and respiration, and is considered a critical global public health hazard (Toscano and Guilarte, 2005). Despite extensive efforts to eliminate the use of Pb, it continues to be a serious problem in many parts of the U.S. In 1991 the U.S. Centers for Disease Control and Prevention determined that blood Pb levels less than 10 μg/dL, were considered safe, however recent studies in humans and animals have shown that the neurotoxic effects of Pb can occur at much lower blood Pb levels (Gilbert and Weiss, 2006). Low-level Pb exposure is a risk factor for learning disabilities and attention deficit hyperactivity disorder (ADHD) in children and many children with these behavioral syndromes also demonstrate deficits in auditory temporal processing, suggesting a link between developmental Pb exposure, behavioral dysfunction and auditory temporal processing (Gray, 1999; Otto and Fox, 1993; Lurie *et al.*, 2006; Breier *et al.*, 2003; Montgomery *et al.*, 2005).

Sources of environmental Pb

Pb is a natural heavy metal that has been widely dispersed throughout the environment because of its use in many industrial procedures and products. The neurotoxic effects of Pb have been recognized for thousands of years and Pb has long been considered a significant global environmental health risk (Gidlow, 2004; Toscano and Guilarte, 2005; Bellinger, 2008).

Classical sources of environmental Pb include house paint, gasoline, lead pipes, and solder for food cans. Entry into biological systems is mainly attributed to its ingestion and respiration. Leaded paint can degenerate into chips and dust that can contaminate soil and water, or be a direct source of exposure if inhaled or swallowed (Toscano and Guilarte, 2005). Drinking water can become contaminated from the lead pipes that supply water to older houses. Canned food can become contaminated from the Pb solder used to seal the joints. Atmosphere and soil accumulation of Pb can be attributed to industrial emissions and burning of leaded fuels (Toscano and Guilarte, 2005; Needleman and Bellinger, 1991). In the United States, extensive efforts have been made over the past several decades to eliminate these sources of environmental Pb exposure. Laws prohibiting the use of Pb in house paint, gasoline, and solder in food cans has resulted in an 85 % decrease in the number of young children with potentially harmful blood lead levels in the last 20 years (Needleman and Bellinger, 1991). Despite these measures, Pb continues to persist in the environment. Pb house paint and pipes continue to remain in older housing, and off-road vehicles continue to burn leaded fuels. In addition to these classical sources of exposure, Pb can still be found as an integral part of many industrial processes, hobbies, tobacco smoke, lip stick, and recently in the surface paint of children toys (Bellinger, 2004; Bellinger, 2008; Gilbert and Weiss, 2006; Toscano and Guilarte, 2005).

Behavioral and cognitive impairments associated with Pb exposure

The developing central nervous system is particularly vulnerable to low levels of Pb and over the years there have been numerous reports on the behavioral and cognitive

impairments associated with Pb exposure (Costa *et al.*, 2004; Braun *et al.*, 2006; Lidsky and Schneider, 2003; Lanphear *et al.*, 2000; Canfield *et al.*, 2003; Goldstein, 1992; Finkelstein *et al.*, 1998). Cognitive impairment has been the most extensively studied effect of Pb exposure and is usually assessed by measuring IQ scores (Needleman and Bellinger, 1991). The current CDC screening guideline for blood Pb levels is 10 μg/dL, however current studies suggest that no level of Pb exposure appears to be safe (Gilbert and Weiss, 2006). For example, decreases in the IQ scores of children may be greater at blood Pb levels below 10 μg/dL than above this level (Bellinger, 2008). Canfield et al., reported that every 1 μg/dL blood lead level increase corresponded with a 1.37 IQ decrease, for blood lead levels under 10 μg/dL; with a total decrease of 7.4 IQ as lifetime average blood lead levels increased from 1-10 μg/dL (Canfield *et al.*, 2003). A recent study by Lanphear et. al., reported that cognitive deficits are associated with blood Pb concentrations lower than 5 μg/dL. The findings from this study found that for children, every 1 μg/dL increase corresponded with an observed 0.7-point decrease in mean arithmetic scores, a 1-point decrease in mean reading scores, a 0.1-point decrease on mean nonverbal reasoning scores, and a 0.5-point decrease in mean short-term memory scores (Lanphear *et al.*, 2000).

It is also becoming increasing clear that low levels of Pb exposure can cause behavioral syndromes in children (Chiodo *et al.*, 2004). Recent studies have suggested that even "subclinical" lead exposure is a risk factor for antisocial and delinquent behaviors (Bellinger, 2004). Recent studies have focused on studying the link between Pb exposure and ADHD.

Early reports by Bellinger, et al., described a significant relationship between childhood Pb exposure, attention, and executive function (Bellinger and Dietrich, 1994; Needleman and Bellinger, 1991). A recent analysis performed by Braun et al., reported a significant dose-response relationship between childhood Pb exposure and ADHD, and further reported that environmental Pb exposure accounts for 290,000 cases of ADHD in U.S. children (Braun *et al.*, 2006).

Although there appears to be a significant link between Pb exposure, behavioral syndromes, and cognitive deficits, the underlying cause remains largely unknown. Cognitive and behavioral dysfunction observed following Pb exposure is most likely a manifestation of the combined effects of Pb on a number of different biological processes that may be due to multiple cellular targets and cell types. Of relevance to the current study, Widzowski et al. demonstrated that Pb accumulates evenly in all areas of the brain and suggested that Pb may elicit specific effects on different brain regions by targeting specific proteins unique or enriched in that brain region (Widzowski and Cory-Slechta, 1994). Therefore, in order to improve risk assessment and to help identify the biochemical mechanisms that contribute to the adverse effects of Pb on biological systems, it is important to identify potential protein targets for the neurotoxic actions of Pb and elucidate their underlying mechanisms.

Known Mechanisms of Pb Neurotoxicity

Although, the toxic effects of Pb cannot be explained by a single molecular mechanism, the ability of Pb to substitute for other divalent cations, particularly calcium and zinc, at numerous

cellular sites is a common factor to many of its toxic actions (Garza *et al.*, 2006; Lidsky and Schneider, 2003). The substitution of Pb for divalent cations has the potential to affect many different biologically significant processes, including metal transport, energy metabolism, apoptosis, ionic conduction, excitotoxicity, neurotransmitter storage and release processes, altered activity of first and second messenger systems, protein maturation, and genetic regulation.

Of relevance to the current study is the concept that Pb is thought to interfere with gene expression by competing for Zn^{2+}-binding sites of transcription factors, such as zinc-finger proteins (Zawia, 2003; Basha *et al.*, 2003). Numerous studies have reported that Pb exposure interferes with the DNA binding of the zinc finger transcription factor Specificity protein 1 (Sp1) both in vivo and in vitro (Crumpton *et al.*, 2001; Zawia *et al.*, 1998; Atkins *et al.*, 2003; Basha *et al.*, 2003; Hanas *et al.*, 1999). Sp1 recognizes a GC-rich motif present in a variety of mammalian gene promotors (Zawia *et al.*, 1998). Sp1 was initially identified as a transcriptional activator, however it was later reported to also act as a negative regulator of gene transcription (Gong *et al.*, 2000). Several studies have shown that Pb can modulate Sp1 DNA-binding in differentiated PC-12 cells (Zawia *et al.*, 1998; Crumpton *et al.*, 2001; Basha *et al.*, 2003). Basha et al. reported that Pb altered hippocampal Sp1 DNA binding and mRNA expression in Pb exposed rats (Basha *et al.*, 2003). Furthermore, Hanas et al. demonstrated that 1-25 μM Pb concentrations inhibited Sp1 DNA binding in-vitro (Hanas *et al.*, 1999). Transcription factors play a vital role in the regulation of gene transcription and functional impairment due to Pb exposure may disrupt the expression of their target genes, altering normal cellular function.

Pb and the auditory system

Several studies have demonstrated auditory processing deficits in animals and children following Pb exposure, indicating that the auditory system may be a particular target for Pb toxicity. Auditory temporal processing is the processing of neuronal signals in time and space, which allows the listener to resolve complex sounds and to recognize specific signals within a noise background. Children exposed to Pb showed decreased performance in tests requiring appropriately timed reactions, as well as increased latencies in brainstem auditory evoked potentials (Finkelstein *et al.*, 1998; Holdstein *et al.*, 1986). Further, these auditory deficiencies have also been observed in several animal studies. Chicks exposed to low levels of Pb are deficient in a test of central auditory temporal processing called backward masking (Gray, 1999). In addition, our lab found that mice exposed to low levels of Pb exposure during development have deficits in two measures of central auditory brainstem function, the brainstem conduction time and gap encoding in the inferior colliculus (Jones *et al.*, 2008). Together, the results from these studies demonstrate that deficits in auditory temporal processing occur following Pb exposure.

Auditory temporal processing and the Superior Olivary Complex

Auditory temporal processing can be roughly defined as the way in which incoming auditory signals are perceived and processed by the brain. Essentially, incoming auditory signals are analyzed by their frequency, intensity, and temporal features by auditory nuclei in the brain. These characteristics enable the listener to recognize sounds (crying, dogs barking, car alarms, etc.) and comprehend speech (Johnson *et al.*, 2007; Frisina, 2001).

Several brain regions are thought to be associated with auditory temporal processing but the superior olivary complex (SOC) is the first site of binaural auditory processing in the brainstem, and is hypothesized to use auditory temporal information for sound location (Squire *et al.*, 2003).

The SOC plays a number of roles in hearing. The SOC is the initial site where auditory signals from the two ears converge and binaural signals for sound localization are processed. The SOC is important for selective auditory attention, the localization of sound in time and space, decoding complex sounds, and detection of auditory signals within a noise background (Mulders and Robertson, 2004). The SOC is composed of three principal nuclei, the lateral superior oliary nuclei (LSO), the medial superior olivary nuclei (MSO), and the medial nucleus of the trapezoid body (MNTB). The MSO is a specialized nucleus that is believed to be associated with processing the differences in time of arrival of sounds between the two ears (the interaural time difference) (Moore, 2000). The LSO and MNTB perform a similar function, but these nuclei are believed to be involved in the processing of intensity differences of sound between the ears (interaural intensity difference), and are required for high frequency sound localization (Tsuchitani, 1997; Moore, 2000).

Energy metabolism and auditory neurons

Auditory neurons are highly active and require precise timing from auditory signals received from the two ears for temporal processing. In order to ensure accurate processing of auditory information, auditory neurons are capable of firing action potentials at very high rates, up to 600 Hz (Rowland *et al.*, 2000). The increased energy demand required for

the high rates of activity of these specialized neurons depends on reliable and efficient cellular energy production (Rowland *et al.*, 2000; Nothwang *et al.*, 2006; Schneggenburger and Forsythe, 2006; Trussell, 1999). To support these high energy requirements, the auditory system contains a specialized arrangement of mitochondria located near the presynaptic membrane. These complexes are thought to not only supply energy for synaptic processes, but also buffer Ca^{2+} during high rates of activity (Rowland *et al.*, 2000). Therefore, even subtle disruptions in mitochondrial metabolism could compromise the proper function of these neurons.

The voltage dependent anion channel and energy metabolism

VDAC is an ion channel involved in the regulation of mitochondrial physiology and is a critical component in controlling mitochondrial energy production. No studies to date have examined the role of VDAC in auditory neurons, but even small changes in VDAC expression have been shown to compromise energy metabolism. VDAC is primarily located in the mitochondrial outer membrane and regulates mitochondrial permeability to anions, cations, creatine phosphate, inorganic phosphate, ATP, ADP, and other metabolites into and out of the mitochondria (Shoshan-Barmatz and Israelson, 2005). Disrupted VDAC function has been shown to compromise energy metabolism as well as Ca^{2+} homeostasis within the cell (Lemasters and Holmuhamedov, 2006; Shoshan-Barmatz and Gincel, 2003). In addition, it has been suggested that VDAC controls the production of cellular energy beginning with the control of the Ca^{2+} dependent enzymes pyruvate dehydrogenase and iso-citrate dehydrogenase in the mitochondria (Shoshan-Barmatz and

Israelson, 2005). Impaired VDAC function or down-regulation of VDAC expression would suppress mitochondrial uptake of ADP and Pi for synthesis and release of ATP, thereby decreasing levels of cytosolic ATP, and stimulating glycolysis and possibly the phosphocreatine circuit (Shoshan-Barmatz and Israelson, 2005; Lemasters and Holmuhamedov, 2006). Furthermore, studies have demonstrated that decreased VDAC-1 expression results in decreased ATP synthesis, decreased cytosolic ADP and ATP levels, decreased phosphocreatine, and increased creatine kinase activity (Rafalowska *et al.*, 1996; Shoshan-Barmatz *et al.*, 2006). Additional studies have suggested that VDAC has Ca^{2+} binding sites and channel activity can be modulated by glutamate, Ca^{2+}, and other cations (Shoshan-Barmatz and Gincel, 2003; Israelson *et al.*, 2007). Mammals express at least three different VDAC genes (Weeber *et al.*, 2002; Baines *et al.*, 2007). VDAC's have highly conserved structural and electrophysiological characteristics across plant, yeast, mouse, and human species (Sampson *et al.*, 2001). Studies using VDAC knock-out mice have demonstrated that each VDAC isoform appears to have specialized functions. Knock-out of VDAC-1 and VDAC-2 resulted in reductions of mitochondrial respiratory capacity (Wu *et al.*, 1999), whereas knockout of VDAC-3 causes male sterility (Sampson *et al.*, 2001). In addition, VDAC-1 and VDAC-3 knockout mice demonstrated deficits in learning behavior and synaptic plasticity (Weeber *et al.*, 2002). However, selective elimination of one or the other of these isoforms does not produce the same effects, suggesting different functional roles for VDAC-1 and VDAC-3 isoforms (Shoshan-Barmatz *et al.*, 2006).

Proteomics approach

In order to determine if Pb exposure compromises mitochondrial metabolism and energy production within the auditory brainstem by modulating proteins such as VDAC that are critical to ATP production, we utilized a proteomic approach as part an arsenal of techniques that we employed to examine the effect of Pb on energy production within auditory neurons. Proteomics is the protein complement of genomics and can generally be described as the large-scale study of proteins in a cell or tissue at a particular time. Genomic studies are limited since not all mRNAs will be translated into the protein. Furthermore, the level of transcription of specific proteins does not always correspond to the level of expression due to many factors, including RNA splicing, posttranslational protein modifications, etc. To gain a better understanding of a biological system, it is desirable to obtain information at the protein level. Proteomics is an attractive technique in this respect, since protein characterization may include various properties of proteins such as its primary sequence, quantity, modification state, subcellular localization, structure, interaction partners and activity or cellular function (Aebersold and Goodlett, 2001; Grant and Blackstock, 2001).

Proteomics relies on the ability to separate a complex mixture so that individual proteins can be easily analyzed. In this study we used a proteomic method commonly referred to as expression proteomics, which is analogous to differential gene expression and relies on comparing the protein expression levels between the experimental samples and control samples. Expression proteomics is commonly performed by separating proteins using two-dimensional protein electrophoresis followed by protein identification using matrix

assisted laser desorption ionization-time of flight mass spectrometry (MALDI-TOF MS) and a peptide mass fingerprint. First, the proteins are separated according to their isoelectric point (pI) (first dimension). Proteins will migrate towards cathode or anode according to their total charge up to the point where the gel pH equals the pI of a given protein. After this initial separation, proteins are then separated based on their molecular weight using gel electrophoresis (second dimension). Once proteins are separated, the gels are stained and protein expression changes are determined by comparing the protein spot density between the experimental samples and control samples. The differentially expressed protein spots are excised and digested with trypin into peptides. Samples analysis by MALDI-TOF MS generates peptide maps of proteins that can be compared to theoretical protein data bases for protein identification, such as Mascot, PEAKS, OMSSA, and SEQUEST (Freeman and Hemby, 2004).

The use of proteomics as a research tool for studying the central nervous system is rapidly increasing due to recent advances made in methodologies, protein identification capabilities, and instrumentation. Proteomics is a powerful tool for studying biological systems since it allows for the study of a large number of proteins simultaneously in a single sample preparation and is being used to elucidate biomarkers for specific diseases, protein-protein interactions, protein function, biochemical pathways and molecular networks. An increased understanding of protein function in the CNS and biomarkers can aid in the diagnosis, prevention, and treatment of many diseases and brain related disorders (Freeman and Hemby, 2004; Johnson *et al.*, 2005). Not only is proteomics a useful tool for generating data for scientific research but it has great potential for scientific discovery as

well (Freeman and Hemby, 2004; Kim *et al.*, 2004; Drabik *et al.*, 2007).

General Hypothesis

Our overall hypothesis driving the current studies is that Pb disrupts energy metabolism in auditory neurons, leading to impairments in function that play a role in producing auditory temporal processing deficits. We further propose that the voltage dependent anion channel (VDAC), is a key target of Pb, because it plays such a central role in regulating cellular energy metabolism (Shoshan-Barmatz *et al.*, 2006; Gincel *et al.*, 2001). VDAC has also been shown be involved in learning and synaptic plasticity in mice (Weeber *et al.*, 2002), two functions that are disrupted by Pb exposure. Therefore, VDAC may represent a possible cellular target for Pb. The current series of studies is the first to examine the effect of Pb on VDAC both in vitro and in vivo.

SPECIFIC AIMS

Specific Aim I: Determine if low levels of Pb alters VDAC expression and ATP levels in-vitro.

-*Explore the effects of low-levels of Pb exposure on VDAC expression and ATP levels in differentiated cell lines*

Specific Aim II: Use a proteomic approach to examine whether chronic Pb exposure results in decreases of VDAC expression in the murine auditory brainstem. Identify cellular systems (including those involved in energy metabolism) primarily affected by chronic Pb exposure, in the murine auditory brainstem.

- *Separate and identify proteins in the murine auditory brainstem that by that display expression changes following low-levels of Pb exposure during development.*

Specific Aim III: Confirm that central auditory neurons show decreased VDAC expression decreases following Pb exposure.

-*Utilize immunohistochemical techniques to determine that VDAC expression decreases in central auditory neurons following developmental Pb exposure.*

Chapter 1

Low-level Pb exposure results in decreased expression of the voltage-dependent anion channel in-vitro

Abstract:

Lead (Pb) has been shown to disrupt cellular energy metabolism which may underlie the learning deficits and cognitive dysfunctions associated with environmental Pb exposure. The voltage dependent anion channel (VDAC) plays a central role in regulating energy metabolism in neurons by maintaining cellular ATP levels and regulating calcium buffering, and studies have shown that VDAC expression is associated with learning in mice. In this study, we examined the effect of low levels of Pb exposure on VDAC expression in-vitro in order to determine whether Pb decreases VDAC expression in neurons. PC-12 and SH-SY5Y cells were used since they differentiate to resemble primary neuronal cells. VDAC expression levels were significantly decreased 48 h after exposure to Pb in both cell lines. In contrast, exposure to 24 h of hypoxia failed to produce a decrease in VDAC, suggesting that decreased VDAC expression is not a general cellular stress response, but is a specific result of Pb exposure. This decreased VDAC expression was also correlated with a corresponding decrease in cellular ATP levels. Real-time RT-PCR demonstrated a significant decrease in mRNA levels for the VDAC-1 isoform, indicating that Pb reduces transcription of VDAC-1. These results demonstrate that exposure to low-levels of Pb reduce VDAC transcription and expression and is associated with reduced cellular ATP levels.

Introduction

The extensive use of lead (Pb) in a wide variety of industrial processes and products has resulted in the widespread distribution of this toxic heavy metal throughout the environment. Despite extensive efforts to eliminate the use of Pb, it continues to be a serious problem in many parts of the U.S. Pb has been shown to affect many different biological processes, including metal transport, energy metabolism, neurotransmitter storage and release processes, protein maturation, and genetic regulation (Garza *et al.*, 2006; Lidsky and Schneider, 2003). While high levels of Pb exposure induce a variety of physical and behavioral syndromes, low-level Pb exposure during development has been shown to be a risk factor for behavioral syndromes such as learning disabilities and attention deficit hyperactivity disorder (ADHD) (Lidsky and Schneider, 2003; Braun *et al.*, 2006). Although there has been an extensive amount of research devoted to studying the effects of Pb exposure, the molecular mechanisms behind the subtle, neurotoxic effects of low levels of Pb remain largely unknown. However, disrupted energy metabolism is one mechanism that has been proposed as a possible cause of the behavioral abnormalities and brain dysfunction induced by Pb (Sterling *et al.*, 1982).

VDAC is an ion channel located in the mitochondrial outer membrane that plays a central role in regulating energy metabolism in neurons by maintaining cellular ATP levels and regulating calcium buffering (Shoshan-Barmatz *et al.*, 2006; Shoshan-Barmatz and Gincel, 2003). Decreased VDAC expression has been shown to result in decreased ATP synthesis, and decreased cytosolic ADP and ATP levels in vitro (Abu-Hamad *et al.*, 2006). Therefore, a potential mechanism through which Pb could induce decreases in ATP

concentrations might be a decrease in VDAC.

In order to investigate the interactions among Pb, VDAC, and ATP, we used two neuronal cell lines, a differentiated rat pheochromocytoma cell line (PC-12 cells) and a differentiated human neuroblastoma cell line (SH-SY5Y cells). PC-12 and SH-SY5Y cells serve as relevant in-vitro model systems for primary neuronal cells because they stop dividing, grow long neurites, and show changes in cellular composition associated with neuronal differentiation, in response to treatment with nerve growth factor and retinoic acid, respectively (Greene and Tischler, 1976; Vignali *et al.*, 1996).

Cells were differentiated for 6-10 days and total VDAC protein levels were measured following low-level Pb exposure. We found that total VDAC protein expression levels decreased in both cell lines with 48 h of Pb exposure. Interestingly, hypoxia did not result in a change in VDAC expression, indicating that reduced VDAC expression is not a general response to stress, but appears to be specific to Pb exposure. In addition, we found a concomitant decrease in cellular ATP levels with 48 h of Pb exposure, suggesting a correlation between decreased VDAC expression and decreased cellular ATP production. Finally, Real Time RT-PCR demonstrated that the Pb-induced decrease in VDAC protein is the result of decreased transcription of two of the three VDAC isoforms. Taken together, these results show that Pb reduces VDAC transcription and protein expression, and this decrease is correlated with a reduction in cellular ATP levels.

Materials and Methods

PC-12 and SH-SY5Y cell cultures

PC-12 cells were obtained from American Type Culture Collection (Rockville, MD). PC-12 cells were cultured in RPMI medium containing 10% horse serum and 5% fetal calf serum, sodium pyruvate, and antibiotics at 37°C in humidified air containing 5% CO_2. The culture medium was changed every 2-3 days and cells were used between passages 6 and 12. For experiments, approximately 15,000 cells/cm^2 were seeded onto collagen-coated 6-well plates and then allowed to grow for 2 days in RPMI medium. Cells were differentiated using 100 ng/ml nerve growth factor (NGF-7S, Sigma-Aldrich, Inc.), in RPMI medium containing 1% horse serum, sodium pyruvate, and antibiotics. Under these conditions, the cells developed a neuronal phenotype with neurite outgrowth that was already apparent 24 h after seeding, we always used the cells at day 6 of differentiation. For experiments, differentiated cells were treated with different concentrations of lead acetate dissolved in water in RPMI medium containing 1% horse serum, sodium pyruvate, and antibiotics.

SH-SY5Y cells were obtained from American Type Culture Collection (Rockville, MD). SHSY-5Y cells were cultured in DMEM/F12 medium (GIBCO BRL, Grand Island, NY) supplemented with 10% fetal bovine serum (Hyclone), 100U/ml penicillin, 100 μg/ml streptomycin, and 2 mM L-glutamine in an incubator maintained at 5% CO_2 and 37°C. The medium was changed every two days. Cells were treated with 10 μM all-trans-Retinoic Acid (Sigma, St. Louis, MO) in for 8-10 days to induce differentiation. For experiments, differentiated cells were treated with different concentrations of lead acetate in

DMEM/F12 medium containing 1% horse serum, sodium pyruvate, and antibiotics for 1-4 days.

Pb exposure

Cells were exposed to Pb as follows; a 5 mM Pb stock solution was prepared by dissolving the appropriate amount of lead acetate in sterile, double distilled H_2O. Experimental Pb concentrations were prepared by dilution of stock solution in appropriate culture medium. For PC-12 cells, experimental Pb concentrations were prepared in serum free RPMI medium containing 1% horse serum, sodium pyruvate, and antibiotics. For SH-SY5Y cells, experimental Pb concentrations were prepared in DMEM/F12 medium containing 1% horse serum, sodium pyruvate, and antibiotics. Differentiated cells were incubated with 0, 1, 5, 10, and 50 μM of Pb for different time periods (24, 48, 72, or 96 h) at 37°C, with 0 μM Pb samples used as the control group. It is important to note that the concentrations of Pb used in our studies had no effect on the cell viability as indicated by MTT and LDH assays.

Hypoxia

For hypoxia experiments, SH-SY5Y cells were cultured and differentiated as described above, followed by incubation in a controlled atmosphere of 2% oxygen (14 mmHg partial pressure) for 24 h at 37ºC. The gas mixture in the incubator during hypoxia was 2% O_2, 5% CO_2, and 93% N_2.

MTT and LDH assays

MTT and LDH assay kits were obtained from Roche Applied Science (Cat. # 11 465 007 001 and 1 644 793, respectively). For MTT and LDH assays, ~0.25 x 10^5 cells/ml were differentiated on collagen coated 96 well plates. Cells were exposed for 24, 48, 72, or 96 h to a graded series of Pb concentrations (0, 1, 5, 10, 50, 100, 250, 500, 1000, 5000, and 10000 µM Pb). For PC-12 cells, a 2% triton X-100 solution in assay medium was used for a high control. One 96-well plate was used for each time point. Cells were incubated for 24, 48, 72, or 96 h at 37°C with 5% CO_2 and 90% humidity. General assay protocols included with each kit were followed.

Briefly, for the LDH assay, cells were rinsed several times with culture medium prior to Pb exposure. Culture medium was removed and 100 µl of fresh medium containing the graded Pb concentrations was added to each well. At the appropriate time points, 100 µl of supernatant was removed from each well and transferred into the corresponding wells of a new 96-well plate. LDH activity was determined by adding 100 µl of reaction mixture (included with kit) to each well and incubating for 20 minutes in the dark at room temperature. Absorbance measurements were made at 490 nm on a microplate reader (Molecular Devices, Versamax). The reference wavelength was 650 nm.

For the MTT assay, cells were rinsed several times with culture medium prior to Pb exposure. Culture medium was removed and 100 µl of fresh medium containing the graded Pb concentrations or triton X-100 was added to each well (n=8 for each Pb concentration and triton x-100). After incubation for appropriate time points, 10 µl of MTT labeling reagent (included with kit) was added to each well. Plates were incubated with MTT

labeling reagent for 4 hours and then 100 µl of solubilizing solution (included with kit) was added to each well. Plates were incubated overnight before being measured. Absorbance of samples was measured using a microplate reader (Molecular Devices, Versamax). The wavelength for measuring formazan product was 575 nm and reference wavelength was 660 nm.

Western Blot analysis

For all samples, total protein was extracted from cells by homogenizing in a lysis buffer containing 20 mM Tris-HCl (pH 7.5), 150 mM NaCl, 1 mM Na_2EDTA, 1 mM EGTA, 1% triton, 2.5 mM sodium pyrophosphate, 1 mM beta-glycerophosphate and 1 mM Na_3VO_4 (Cell Signaling Technology, Beverly, MA). Additions were made giving final concentrations of 0.5% Na-deoxycholate, 0.5% SDS, 1 µM okadaic acid, 1 mM phenylmethylsulfonyl (PMSF), 0.1 mg/mL benzamidine, 8 µg/mL calpain inhibitors I and II and 1 µg/mL each leupeptin, pepstatin A and aprotinin. Homogenates were sonicated and vortexed for 5 minutes before centrifugation at 50,000 rpm for 20 minutes. Protein concentration of the supernatant was then determined by Bradford protein assay. Proteins were separated by SDS-PAGE using 4-12% gradient bis-tris gels (Bio-Rad criterion precast gel) and transferred to PVDF membranes for immunoblotting. Sources for antibodies were as follows: Total VDAC (Cell signaling technology, Cat.# 4866), and p44/42 Map Kinase (ERK)(Cell signaling technology Cat.# 9102).

Gels were transferred to Immun-Blot PVDF membrane (Bio-Rad) using Criterion (Bio-Rad) transfer cell with plate electrodes for 60 minutes at 100 V and blocked in 5% milk in

TBST (1 x Tris-buffered saline, 0.1% Tween 20, 5% dry milk), incubated overnight at 4°C. Membranes were washed in TBST, and then incubated overnight at 4ºC with VDAC antibody. Membranes were then washed in TBST and incubated with secondary antibody (Vector, HRP-conjugated Anti-Rabbit, PI-1000; 1:2000) for two hours. Membranes were then washed in TBST before imaging with the Fuji LAS-3000 CCD based imaging system (FujiFilm Life Science). Membranes were re-probed with ERK to confirm equal protein loading. Band pixel intensity was measured using the Fuji LAS-3000 software. VDAC band intensities from control and treated groups were normalized to ERK, and plotted using GraphPad (GraphPad Prism 4.0) software. For PC-12 cells, statistical significance was determined by t-test, $p<0.05$ (n=6 samples per group). For SH-SY5Y cells, statistical significance between control, Pb treatment and hypoxia was determined by ANOVA followed by Dunnets post hoc test (n=4 samples per group).

Cellular ATP assay

The cellular ATP levels for each Pb treatment group was determined using an ATP Bioluminescence Assay Kit HSII, Roche Applied Science. Cells were grown and differentiated on collagen-coated plates as described above. Cells from each treatment group were rinsed with sterile PBS, then collected and diluted to ~10^7-cells/mL. 200 µl of the cell suspension and 200 µl of the supplied lysis reagent were placed in a 1.5 ml eppendorf tube and for ~5 minutes. Samples were centrifuged at 10,000 x g for 60 seconds and supernatant was transferred to a fresh eppendorf tube and kept on ice until analysis. For ATP determinations, 50 µl of sample was transferred to a 96-well plate and

luminescence was measured using a microplate luminometer (Berthold Technologies, Centro LB 960). Briefly, 50 µl of luciferase reagent was added to 50 µl of sample by automated injection. Measurement was started after a 1 second delay and integrated from 1 to 10 seconds. Luminescence measurements from control and treated groups were normalized to total protein concentration of sample. Statistical significance was determined by analysis of varience followed by a Dunnets post hoc test, $p<0.05$ (n=6 samples per group).

RNA Isolation

Cell pellets were resuspended in a small volume (<300 µl) of PBS. 8 ml of Trizol Reagent (Invitrogen Corp. Carlsbad, CA) was added and mixed by pipetting to homogenize the cells. After a 10-minute incubation at room temperature, 1.6 ml of chloroform was added and the solution was mixed by shaking for 30 seconds and incubated at room temperature for 3 minutes. Phase separation was performed by centrifugation at 3200 x g for 30 minutes. The upper aqueous layer was removed to a tube containing 4 ml of isopropanol and mixed by inversion. Samples were then precipitated overnight at -20°C. RNA was pelleted by centrifugation at 3200 x g for 15 minutes, the supernatant was removed, and 8 ml of 75% ethanol prepared with DEPC water was added to wash the pellet. Another centrifugation at 3200 x g for 10 minutes was performed, the supernatant was removed, and the pellets were air-dried for 10 minutes. Pellets were resuspended in 400 µl of RNase Free Water from the Qiagen RNeasy Mini kit (Qiagen, Inc., Valencia, CA). 100 µl of each sample was used for further purification according to the "RNA Cleanup"

protocol from the Qiagen RNeasy manual, including the optional DNase treatment. The final elution step was performed with 30 µl of RNase free water. RNA quantity was determined using a NanoDrop ND1000 Spectrophotometer (NanoDrop Technologies, LLC, Wilmington, DE). RNA quality was assessed using an Agilent 2100 Bioanalyzer (Agilent Technologies, Santa Clara, CA) with the RNA 6000 Nano LabChip and reagents to obtain RNA Integrity Numbers (RIN) and 28S/18S ratios.

Real Time RT-PCR Analysis

A Real Time RT-PCR analysis was used to investigate gene expression following Pb exposure in differentiated PC-12 cells. Total RNA was extracted, as described above, from 6 samples, three control groups and three groups treated with 5 µM Pb for 48 h. Real Time RT-PCR was used to analyze the expression of rat GAPDH (NM017008), VDAC-1 (NM031353), VDAC-2 (NM031354), and VDAC-3 (NM031355) genes and MAPK 1/ERK 2 (NM053842) was used for the control or house keeping gene. Reverse transcription and Real-Time PCR expression analysis was conducted by SuperArray Bioscience Corporation in Frederick, MD.

RNA Quality Control

RNA samples were run on the Agilent bioanalyzer. The integrity of RNA was assessed by looking at 18 & 28s rRNA peaks and by the RIN (RNA integrity number). RNA concentrations were measured using the nano drop and all samples had 260/280 ratios above 2.0 and 260/230 ratios above 1.7.

Reverse Transcription and First strand cDNA Synthesis

Equal amounts of RNA (1 µg) were taken for all samples and reverse transcription was performed using RT2 First Strand kit from Superarray Biosciences. This kit uses MMLV Reverse transcriptase and a combination of random primers and oligo dT primers. The kit contains optimized DNA removal buffer that prevents false positive signals due to amplification of genomic contamination and has a built-in external RNA control that verifies lack of enzyme inhibitors and efficient reverse transcription. The total volume of the reaction was 20 µL and was diluted to 100 µL.

PCR

PCR reactions were performed using RT2 qPCR primer assasys (SuperArray, Frederick, MD) on the ABI 7500, with RT2 Real-Time TM SYBR Green PCR master mix PA-012. The total volume of the PCR reaction was 25 µL. The thermocycler parameters were 95°C for 10 min, followed by 40 cycles at 95°C for 15 s and 60°C for 1 min. Samples consisted of 3 biological replicates for the control group and treatment group. Relative changes in gene expression were calculated using the ΔΔCt (threshold cycle) method (Livak and Schmittgen, 2001). PCR for all the genes for each sample was done in triplicate and the average, standard deviation and % CV was calculated for all technical replicates. Data was normalized using the MAPK1 gene. Once data had been normalized (Δ Ct) the average of the 3 biological replicates in each group was used to calculate the ΔΔ Ct and fold change (fold change = $2^{-\Delta\Delta Ct}$). The p value is calculated using a 2-tailed student's t-test.

Results

Low-level Pb exposure does not induce neuronal death

In order to study the interactions among Pb, VDAC, and ATP we used two different neuronal cell lines, differentiated SH-SY5Y and PC-12 cells. These two cell lines were used because they are established model systems for primary neurons (Greene and Tischler, 1976; Robson and Sidell, 1985; Vignali *et al.*, 1996). In addition, we reasoned that if Pb induces decreased VDAC expression in both neuronal cell lines, then this is a general effect of Pb on neurons and is not restricted to particular neuronal subtype. Because our in vivo studies have demonstrated that low-levels of Pb exposure during development does not result in neuronal death (Jones *et al.*, 2008), we first established that low-level Pb does not result in cell death in vitro.

Differentiated SH-SY5Y and PC-12 cells were exposed to a graded series of Pb concentrations and cell viability was assessed by using both MTT and LDH assays following 24, 48, 72, or 96 h of exposure (Figures 1&2). In PC-12 cells, only the higher concentrations of Pb >1000 μM at the 48 h and 72 h time points elicited a significant loss of cell viability (Figure 1). SH-SY5Y cells were even more resistant to cell death following Pb exposure compared to PC-12 cells, demonstrating significant cell loss at 10,000 μM Pb for all time points examined (Figure 2). Thus, Pb did not induce neuronal death at low doses in vitro.

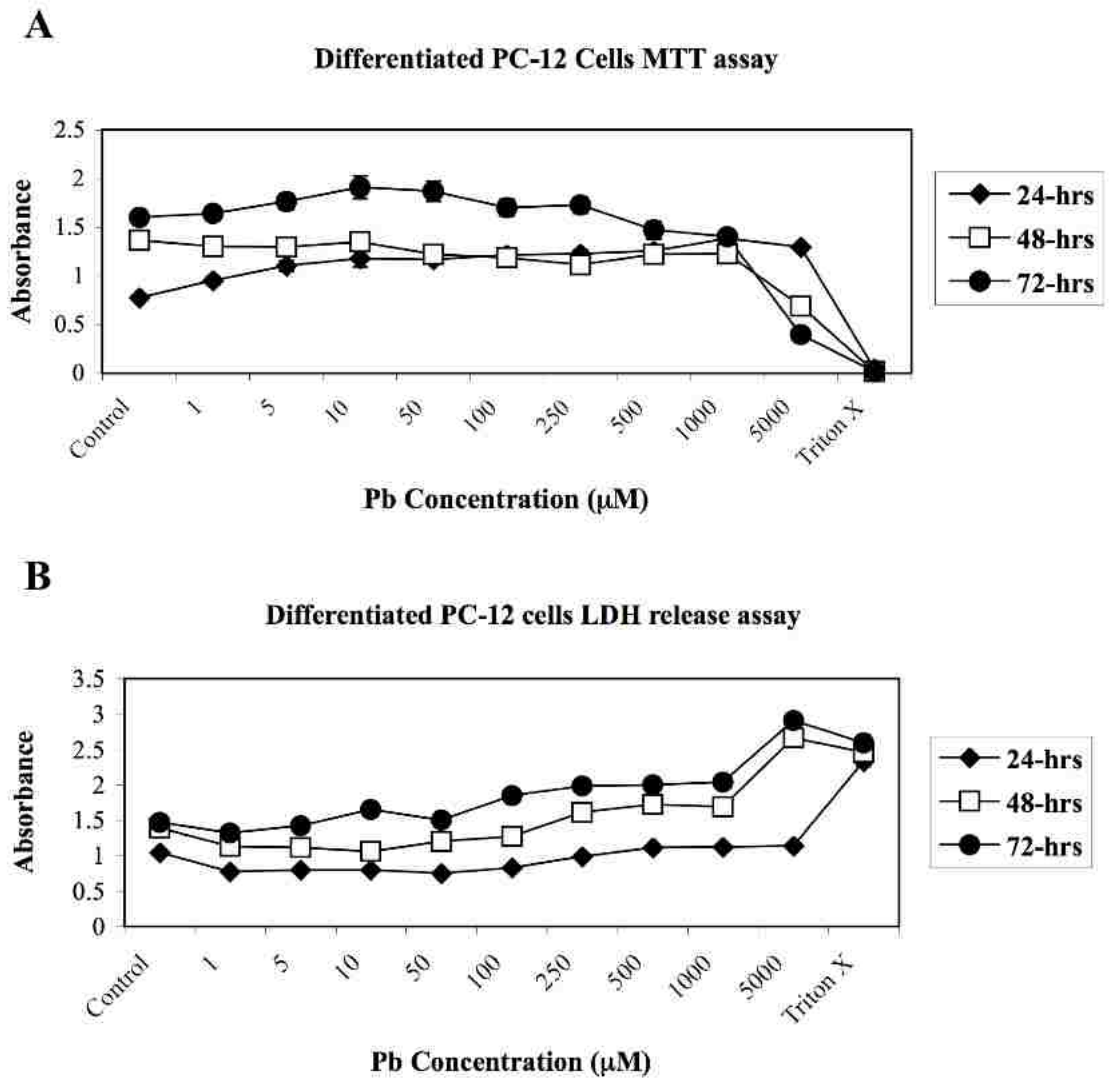

Figure 1: Low level Pb exposure does not result in cell death of differentiated PC-12 cells. Cells were exposed for 24, 48, or 72 h to a graded series of Pb concentrations (0, 1, 5, 10, 50, 100, 250, 500, 1000, and 5000 μM Pb). Triton X-100 was used as a positive control because it results in cell lysis. A) MTT assay demonstrates only the higher concentrations of (Pb >1000 μM) at the 48 h and 72 h time points elicited a loss of cell viability. Cells treated with triton X-100 could not reduce the MTT to formazan and no absorbance was measured for these samples. B) Similar results were demonstrated by LDH release assays. Decreases in cell viability were only observed for higher concentrations of Pb (> 1000 μM) at 48 h and 72 h. Maximum amount of LDH release was determined by treating cells with triton X-100.

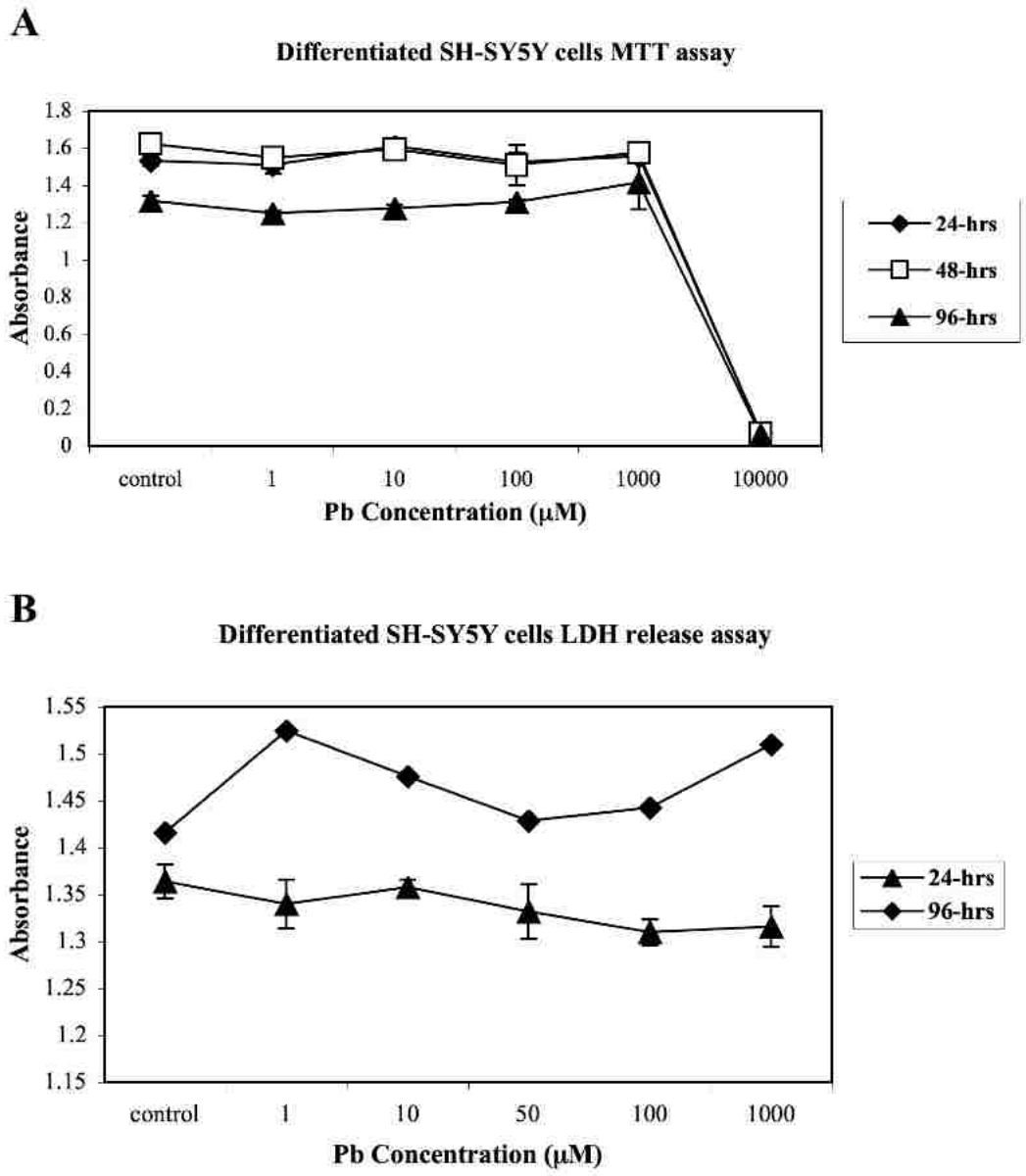

Figure 2: **MTT and LDH assays for differentiated SH-SY5Y cells demonstrates that low-level Pb exposure does not result in cell death**. Cells were exposed for 24, 48, or 96 h to a graded series of Pb concentrations (0, 1, 10, 100, 1000, and 10000 μM Pb). A) MTT assay demonstrates that only the 10000 μM Pb concentration results in a significant loss of cell viability for all time points. B) Similarly, LDH release assays demonstrate that cells exposed to Pb concentrations ≤1000 μM for 24 h and 96 h displayed no decrease in cell viability.

Low dose Pb exposure reduces VDAC expression in vitro

In order to determine whether low dose Pb exposure decreases VDAC expression in vitro, we exposed differentiated PC12 cells to 0, 1, 5, 10, and 50 μM of Pb for 24, 48, and 72 h. These Pb concentrations had no apparent effect on the cell viability at these time points, as indicated by MTT and LDH assays described above (Figures 1&2). A western blot analysis using an antibody directed at total VDAC was then used to compare VDAC expression levels between the Pb treatment groups and the no Pb control groups. The results indicated that VDAC expression levels began to decrease within 48 h of exposure to Pb, with large decreases observed for the 5 and 10 μM Pb concentrations at the 48 h time point (Figure 3). It is important to note that these are relatively low levels of Pb, and the 5-10 μM range has been widely used in many in vitro studies examining the effects of Pb on its molecular targets (Cordova *et al.*, 2004; Zhao *et al.*, 1998; Leal *et al.*, 2002). Therefore, we selected 5 and 10 μM Pb exposure at 48 h to further investigate the effects of Pb on VDAC expression. Additional experiments at these doses at 48 h confirmed that the expression of total VDAC in the 5 μM and 10 μM treatment groups was significantly decreased by 44% and 31% respectively compared to control group (Figure 4).

Hypoxia fails to decrease VDAC expression in-vitro

The results from the above experiments demonstrate that exposing differentiated PC-12 cells to low-levels of Pb results in a significant decrease in VDAC expression levels. In order to determine if Pb induces VDAC expression in neurons, and is not restricted to a particular neuronal subtype, we compared VDAC expression levels in differentiated SH-

SY5Y cells following a 48 h 10 μM Pb exposure. We found that exposing SH-SY5Y cells to 10 μM Pb for 48 h results in a significant decrease in VDAC expression (Figure 5). Furthermore, decreased VDAC expression is not due to a general cellular stress response, because VDAC expression does not change following 24 h of hypoxia (Figure 5). These results demonstrate that Pb decreases VDAC expression in neurons, and this reduction is a specific response to Pb exposure.

A

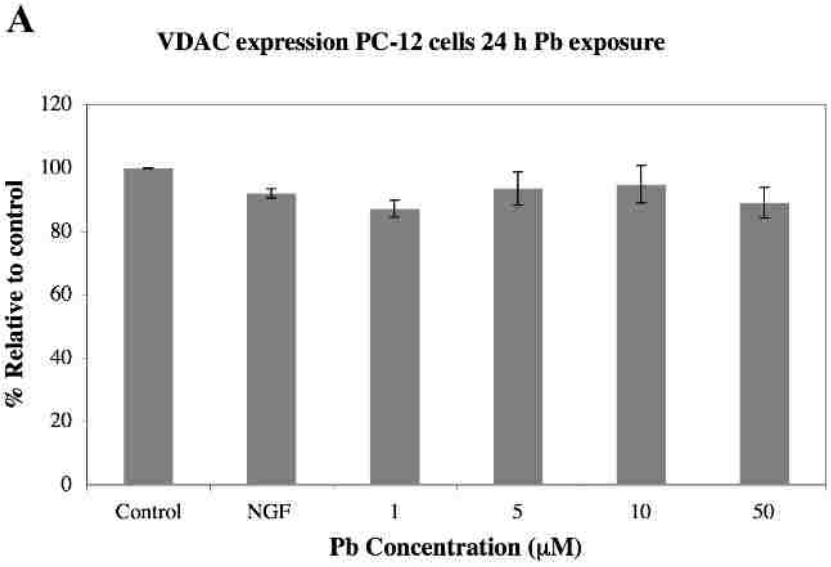
VDAC expression PC-12 cells 24 h Pb exposure
% Relative to control
120
100
80
60
40
20
0
Control
NGF
1
5
10
50
Pb Concentration (μM)

B

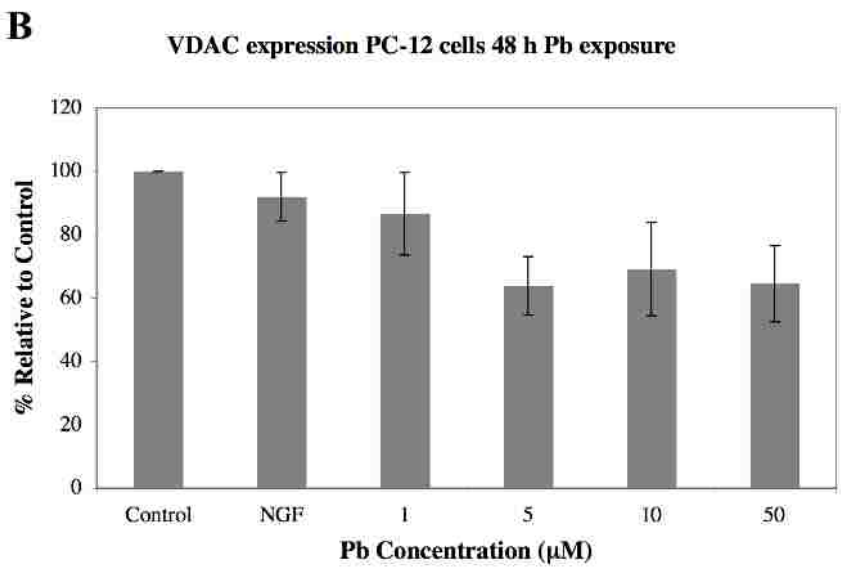
VDAC expression PC-12 cells 48 h Pb exposure
% Relative to Control
120
100
80
60
40
20
0
Control
NGF
1
5
10
50
Pb Concentration (μM)

C

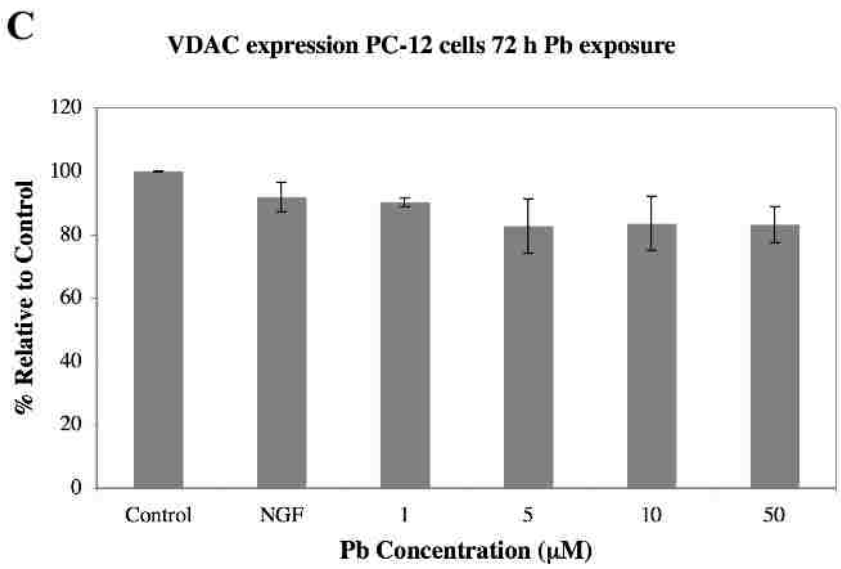
VDAC expression PC-12 cells 72 h Pb exposure
% Relative to Control
120
100
80
60
40
20
0
Control
NGF
1
5
10
50
Pb Concentration (μM)

Figure 3: Pb results in decreased VDAC expression. Differentiated PC-12 cells were exposed to a graded series of Pb concentrations (0, 1, 5, 10, and 50 μM) and VDAC expression was measured by western blot analysis after A) 24 h, B) 48 h, and C) 72 h of exposure. VDAC expression levels began to decrease within 48 h of exposure to Pb, with large decreases observed for the 5 and 10 μM Pb concentrations at the 48 h time point. Data are presented as % relative to control (with control density considered to be 100%) , mean ± SEM (n=3).

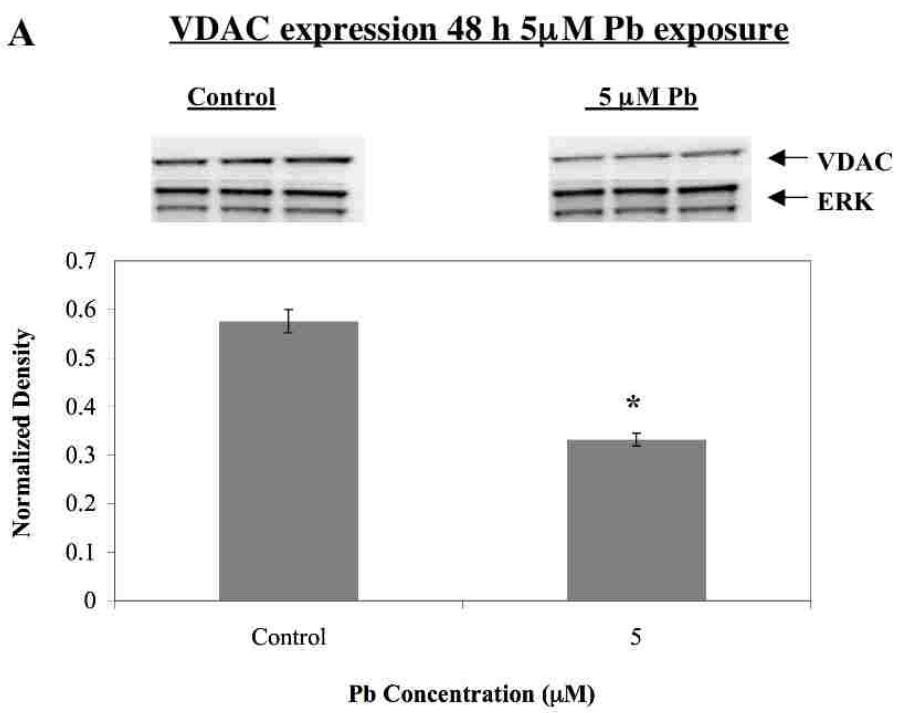
A
VDAC expression 48 h 5μM Pb exposure
Control
5 μM Pb
VDAC
ERK
Normalized Density
0.7
0.6
0.5
0.4
0.3
0.2
0.1
0
*
Control
5
Pb Concentration (μM)

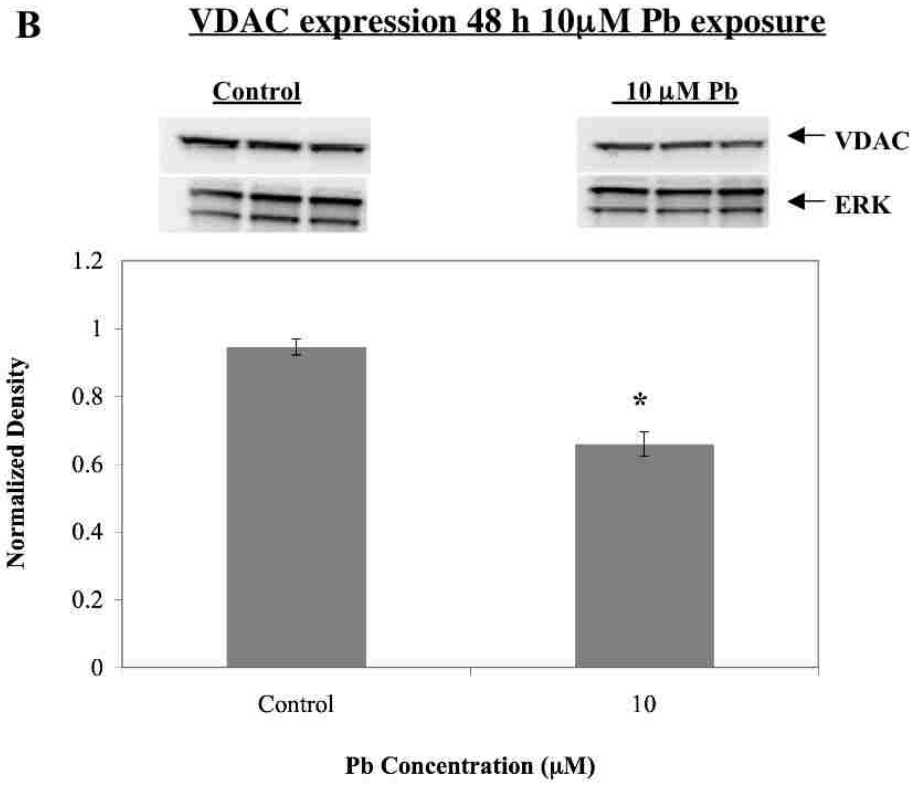
B
VDAC expression 48 h 10μM Pb exposure
Control
10 μM Pb
VDAC
ERK
Normalized Density
1.2
1
0.8
0.6
0.4
0.2
0
*
Control
10
Pb Concentration (μM)

Figure 4: Pb exposure causes a significant decrease of VDAC expression at 48 h. Differentiated PC-12 cells were exposed to 5 μM and 10 μM Pb concentrations for 48 h and VDAC expression was quantified by western blot analysis. A) 48 h exposure to 5 μM Pb results in a significant decrease in VDAC expression (~44% relative to control, n=6). B) Similarly, 48 h exposure to 10 μM Pb produced a significant decrease in VDAC expression compared to controls (n=6, ~31% relative to control). * $p<0.05$; t-test.

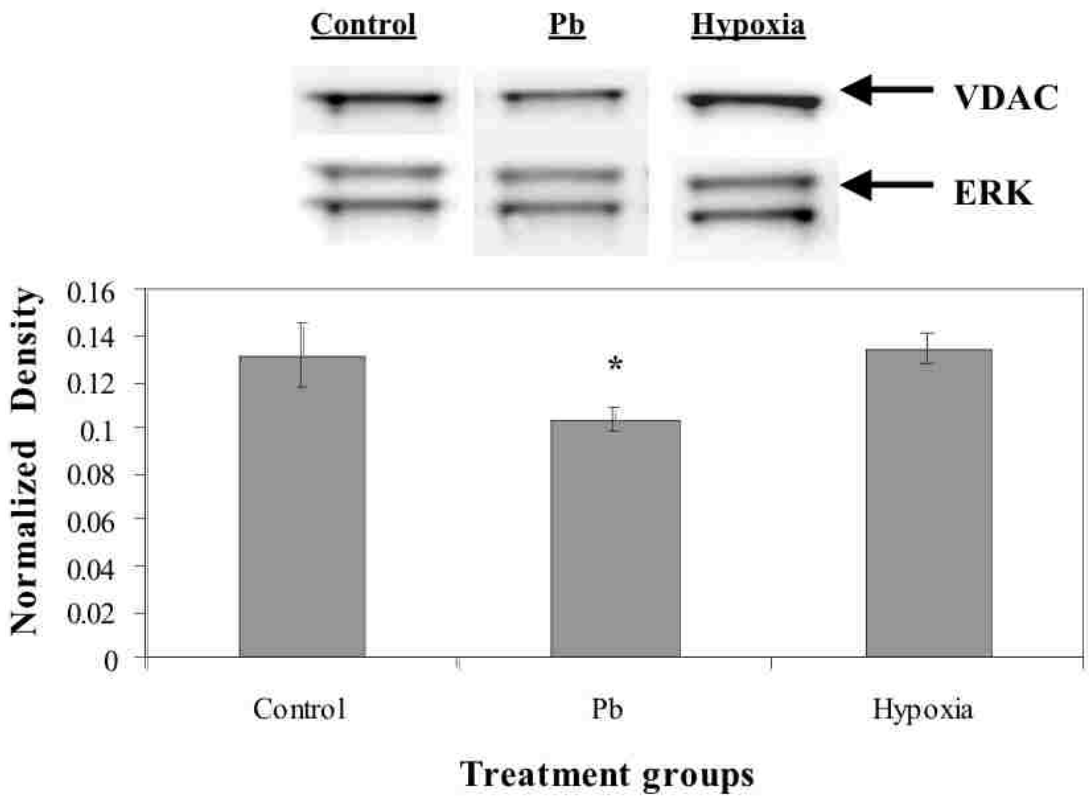

Figure 5: Hypoxia fails to decrease VDAC expression. Differentiated SH-SY5Y cells were exposed to 24 h Hypoxia or 10 μM Pb for 48 h. A 48 h exposure to 10 μM Pb resulted in a significant decrease in VDAC expression. In contrast, exposure to 24 h hypoxia fails to produce decreases in VDAC expression, demonstrating that decreased VDAC expression is not a general stress response, but is a specific effect of Pb exposure. *p<0.5; ANOVA followed by Dunnets post hoc (n=3).

Pb reduces cellular ATP levels

The above findings demonstrate that VDAC expression begins to decrease 48 h following Pb exposure, therefore we expected to see a corresponding decrease in cellular ATP since VDAC plays such a central role in regulating cellular energy metabolism. To determine if the Pb induced decrease in VDAC expression corresponded with decreases in cellular ATP levels, a luciferase driven bioluminescence assay was used to measure ATP levels following Pb exposure. Differentiated PC-12 cells were incubated with 0, 1, 5, 10, and 50 μM of Pb, and cellular ATP levels were determined using a luciferase driven bioluminescence assay. ATP levels were compared between the treatment groups to the no Pb control group. To determine if Pb itself could directly interfere with the bioluminescence assay, we exposed differentiated PC-12 cells with the Pb concentrations listed above and measured the cellular ATP levels following a 30 minute incubation. After 30 minutes of exposure, Pb concentrations failed to produce a significant difference in cellular ATP levels when compared to the no Pb control group (Figure 6A), demonstrating that Pb itself does not interfere with bioluminescence assay.

In contrast, after a 48 h incubation with Pb, cellular ATP levels for all treatment groups were found to be significantly decreased by ~35-45% relative to the no Pb control group (Figure 6B). The observed decreases in cellular ATP levels appear to correspond with the decreases in VDAC expression after 48 h of exposure to Pb, suggesting that ATP synthesis may be compromised by Pb induced decreases in VDAC expression.

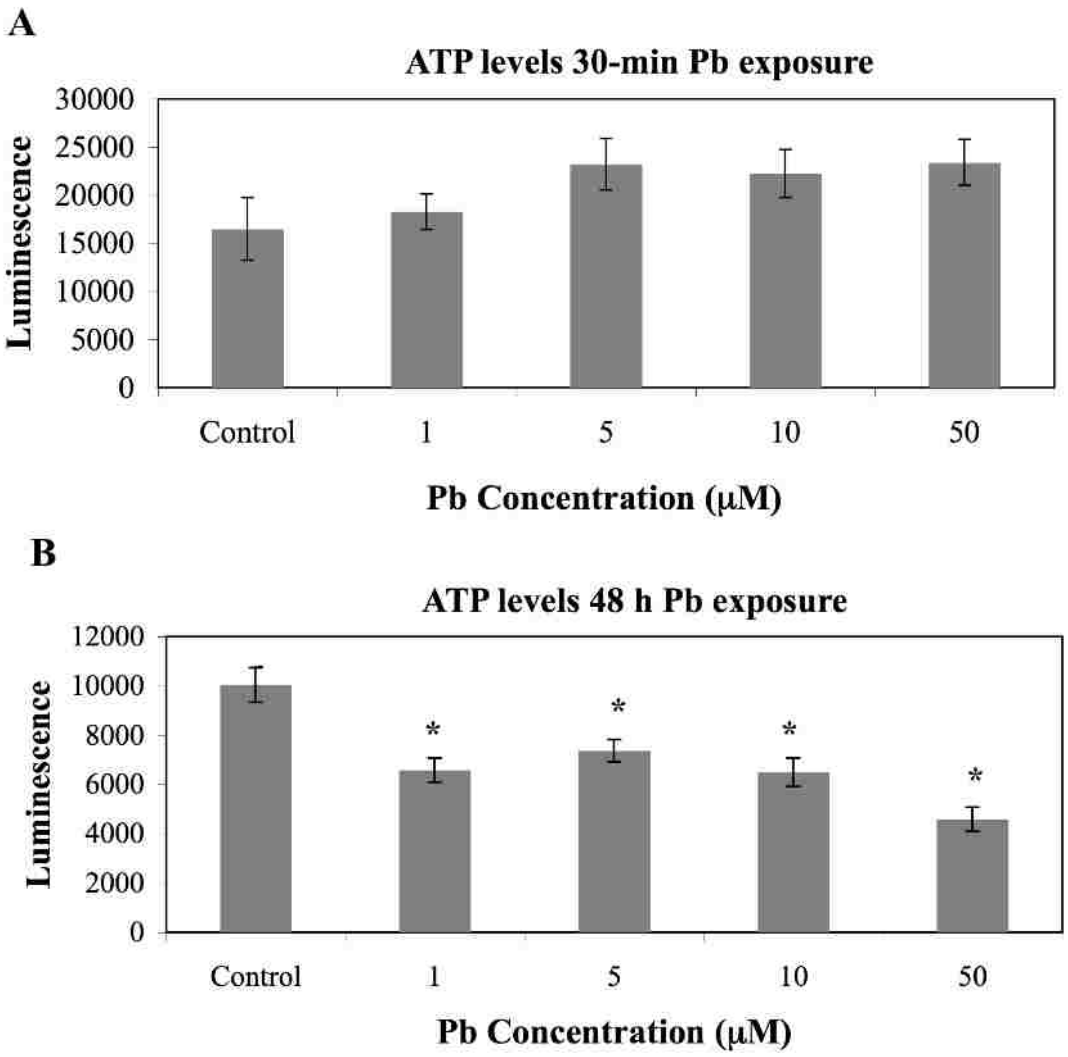

Figure 6: Pb exposure results in reduced levels of cellular ATP. A bioluminescence assay was used to measure cellular ATP levels in differentiated PC-12 cells following exposure to a graded series of Pb concentrations (0, 1, 5, 10, and 50 μM). A) After 30 minutes of exposure, Pb concentrations failed to produce a significant difference in cellular ATP levels when compared to the no Pb control group, demonstrating that Pb itself does not interfere with the bioluminescence assay itself. B) In contrast, exposure to Pb concentrations for 48 h produced a significant decrease (~35-45% relative to the no Pb control group) in cellular ATP levels at all levels of Pb. * $p < 0.05$; ANOVA followed by Dunnets post hoc test (n=6).

Pb produces decreased gene transcription of VDAC 1

The cellular effects of Pb are widespread and are elicited through a variety of different mechanisms, including altered gene transcription (Garza *et al.*, 2006). Pb is thought to interfere with gene expression by competing for the metal-binding sites of transcription factors, such as zinc-finger proteins (Zawia, 2003; Basha *et al.*, 2003). Therefore, the Pb-induced decrease in VDAC protein expression might be due to decreased transcription of the VDAC gene. In order to test this hypothesis, we used real time RT-PCR to determine whether Pb exposure results in decreased gene expression for one or more of the three isoforms of VDAC. Total RNA was extracted from differentiated PC-12 cells following a 48 h exposure to 5 μM Pb concentration. Real time RT-PCR was then used to determine the mRNA levels for VDAC-1, VDAC-2, and VDAC-3, relative to the MAPK control gene. Figure 7 shows that Pb exposure caused a significant decrease (14%) in the levels of VDAC-1 mRNA. Pb also induced a decreased trend for mRNA levels of the VDAC-2 gene but this decrease was not statistically significant. In contrast, there was no observed decrease in mRNA levels for VDAC-3. It is important to note that Pb did not induce a significant difference in mRNA levels between our control gene MAPK, and GAPDH a commonly used housekeeping gene. Thus, the decreased protein expression of VDAC that is observed following Pb exposure in vitro is primarily due to decreased transcription of VDAC-1.

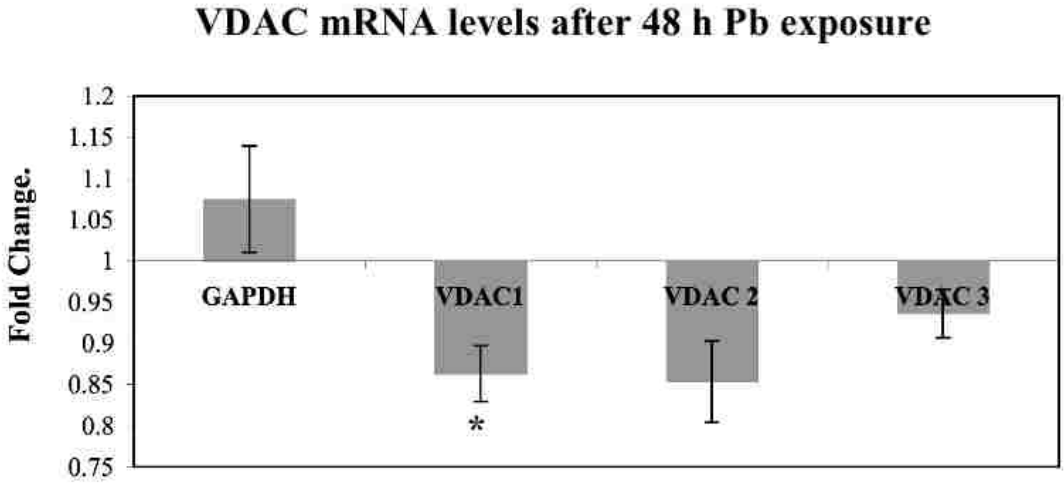

Fold Change avg PB/avg Control	VDAC1	VDAC 2	VDAC 3	GAPDH
	0.86	0.85	0.94	1.06
p value	0.03	0.09	0.48	0.52

Figure 7: Pb produces significant decreases in mRNA levels for VDAC-1. Differentiated PC-12 cells were exposed to Pb, followed by a real time RT-PCR analysis to determine the mRNA levels for VDAC-1, VDAC-2, and VDAC-3. A 48 h exposure to 5 μM Pb results in a significant decrease (14% relative to control) in the levels of VDAC-1 mRNA. Pb also induces a decreased trend for mRNA levels of the VDAC-2 gene, but this decrease was not statistically significant. In contrast, there was no observed decrease in mRNA levels for VDAC-3. Data was normalized using the MAPK1 gene. Once data had been normalized (Δ Ct), the average of the 3 biological replicates in each group was used to calculate the ΔΔ Ct and fold change (fold change = $2^{-\Delta\Delta Ct}$). It is important to note that Pb did not induce a significant difference in mRNA levels between our control gene MAPK, and GAPDH a commonly used housekeeping gene. *$p<0.05$; 2-tailed student's t-test (n=3).

Discussion

In this study, we found that low levels of Pb exposure results in decreased VDAC expression in differentiated PC-12 and SH-SY5Y cells. Results from MTT and LDH assays demonstrated that the low levels of Pb exposure used for these experiments had no affect on cell viability for either cell line. For PC-12 cells, we found that total VDAC expression levels began to decrease 48 h after Pb exposure, with larger decreases observed for 5 and 10 μM Pb concentrations. Exposing SH-SY5Y cells to 10 μM Pb for 48 h resulted in a significant decrease in VDAC expression, whereas exposure to 24 h of hypoxia failed to produce any decrease in VDAC expression. These findings demonstrate that decreased VDAC expression is a specific response to Pb exposure. In addition, Pb exposure for 48 h resulted in a corresponding decrease of cellular ATP levels, suggesting a relationship between decreased ATP levels and decreased VDAC expression. Furthermore, real time RT-PCR established that the decrease in VDAC protein expression occurs as a result of a significant decrease in gene expression for VDAC-1.

Involvement of mitochondrial VDAC in neuronal function

Mitochondria are membrane enclosed organelles that perform essential cellular functions including ATP production and intracellular Ca^{2+} signaling. Neurons require large amounts of ATP for establishing ionic gradients across cell membranes and to fuel neurotransmission and synaptic plasticity (Kann and Kovacs, 2007). VDAC is an ion channel located in the mitochondrial outer membrane and is considered to be essential for the regulation of mitochondrial function (Blachly-Dyson and Forte, 2001). VDAC regulates mitochondrial

metabolism by controlling the flow of anions, cations, creatine phosphate, Pi, ATP, ADP, and other metabolites across the mitochondrial outer membrane (Shoshan-Barmatz *et al.*, 2006; Shoshan-Barmatz and Gincel, 2003; Shoshan-Barmatz and Israelson, 2005). Mammals express at least three different VDAC genes; VDAC 1, 2, and 3 (Weeber *et al.*, 2002; Baines *et al.*, 2007). VDAC's have highly conserved structural and electrophysiological characteristics across plant, yeast, mouse, and human species (Sampson *et al.*, 1997). Studies using VDAC knock-out mice suggest that each VDAC isoform appears to have specialized functions. The knockout of VDAC-1 combined with VDAC-2 result in reductions of mitochondrial respiratory capacity (Wu *et al.*, 1999), where as knockout of VDAC-3 causes male sterility (Sampson *et al.*, 2001). Our real time RT-PCR analysis demonstrated that Pb reduced gene expression of the VDAC-1 and potentially the VDAC-2 isoforms, which have been associated with mitochondrial respiration. Reduced VDAC expression may impair normal mitochondrial ATP synthesis and thus compromise neuronal activity.

Pb exposure decreases VDAC expression in-vivo

Recently, our lab has demonstrated that low-level Pb exposure during development results in auditory processing deficits in mice (Jones *et al.*, 2008). The auditory brainstem contains specialized neurons that are highly active and capable of extremely high rates of synaptic activity (Oertel, 1999). High levels of ATP are necessary for auditory neurons to maintain the high rates of firing that are required for accurate processing of auditory information (von Gersdorff and Borst, 2002; Rowland *et al.*, 2000). While we are the first

to demonstrate Pb-induced decreases in VDAC expression within neurons, other studies have found a decrease in ATP concentrations following Pb exposure in rat brain synaptosomes (Rafalowska *et al.*, 1996). The ability of Pb to inhibit VDAC expression may result in decreased levels of neuronal ATP, leading to deficits in cellular energy metabolism. This compromised cellular energy metabolism would be detrimental to neurons with high-energy requirements, such as brainstem auditory neurons.

Mechanisms of Pb neurotoxicity

While various mechanisms have been proposed to explain the neurotoxic effects of Pb, the ability of Pb to substitute for other divalent cations, particularly calcium and zinc, at numerous cellular sites has emerged as a common theme for many of its toxic actions (Garza *et al.*, 2006; Lidsky and Schneider, 2003). The substitution of Pb for divalent cations has the potential to affect many different biologically significant processes, including metal transport, energy metabolism, apoptosis, ionic conduction, excitotoxicity, neurotransmitter storage and release processes, altered activity of first and second messenger systems, protein maturation, and genetic regulation (Garza *et al.*, 2006; Lidsky and Schneider, 2003). In addition, Pb is thought to interfere with gene expression by competing for the metal-binding sites of transcription factors, such as zinc-finger proteins (Zawia, 2003; Basha *et al.*, 2003). Numerous studies have reported that Pb exposure interferes with the DNA binding of the zinc finger transcription factor Sp1 both in-vivo and in-vitro (Crumpton *et al.*, 2001; Zawia *et al.*, 1998; Atkins *et al.*, 2003; Basha *et al.*, 2003; Hanas *et al.*, 1999). Although it is not known if Sp1 regulates VDAC gene

transcription, all three VDAC isoforms contain Sp1 binding sites (Sampson *et al.*, 1997) that could be modified by Pb. Future experiments will determine whether Pb exposure decreases VDAC transcription by altering Sp1 binding.

Summary and Conclusions

The current study demonstrates that VDAC may represent a novel target for Pb in the CNS, by reducing VDAC transcription and expression in two different neuronal cell lines. This decrease is correlated with a decrease in cellular ATP levels, linking decreased VDAC expression with decreased ATP. The loss of VDAC following Pb exposure may impair mitochondrial function and compromise neuronal activity. These effects are likely to be magnified in highly active neurons, such as those found in the auditory brainstem. Even subtle impairments in cellular energy producing processes could compromise normal neuronal signaling, and lead to the deficits in auditory temporal processing that we have observed following Pb exposure in vivo (Jones *et al.*, 2008).

Chapter 2

Chronic low-level Pb exposure during development alters proteins involved in energy metabolism in auditory neurons of the brainstem

Abstract

Low level Lead (Pb) exposure is a risk factor for behavioral and cognitive dysfunctions such as learning disabilities and ADHD. The mechanism by which Pb produces these behavioral deficits is unknown. Pb exposure during development is associated with auditory temporal processing deficits in both humans and animals, while similar auditory processing deficits are found in children with learning disabilities and ADHD. To identify cellular changes that might underlie this functional deficit, proteins expression changes following Pb exposure during development were identified in auditory regions of the brainstem using proteomic analysis. CBA/CaJ mice were exposed to no Pb (control), 0.01 mM (very low), 0.1 mM (low), or 2 mM (high) Pb acetate during development. At P21, the ventral brainstem region (VBS) containing several auditory nuclei, including the Medial Nucleus of the Trapezoid Body (MNTB), and the medial (MSO) and lateral superior olivary (LSO) nuclei, was separated from the total brainstem. Proteomic analysis (isolation and separation of proteins by 2D-PAGE; analysis by MALDI-MS) revealed that chronic Pb exposure alters the expression of a number of different classes of proteins including those involved in the regulation of cellular energy metabolism. This group includes creatine kinase B (CKB) and the voltage dependent anion channel 1 (VDAC). VDAC is an ion channel that regulates mitochondrial function and ATP production. Immunohistochemistry confirms that Pb exposure results in decreased expression of VDAC in auditory nuclei.

Thus, the Pb-induced decrease in VDAC could have a significant effect on the function of auditory neurons, leading to deficits in auditory temporal processing.

Introduction

The extensive use of lead (Pb) in a wide variety of industrial processes and products has resulted in the widespread distribution of this toxic heavy metal throughout the environment. Environmental Pb can enter biological systems through ingestion and respiration, and is considered a critical global public health hazard (Toscano and Guilarte, 2005). Despite extensive efforts to eliminate the use of Pb it continues to be a serious problem in many parts of the U.S. In 1991 the U.S. Centers for Disease Control and Prevention determined that blood Pb levels less than 10 μg/dL, were considered safe, however recent studies in humans and animals have shown that the neurotoxic effects of Pb can occur at much lower blood Pb levels (Gilbert and Weiss, 2006). Low-level Pb exposure is a risk factor for learning disabilities and attention deficit hyperactivity disorder (ADHD) (Lidsky and Schneider, 2003; Braun *et al.*, 2006). Many children with these behavioral syndromes also demonstrate deficits in auditory temporal processing, suggesting a disturbing link between developmental Pb exposure, behavioral dysfunction and auditory temporal processing (Gray, 1999; Otto and Fox, 1993; Lurie *et al.*, 2006; Breier *et al.*, 2003; Montgomery *et al.*, 2005).

Auditory temporal processing is the processing of central auditory neuronal signals in time and space, which allows the listener to resolve complex sounds and to recognize specific signals within a noise background. Children exposed to Pb showed decreased

performance in tests requiring appropriately timed reactions, and additionally, demonstrate increased latencies in brainstem auditory evoked potentials (Finkelstein *et al.*, 1998; Holdstein *et al.*, 1986). These auditory deficiencies have also been observed in several animal studies. For example, chickens exposed to low-levels of Pb are deficient in a test of central auditory temporal processing called backward masking (Gray, 1999). We have recently documented that mice exposed to low levels of Pb during development demonstrate alterations of two measures of central auditory brainstem function, the brainstem conduction time and gap encoding in the inferior colliculus. (Jones *et al.*, 2008) Taken together, our studies, and those of others, suggest that Pb targets the central auditory system, producing deficits in auditory temporal processing.

Auditory neurons have extremely high rates of neuronal activity, firing action potentials at very fast rates (Rowland *et al.*, 2000), and precise timing of the information arriving from the two ears is required in order for accurate temporal processing to occur. The increased energy demand needed by auditory neurons depends on reliable and efficient cellular energy production (Rowland *et al.*, 2000; Nothwang *et al.*, 2006; Schneggenburger and Forsythe, 2006). Pb has been shown to alter energy metabolism within the brain, resulting in decreases in cytosolic ATP levels and increased concentrations of creatine phosphate (Rafalowska *et al.*, 1996). If low-level Pb exposure results in disrupted energy metabolism in central auditory neurons, then accurate temporal processing could be severely comprised.

The current study was undertaken to determine if developmental Pb exposure results in impairment of energy metabolism in central auditory neurons. We utilized a proteomic

approach to identify Pb-induced changes in proteins involved in energy metabolism within the murine auditory brainstem. Proteomics is an attractive method for this type of study because it allows for a large-scale analysis of proteins from the Pb-challenged CNS. Proteins were isolated from control and Pb-exposed mice and were separated using two-dimensional gel electrophoresis (2D-PAGE), followed by matrix assisted laser desorption ionization-time of flight mass spectrometry (MALDI-TOF MS) and a MASCOT peptide mass fingerprint database search to identify proteins of interest. This is an ideal technique with which to explore the effects of chronic Pb exposure on protein expression since it provides information about the protein's relative mass, isoelectric point, and allows for the screening of a large number of proteins simultaneously in a single sample preparation.

We found that chronic low-level Pb exposure results in the differential expression of proteins involved in several diverse cellular pathways including energy metabolism, signal transduction, and cytoskeletal organization. However, the majority of proteins that changed expression following developmental Pb exposure were involved in cellular energy metabolism, including brain type creatine kinase (CKB) and the voltage dependent anion channel (VDAC). VDAC regulates mitochondrial ATP production and cellular ATP levels by controlling the flow of metabolites (ATP, ADP, phosphocreatine, etc.) across the outer mitochondrial membrane. Immunohistochemistry demonstrated that brainstem neurons, including auditory neurons, show a significant decrease in VDAC staining with Pb exposure. Because auditory neurons are so highly active, the Pb-induced decrease in VDAC expression could alter the function of auditory neurons by compromising energy metabolism within these cells.

Experimental Procedures

Chronic Pb exposure

Breeding pairs of CBA mice were obtained from The Jackson Laboratory (Bar Harbor, Maine). Mice used in these studies were maintained in microisolator units and kept in the University of Montana specific pathogen free animal facility. Cages, bedding, and food were sterilized by autoclaving and mice were handled with aseptic gloves. Mice were allowed food and water ad libitum. All animal use was in accordance with NIH and University of Montana IACUC guidelines. Thirteen breeding pairs of CBA mice were randomly assigned to three groups having unlimited access to water (pH 3.0) containing 0 mM (control), 0.01 mM (very low), 0.1 mM (low) or 2 mM (high) Pb acetate. Breeding pairs were given leaded water when they were paired so that offspring were exposed to Pb throughout gestation and through the dam's milk until postnatal day 21 (P21) when mice were sacrificed.

Blood lead levels

Blood was collected from deeply anesthetized mice by retro-orbital puncture. Blood Pb levels were measured by the Montana Health Department in Helena, MT. It should be noted that the means for the No Pb group include values of <1.0 which were included in the data set as equal to 1.0.

Sample preparations

The auditory region of the mouse brainstem was isolated using a 1 mm mouse brain matrix. A 2mm thick section was cut and then flash frozen on a microscope slide using liquid nitrogen and dissected into three separate regions: the cochlear nucleus (CN); the ventral brainstem region (VBS), containing the superior olivary complex (SOC) which consists of three principle auditory nuclei, the lateral superior olive (LSO), medial superior olive (MSO), and the medial nucleus of the trapezoid body (MNTB); and the dorsal brainstem region (DBS) (Figure 8A). The three fractions were placed in microfuge tubes, flash frozen with liquid nitrogen, and stored at –80°C. Brainstem sections from approximately 10 mice were dissected and used for protein extraction. Figure 8B summarizes the procedure from protein extraction through protein identification.

To simplify the proteome and increase the sensitivity of the assay, proteins were extracted according to their subcellular localization. Approximately 50 mg wet tissue was added to ice cold fractionation buffer (ice-cold PBS containing 3 mM EDTA and a protease/phosphatase inhibitor cocktail: 1 mM PMSF, 1 μg/ml pepstatin A, 1 μg/ml aprotinin, 1 μg/ml leupeptine, 1 μM okadaic acid (phosphatase inhibitor) and tissue was sheared using a 1ml pipette tip. The sample was then centrifuged at 1,000 x g for approximately 10 minutes and the supernatant was discarded. Proteins were extracted using a subcellular proteome extraction kit (Calbiochem ProteoExtract Subcellular Proteome Extraction Kit). The extraction separates the proteins into four fractions, cytosolic proteins, membrane proteins, nuclear proteins, and cytoskeletal proteins (Figure 9).

A

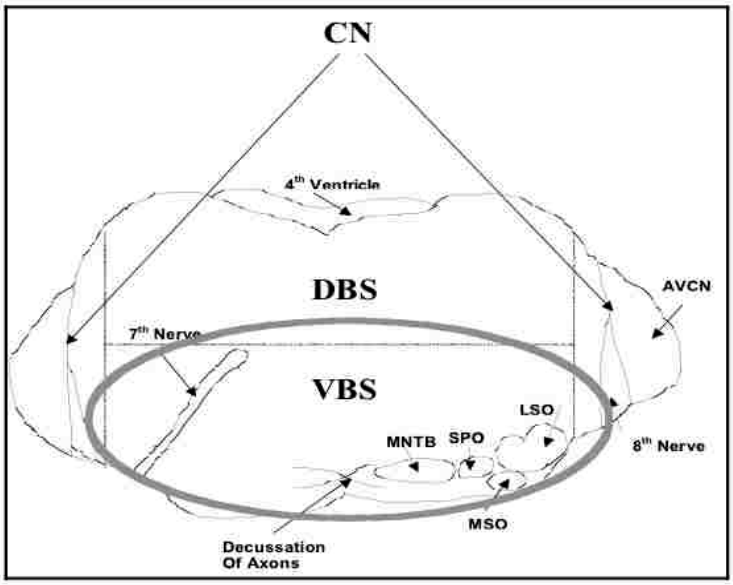
CN
4th Ventricle
DBS
AVCN
7th Nerve
VBS
LSO
MNTB
SPO
8th Nerve
MSO
Decussation
Of Axons

B

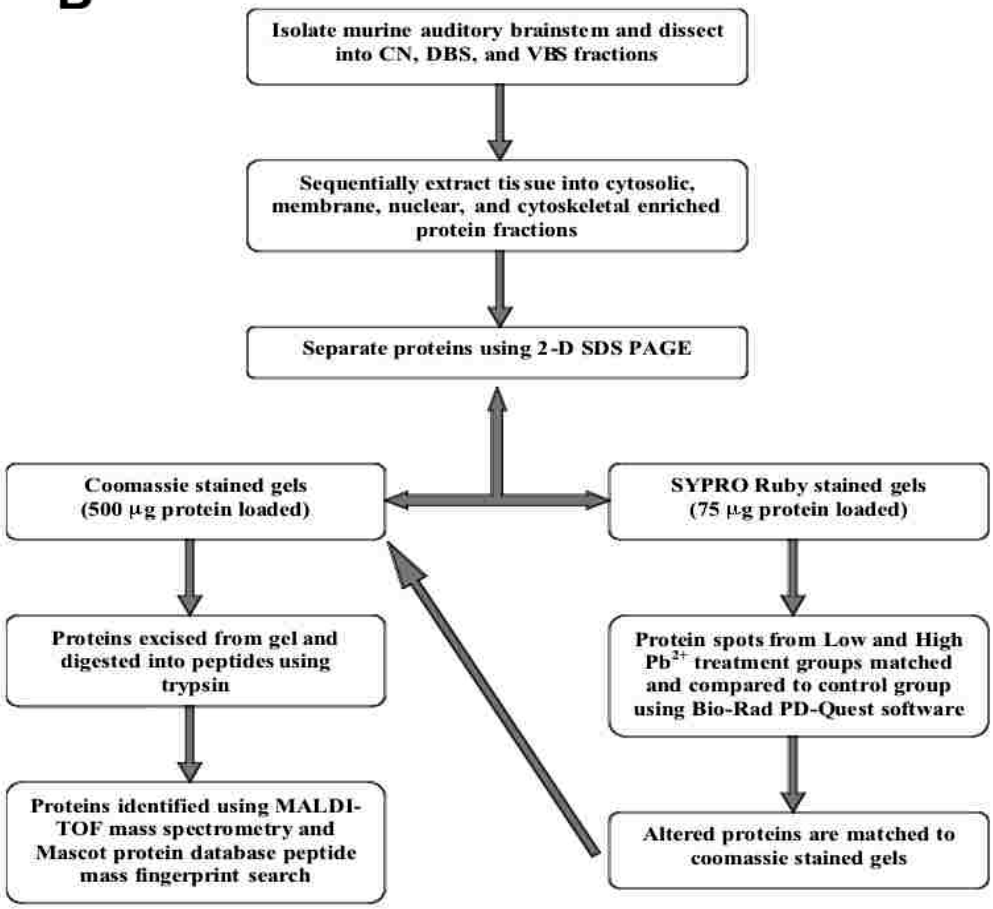
Isolate murine auditory brainstem and dissect into CN, DBS, and VBS fractions
Sequentially extract tissue into cytosolic, membrane, nuclear, and cytoskeletal enriched protein fractions
Separate proteins using 2-D SDS PAGE
Coomassie stained gels (500 μg protein loaded)
SYPRO Ruby stained gels (75 μg protein loaded)
Proteins excised from gel and digested into peptides using trypsin
Protein spots from Low and High Pb2+ treatment groups matched and compared to control group using Bio-Rad PD-Quest software
Proteins identified using MALDI-TOF mass spectrometry and Mascot protein database peptide mass fingerprint search
Altered proteins are matched to coomassie stained gels

Figure 8: Illustration of brainstem area from which proteins were extracted and summary of the various steps of the proteomic analysis. A) Illustration of brainstem area from which proteins were extracted. A 2 mm brainstem slice is obtained and cochlear nucleus sections (CN) containing the anteroventral cochlear nucleus (AVCN) are removed and the remaining tissue separated into a ventral brainstem region (VBS) and a dorsal brainstem region (DBS). The VBS (outlined in the gray circle) is isolated in order to obtain tissue enriched with auditory nuclei, and then compared to the DBS region. The DBS is used to represent the non-auditory brainstem. The VBS contains the Superior Olivary Complex (SOC), which is composed of several principle auditory nuclei including the lateral superior olivary nuclei (LSO), medial superior olivary nuclei (MSO), superior olivary nuclei (SPO), and the medial nucleus of the trapezoid body. This is the region where auditory signals from the two ears converge and is the site of initial processing of the binaural signals that allows listeners to localize sound in time and space. Protein expression changes found in the VBS were then compared to the DBS to determine if protein expression changes were specific to the auditory region of the brainstem. B) Flowchart of the proteomic analysis. Briefly, proteins were extracted from VBS and DBS tissue according to cellular localization. Proteins from the different cellular fractions were then separated by 2-D SDS-PAGE. Comparative gels were stained with SYPRO ruby and protein expression from the low and high Pb treatment groups were compared to the no Pb control using Bio-Rad PDQuest software. Proteins displaying a significant expression change (± 1.4 fold) were then matched to a coomassie stained gel for identification by MALDI-TOF MS and a mascot peptide mass fingerprint search.

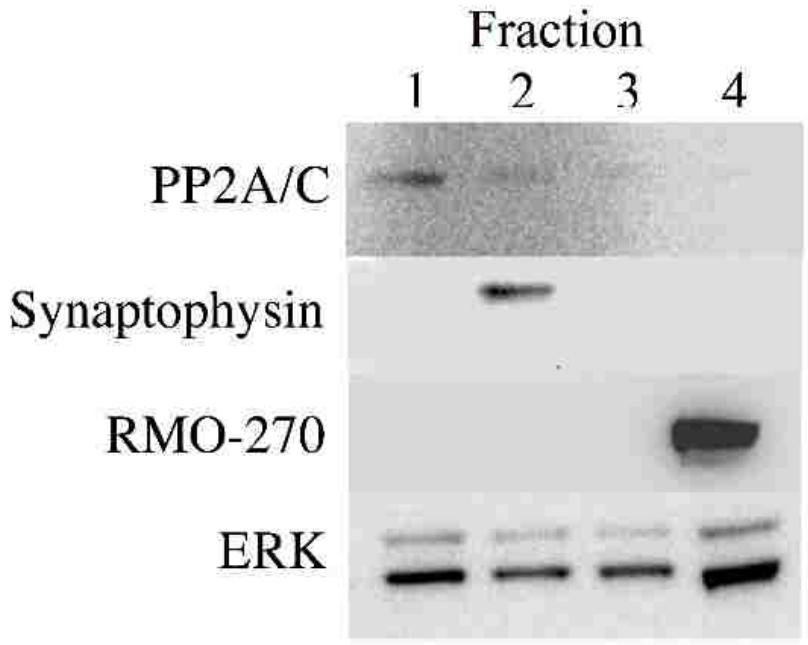

Figure 9: Calbiochem sub-proteome extraction. In order to simplify the proteome and increase the sensitivity of the 2-D gel assay, proteins were extracted from the tissue according to their subcellular localization. A Calbiochem sub-proteome extraction kit was used to separate the proteins into four different cellular fractions; (1) cytosolic, (2) membrane, (3) nuclear, and (4) cytoskeletal fractions. Western blot analysis was used to test the efficiency of the extraction on mouse brainstem tissue. Protein phosphatase 2 (PP2A/C) is primarily a cytosolic protein and was largely restricted to the cytosolic fraction. Synaptophysin is a membrane bound protein and was found in the membrane fraction. RMO 270 is an antibody directed towards Neurofilament medium and was isolated in the cytoskeletal fraction. ERK is an enzyme that translocates from the nucleus to the membrane and was found in all fractions. Results from the western blot analysis demonstrate that the sub-proteome extraction can efficiently isolate proteins according to their localization within the cell.

After extraction, the protein concentration was determined for each fraction using a BCA protein assay and samples were stored at –80°C. To concentrate proteins and remove any impurities such as salts and detergents that may interfere with 2D-PAGE separation, protein was precipitated using a protein precipitation kit (Calbiochem ProteoExtract Protein Precipitation Kit). Precipitated protein was then prepared for isoelectic focusing (IEF) by re-suspending proteins in 185 ml of 7 M urea, 2 M thiourea, 1% (w/v) ASB-14 detergent, 40 mM tris base, and 0.001% Bromophenol Blue.

Two-dimensional gel electrophoresis

Comparative Gels stained with SYPRO Ruby

In order to compare spot densities and identify proteins that changed between Pb-treatment groups, 75 μg of total protein from each treatment group for each cellular fraction was loaded onto an 11-cm IPG strip (Bio-Rad, pH 3-10). The spots on the comparative gels were then matched to a second group of gels loaded with 500 μg of total protein from each fraction and used for protein identification by mass spectrometry. Proteins were loaded onto gels by placing protein samples in a 12-well re-hydration tray. IPG strips were placed on protein samples and protein samples were allowed to enter the strip for approximately 60 minutes. A layer of mineral oil was then placed over the strips and left in the tray overnight (approximately 16 h). The IPG strips were next subjected to isoelectric focusing at 250 V for a 15 minute warm up and then ramped to 8,000 V for 2-5 h depending on sample content. The voltage was limited by a 50 μA/gel current restriction. After reaching 8000 V, the samples were focused for an additional 5 h. In preparation for

the second dimension, all sulfhydryl groups were reduced and alkylated. IPG strips were first placed an 11 cm rehydration tray containing approximately 1 ml of reducing solution (3.6 mg Urea, 0.2 mg DTT, 2.0 ml 10% SDS, 2.5 ml 1.5 M tris (pH 8.8), 2.0 ml Glycerol, and 1.0 ml H_2O) for 30 minutes. After 30 minutes the reducing solution was decanted and channels were refilled with an alkylating soluton (3.6 g Urea, 0.25 g Iodoacetamide, 2.0 ml 10% SDS, 2.5 ml 1.5 M tris (pH 8.8), 2.0 ml Glycerol, 1.0 ml H_2O, and a very small amount of Bromophenol blue) for 30 minutes. After IPG strips had been equilibrated, they were positioned in a 12.5% TRIS-HCl criterion gel (Bio-Rad criterion precast gel) and overlayed with a layer of molten agarose. Gels for all treatment groups were run simultaneously in a Bio-Rad criterion dodeca cell, which is capable of running up to 12 gels simultaneously. Gels were run for approximately 1 hour at 20°C at a constant voltage of 200 V.

Comparative Gel Staining and Imaging

2-D gels were removed from the gel cassette, and the comparative gels (75 μg total protein) were stained with SYPRO ruby fluorescent gel stain (Bio-Rad SYPRO Ruby protein gel stain). Gels were washed for 30 min in 10% methanol, 7% acetic acid. After 30 minutes the wash solution was removed and gels were covered with SYPRO Ruby protein gel stain. Gels were stained for approximately 3 hours with gentle agitation and then rinsed in 10% methanol, 7% acetic acid for 60 minutes to decrease background fluorescence. Finally, gels were washed in water for 15 minutes before imaging. Gel images were recorded using a Bio-Rad Versa Doc CCD based imaging system (Bio-Rad, Versadoc

imaging system, Model 300).

Image Analysis

Gel images were analyzed using Bio-Rad PDQuest 2-D Gel Analysis Software Version 6.2. The comparative gels from each protein extraction were grouped together according to Pb treatment and cellular fraction. The average spot density for each protein spot was then used to compare the spot density among control, low and high Pb treated animals. Comparative gels were normalized using the PDQuest software for normalization among multiple gels.

Protein Identification Gels

As described above, the SYPRO ruby-stained comparative gels were used to identify protein spots that changed in density following Pb exposure. SYPRO ruby is a very sensitive stain and changes in spot density can be detected using small amounts of protein per gel. This is important because it allowed us to use smaller numbers of animals per treatment group. However, more protein is needed per spot to accurately identify the protein using MALDI-TOF mass spectrometry. Therefore, one 2-D master gel per protein fraction was run using 500 μg total protein and stained with Coomassie blue (Bio-Rad Bio-Safe Coomassie) for approximately one hour and then destained using distilled water. Coomassie stained gel images were recorded and digitalized using a Bio-Rad desktop densitometer (Bio-Rad GS-800). Proteins of interest that were identified on the SYPRO ruby stained gels were then matched to the Coomassie stained gels using PDQuest

software. Protein spots that exhibited a greater than ±1.4 fold change between no vs. low and no vs. high Pb treated animals on the SYPRO ruby gels were identified in the Coomassie gel and identified by mass spectrometry. In addition to these protein spots of interest, approximately 100 additional high quality protein spots from each Coomassie stained gel were excised and used to create a proteomic profile for each cellular fraction (Appendix A).

In gel trypsin digestion

Protein spots were excised from Coomassie stained gels using a ProteomeWorksTM Spot Cutter (Bio-Rad) and gel plugs transferred to a 96 well plate. The proteins were enzymatically digested and the tryptic peptides were ZipTip purified. Briefly, gel plugs were destained by washing plugs for 30 minutes in 200 μl of 50% H_2O/50% acetonitrile, dried in a non-humidified oven (37°C) for approximately 2 hours, and then trypsinized using a 50 ml trypsin solution (12.5 ng trypsin/l 25mM NH_4HCO_3 in 50% acetonitrile). The sample was then incubated at 4ºC in the trypsin solution for 20 minutes, excess trypsin was removed and the sample overlayed with 30 μl of 25 mM NH_4HCO_3 and allowed to incubate overnight at 37ºC. The following morning the supernatant containing peptides was removed and placed in a fresh 0.5 ml eppendorf tube. The sample was then extracted two times with 200 μl 0.1% trifluoroacetic acid/60% acetonitrile and reduced to approximately 10 μl. The extraction was ZipTip (Millipore ZipTip, P10 C18) purified following the manufacturer's protocol. After ZipTip purification, the tryptic peptides were eluted from the ZipTip with 4 μl 60% Acetonitrile/0.2% formic acid. For analysis by

MALDI time-of-flight (MALDI-TOF) mass spectrometry, 10 μg -cyano hydroxycinnamic acid matrix is dissolved in 1 ml of 50% acetonitrile and then spiked with 2 μl of Bruker peptide calibration standard. The MALDI-TOF matrix is mixed 1:1 with peptide before samples are spotted on the MALDI-TOF sample plate.

Mass Spectrometry

Peptide mass spectra were recorded in positive ion mode on a Voyager-DE Pro MALDI time-of-flight mass spectrometer (Applied Biosystems, Foster City, CA. USA). Mass spectra were obtained by averaging 500 individual laser shots. A calibration standard mixture (Bruker peptide calibration standard) containing 7 different peptide standards was used as internal calibration standards. The selected proteins were identified by MALDI-TOF mass spectrometry and Mascot protein database search. In order to accept a Mascot database hit as a correct protein identification, several criteria have to be met. First, the protein match must have a MOWSE (Molecular Weight Search) score of at least 62 to be considered significant ($p<0.05$). In addition, most of the identified proteins have an average sequence coverage of greater than 25%. Finally, the experimental molecular weights and isoelectric points (pIs) have to be a close approximation of the protein's theoretical molecular weight and/or pI.

Database search

The peptide mass data was used to identify proteins using a Mascot protein database search engine against the MSDB database (MSDB is a non-identical protein sequence

database maintained by the Proteomics Department at the Hammersmith Campus of Imperial College London. MSDB is designed specifically for mass spectrometry applications) (http://www.matrixscience.com/). The following search parameters were used: MSDB database; Taxonomy, mus musculus (house mouse); maximum missed cleavages, 1; variable modifications, carbamidomethyl (C) and oxidation (M); and peptide tolerance, ± 0.2 Da. The Mascot search engine was used to calculate a theoretical molecular weight, isoelectric point, and search (MOWSE) score for each experimental peptide mass spectra (protein score in -10*Log(P), where P is the probability that the observed match is a random event. Protein scores greater than 62 are significant ($p<0.05$).

Total Ventral Brainstem (VBS) protein extraction and Western Blots

VBS brainstem sections from each experimental group were dissected from individual CBA mice. Total protein from each VBS section was extracted by homogenizing in a lysis buffer containing 20 mM Tris-HCL (pH 7.5), 150 mM NaCl, 1mM Na_2EDTA, 1 mM EGTA, 1% triton x, 2.5 mM sodium pyrophosphate, 1 mM beta-glycerophosphate and 1 mM Na_3VO_4 (Cell Signaling Technology, Beverly, MA). Additions were made giving final concentrations of 0.5% Na-deoxycholate, 0.5% SDS, 1 μM okadaic acid, 1 mM PMSF, 0.1 mg/mL benzamidine, 8 μg/mL calpain inhibitors I and II and 1 μg/mL each leupeptin, pepstatin A and aprotinin. Homogenates were sonicated and vortexed for approximately 30 seconds before centrifugation at 50,000 rpm for 20 minutes. Proteins were separated by SDS-PAGE using 4-12% gradient bis-tris gels (Bio-Rad criterion precast gel) and transferred to PVDF membranes for immunoblotting. Sources for antibodies were as

follows: Total VDAC (Cell signaling technology, Cat. # 4866), Creatine Kinase B (Abcam Inc., Cat. # ab38211), Erk (Cell signaling technology, Cat. # 9102), and total aldolase (Cell Signaling Technology, Cat. # 3188).

Immunoblotting

Protein concentrations for the whole cell lysate were quantified using the BCA Protein Assay kit (Pierce) and 20 μg of protein/sample was used for immunoblotting of brain type creatine kinase (CKB), total aldolase, total VDAC, and ERK. Proteins were suspended with an equal volume of Laemmli buffer, heated at 95°C for 5 min, loaded, and separated on 18-well Criterion Bis-Tris 4-12% pre-cast gels (Bio-Rad). The MagicMark XP western standard (Invitrogen) was used to determine the approximate molecular weight of each protein. Gels were transferred to Immun-Blot PVDF membrane (Bio-Rad) using Criterion (Bio-Rad) transfer cell with plate electrodes for 60 minutes at 100 V and blocked in 5% milk in TBST (1 x Tris-buffered saline, 0.1% Tween 20, 5% dry milk), incubated overnight at 4°C. Membranes were washed in TBST, and then incubated overnight at 4ºC with antibodies directed against total VDAC (Cell signaling technology, Cat. # 4866; 1:1000), Creatine Kinase B (Abcam Inc., Cat. # ab38211; 1:400), and total Aldolase (Cell signaling technology, Cat. # 4866; 1:1000). Membranes were then washed in TBST and incubated with 2º-antibody (Vector, HRP-conjugated Anti-Rabbit, PI-1000; 1:2000) for two hours. Membranes were then washed in TBST before imaging with the Fuji LAS-3000 CCD based imaging system (FujiFilm Life Science). Membranes were reprobed with total ERK (Cell signaling technology #9102; 1:1000) to confirm equal protein loading. Band pixel intensity

was measured using the Fuji LAS-3000 software. Band intensities from treated groups were normalized to a percentage of control samples, and plotted using GraphPad (GraphPad Prism 4.0) software. Statistical significance was determined by an analysis of variance followed by dunnets post hoc, $p<0.05$ (n=3-4 animals per group).

Immunohistochemistry

At P21, mice from both treatment groups (n=3 to 4 per group) were deeply anesthetized and perfused transcardially with 4% Na-periodate-lysine-paraformaldehyde fixative (PLP, final concentrations 0.01 M sodium periodate, 0.075 M lysine, 2.1% paraformaldehyde, 0.037 M phosphate). Brains were removed and post-fixed for 2 hours at 4°C in PLP, rinsed 3 times for 10 minutes each in PBS and transferred to a 30% sucrose solution in PBS overnight at 4°C. Brains were bisected between the forebrain and brainstem and tissue was embedded cut-side down into 1.5 cm square embedding cups filled with optimal cutting temperature (O.C.T.) compound. Brains were then frozen in liquid nitrogen and stored at -20°C. Ten micron tissue sections were cut on a Thermo Shandon Cryotome Cryostat (Thermo Shandon, Pittsburgh PA) and a one in three series of sections was collected for each brain.

Sections were thawed to room temperature and then rinsed in PBS three times for 10 minutes each. Slides were then permeabilized for 30 minutes with 0.5% Triton X-100 in PBS and immunostained as previously described (Lurie *et al.*, 2000)(Wishcamper *et al.*, 2001). Briefly, tissue sections were blocked for 20 minutes with 4% Normal Goat Serum (Vector Labs, Burlingame CA) in PBS containing 1% azide (PAB) and incubated with

primary antibody, rabbit anti-VDAC (Cell Signaling Technologies, Boston MA) diluted 1:200 in PAB, for 24 hours in a humid chamber at 4°C. The tissue was rinsed and then stained with the secondary antibody, Alexa Fluor 488 anti rabbit IgG (Invitrogen, Carlsbad CA) diluted 1:400 for 1 hour at room temperature in the dark. Sections were then rinsed in PBS followed by distilled water and the slides were coverslipped with FluorSave (Calbiochem, San Diego CA) and stored in the dark at 4°C.

Antibodies

The polyclonal antibody against voltage dependent anion channel (VDAC) was raised by immunizing rabbits with a synthetic peptide (KLH coupled) corresponding to the amino terminus of human VDAC-1 and purified using protein A and peptide affinity chromatography (Cat. No. 4866, Cell Signaling Technologies, Boston MA). VDAC detects endogenous levels of total VDAC protein that is ubiquitously expressed and located in the outer mitochondrial membrane.

Tissue Analysis

All fluorescent slides were viewed at 60x magnification using a Nikon Eclipse TE 300 confocal microscope and the BioRad Radiance 2000 Laser Scanning System connected to a Dell PC. Two auditory brainstem regions, the medial nucleus of the trapezoid body (MNTB) and the lateral superior olivary complex (LSO) and one non-auditory brainstem region, the motor trigeminal nucleus (Mo5) were analyzed. Images from MNTB were taken at 60x magnification with a 2.3 zoom feature while images from LSO and Mo5 were taken

with no zoom. The center of each region was determined by examining a series of hematoxylin and eosin stained sections. Two sections from the center of each region of interest were selected. Slides were blinded and images were collected and then converted from color tiff files to black and white, 12 bit tiff files. Five areas of interest were analyzed from each blinded image and the integrated optical density of the immunostaining was measured using MediaCybernetics Image-Pro software (Bethesda MD). Integrated optical density measurements were used for quantification of immunostaining because it analyzes both the area of immunostained tissue that met threshold as well as the intensity of the immunostaining. Immunostaining within five randomly placed area of interest boxes (2665 square microns) within MNTB, LSO and Mo5 in control and Pb-exposed mice was then quantified and averaged. From each mouse, the IOD in the five area of interest boxes were measured per image and the IOD in 10 area of interest boxes were measured per mouse. Statistical differences in immunostaining between control and Pb exposed animals were analyzed using Synergy Software's KaleidaGraph software (Reading PA).

Statistical Analysis

Data are expressed as mean SEM and were analyzed using one-way analysis of variance with Dunnett's post-hoc analyses where appropriate; $p<0.05$ was considered significant.

Results

The present study uses four different doses of Pb in the drinking water, the no Pb control, very low Pb (0.01 mM), low Pb (0.1 mM) and high Pb (2 mM). Blood lead levels (mean ± SEM) of the mice used in the proteomic studies are as follows: No Pb controls (1.38 ± 0.14 μg/dL), Very Low Pb (8.0 ± 0.4 μg/dL), Low Pb (42.3 ± 1.97 μg/dL), and High Pb (279 ± 44.11 μg/dL). The low dose of Pb produces a low blood Pb level while the high dose resulted in small decreases in both body weight and size of the mice (data not shown) suggesting that the high dose is a potentially toxic dose. In contrast, our very low and low Pb dose exhibited no change in body size and weight, and thus was considered to be a sub-toxic dose. We focused on the proteomic changes observed at low levels of Pb, particularly those involved in energy metabolism, because auditory temporal processing deficits are seen following low Pb-exposure (Jones *et al.*, 2008). Futhermore, the blood lead levels of our low Pb animals has been commonly used to demonstrate the neurotoxic effects of Pb in rodents (Lasley and Gilbert, 2000).

Proteomic analysis of control mice

In order to determine whether Pb exposure preferentially altered expression of proteins involved in energy metabolism, a proteomic analysis using 2-D gel electrophoresis was performed. This technique yielded a large number of identifiable proteins in both control and Pb-exposed mice. Representative 2-D gel maps of overall protein expression from the cytosolic, membrane, and cytoskeletal fractions of the VBS are shown in Figure 10. Proteins are widely distributed across the entire pI range of the gel and the majority of the

proteins are located between 20 and 120 kDa. A total of 187 protein spots were identified in the three cellular fractions, with an average of approximately 60 protein spots per fraction (Appendix A). For this analysis, it is important to note a specific protein may exist in several post-translationally modified forms and be represented by multiple spots distributed across a wide range of isoelectric points (pI). In addition, specific proteins may exist in different cellular compartments and can be found in one or more cellular fractions. Several of the proteins were identified in multiple spots in a single fraction, indicating possible posttranslational modifications such as phosphorylation. An example of this is the medium weight neurofilament protein (NFM), which was identified as multiple spots distributed across an entire pI range within the cytoskeletal fraction (Figure 10C). Our previous studies have found that developmental Pb exposure increases the phosphorylation of NFM in the mouse auditory brainstem (Jones *et al.*, 2008) and this is reflected in the altered distribution of the protein within the 2-D gel following Pb exposure. There were also several instances where a single protein was identified in multiple cellular fractions, suggesting the possible trafficking of the protein between cellular compartments. For example, β-actin was identified in all three cellular fractions (Figure 10).

Proteomic Analysis of Pb exposed mice

In order to determine whether proteins involved in energy metabolism represented the major class of Pb-induced protein expression changes within the VBS region (containing auditory nuclei), two-dimensional gels were run for each Pb treatment group and changes in protein expression between control and Pb treated groups were found by map matching.

Representative 2-D gel maps from no, low, and high Pb treated animals are shown in Figure 4. It is important to note that 2-D gel maps have been normalized to ensure that spot signal intensity can be compared between the no Pb control and the Pb treatment groups. Several proteins have been circled that show increases in protein expression following Pb treatment, including Heat Shock Protein 60 (HSP 60) and Creatine Kinase B (CKB) (Figure 11), demonstrating that this technique is able to identify changes in protein expression. We utilized a differential extraction protocol in order to localize protein changes to specific cellular compartments (as described in Methods).

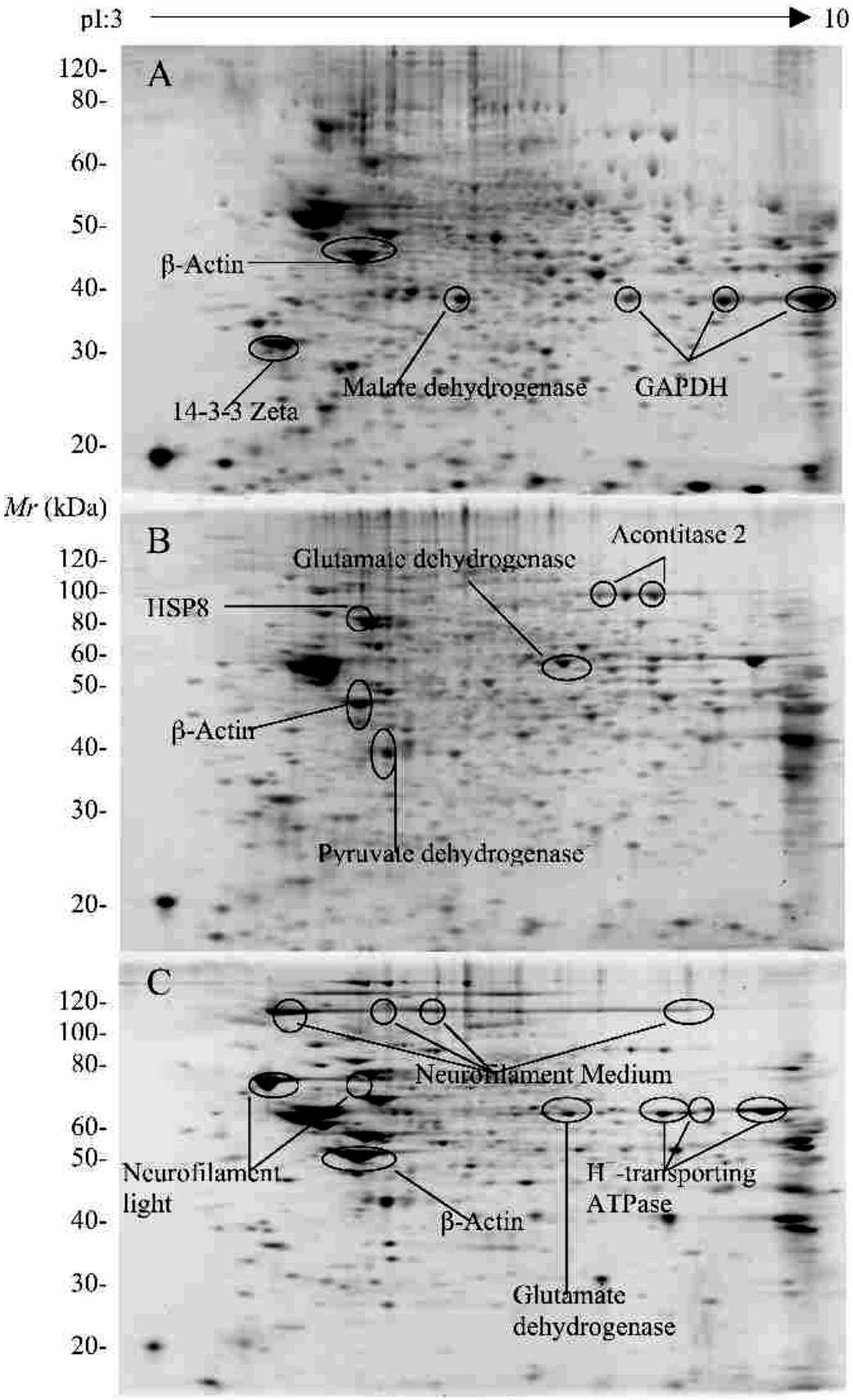
pI:3
10
Mr (kDa)
A
120-
80-
60-
50-
40-
30-
20-
β-Actin
Malate dehydrogenase
GAPDH
14-3-3 Zeta
B
120-
100-
80-
60-
50-
40-
30-
20-
Glutamate dehydrogenase
Acontitase 2
HSP8
β-Actin
Pyruvate dehydrogenase
C
120-
100-
80-
60-
50-
40-
30-
20-
Neurofilament Medium
Neurofilament light
β-Actin
H -transporting ATPase
Glutamate dehydrogenase

Figure 10: Representative two-dimensional gel maps of overall protein expression in VBS from No Pb (Control) mice. Protein expression from (A) cytosolic fraction, (B) membrane fraction, and (C) cytoskeletal fractions are shown. Approximately 60 protein spots were identified for each cellular fraction for a total of 187 protein spots in the three fractions. The majority of the proteins are located between 20 and 120 kDa, and are widely distributed across the entire pI range (pI: 3-10). Many proteins are identified as multiple spots in a single fraction, suggesting possible posttranslational modifications such as glycosylation or phosphorylation. Note that the medium weight neurofilament protein (NFM) (known to exist in several different phosphoryolation states within the cell) is identified as multiple spots distributed across an entire pI range within the cytoskeletal fraction. In addition, several proteins such as β-actin, are identified in multiple cellular fractions, suggesting the possible trafficking of these proteins between cellular compartments.

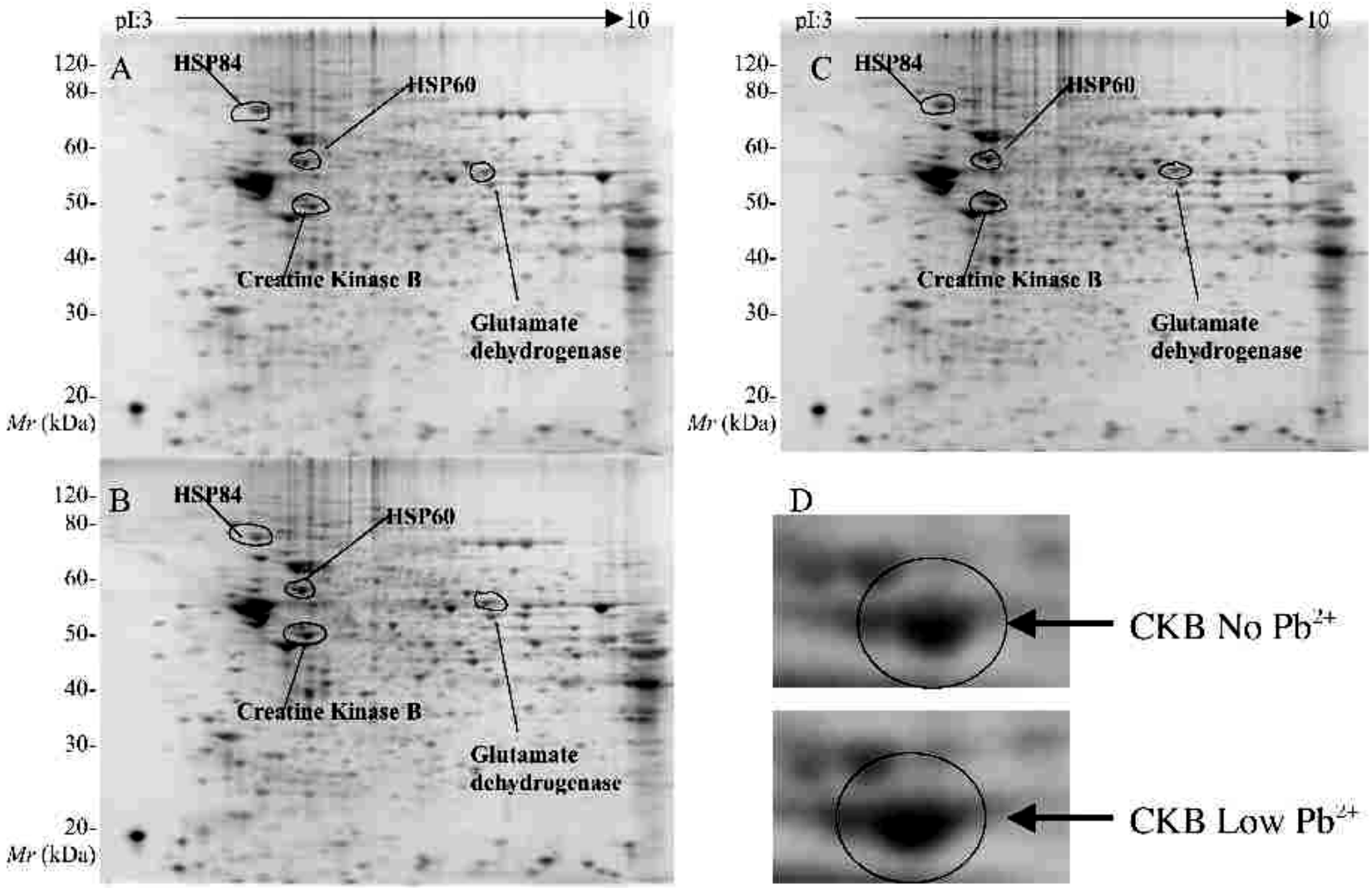
pI:3
10
A
HSP84
HSP60
Creatine Kinase B
Glutamate dehydrogenase
120-
80-
60-
50-
40-
30-
20-
Mr (kDa)
B
HSP84
HSP60
Creatine Kinase B
Glutamate dehydrogenase
C
HSP84
HSP60
Creatine Kinase B
Glutamate dehydrogenase
D
CKB No Pb2+
CKB Low Pb2+

Figure 11: Representative 2-D gel maps of VBS membrane fraction from (A) No Pb control, (B) Low Pb, and (C) High Pb treated animals. In order to identify Pb-induced protein expression changes within the VBS region, two-dimensional gels were run for each Pb treatment group (both the VBS and DBS fraction) and changes in protein expression between control and Pb treated groups were found by map matching. Several proteins that were differentially expressed in the VBS membrane fraction following low Pb treatment have been circled, including Heat Shock Protein 60 (HSP 60), Heat Shock Protein 84 (HSP 84), glutamate dehydrogenase, and Creatine Kinase B (CKB). (D) Expanded view of CKB illustrates an increase in protein expression with Pb exposure. Quantification of this spot reveals that low Pb induced a +1.5 fold expression change in CKB in the membrane fraction.

Tissue samples from each treatment group were pooled in order to obtain enough tissue for the differential extraction. It should be noted that pooling samples does not allow for the statistical comparison of protein expression changes between individual animals. However, since the mechanisms of Pb toxicity are not well defined, we used the proteomic analysis as a general screen to identify proteins that changed expression in the VBS compared to the rest of the brainstem (dorsal brainstem (DBS); see Figure 8). Protein spots displaying an expression change of ±1.4 fold or greater were excised from the gel and identified by MALDI-TOF mass spectrometry and a peptide mass fingerprint search. In order to identify those protein changes that were specific to the auditory region and were not a general effect of Pb on the brain, we performed an additional proteomic analysis of the DBS brainstem fraction from the same mice and compared the results to the VBS brainstem fraction (Tables 1-3). In this way we were able to identify and focus on proteins that changed specifically within auditory regions.

Protein Name	SSP#	VBS Protein (fold change)	DBS Protein (fold change)	Mr/pI Theoretical	Mr/pI Calculated	Mascot Score	Sequence Coverage	Function
No Pb^{2+} vs. Low Pb^{2+}								
Dihydropyrimidinase-related protein 2 (Symilarity)	2806	+1.6	NC	62/6.0	64/5.2	92	28%	Neuronal development
ATPase, H+ transporting, V1 subunit E isoform 1	9301	+1.5	NC	26/8.4	32/9.5	81	31%	Vesicular proton pump subunit
ATPase, H+ transporting, V1 subunit A isoform 1	2812	-1.4	-1.5	68/5.5	65/5.2	120	25%	Vesicular proton pump subunit
Glyceraldehyde-3-phosphate dehydrogenase (phosphorylating)	9403	+1.7	NC	36/8.4	36/9.5	78	39%	Energy generation, Glycolysis
Fructose-bisphosphate aldolase A	9502	+1.6	NC	39/8.3	42/9.5	111	43%	Energy generation, Glycolysis
Fructose-bisphosphate aldolase C (Aldolase 3)	5503	-1.6	NC	39/6.8	41/6.2	114	49%	Energy generation, Glycolysis
14-3-3 zeta protein	203	-1.5	NC	28/4.7	30/4.7	89	39%	Synaptic plasticity
Guanosine diphosphate (GDP) dissociation inhibitor	1802	-1.4	NC	51/5.0	59/4.9	125	42%	Neurotransmitter release
Heat shock protein, 60kD	2808	+1.6	NC	61/5.7	61/5.2	81	15%	Molecular chaperone
No Pb^{2+} vs. High Pb^{2+}								
Dihydropyrimidinase-related protein 2 (Symilarity)	2806	+1.8	-1.4	62/6.0	64/5.2	92	28%	Neuronal development
Heat shock protein, 60kD	2808	-1.6	+1.4	61/5.7	61/5.2	81	15%	Molecular chaperone
L-lactate dehydrogenase B chain (LDH-B)	3401	-1.4	NC	36/5.7	36/5.3	143	39%	Energy generation, Glycolysis
Pyruvate kinase isozyme M2	6801	-1.5	NC	58/7.4	58/6.7	70	24%	Energy generation, Glycolysis
Glutamate dehydrogenase [NAD(P)] precursor	7703	-1.5	NC	61/8.1	54/6.8	92	25%	Glutamate turnover, glutamate breakdown

Table 1: Cytosolic protein fold change in VBS and DBS following chronic Pb exposure during development. Protein fold change of ±1.4 or greater were considered to reflect a significant effect of Pb exposure on protein expression. Theoretical and calculated molecular weight and isoelectric point (Mr/pI) are shown for each protein. Mascot search scores (MOWSE score) of greater than 62 are considered significant.

Protein Name	SSP#	VBS Protein (fold change)	DBS Protein (fold change)	Mr/pI Theoretical	Mr/pI Calculated	Mascot Score	Sequence Coverage	Function
No Pb^{2+} vs. Low Pb^{2+}								
Fructose Bisphosphate (aldolase A)	9407	+1.5	NC	39/8.4	42/9.5	73	32%	Energy generation, Glycolysis
Alpha enolase	3502	+1.8	NC	47/6.4	49/5.6	71	24%	Energy generation, Glycolysis
Creatine Kinase B	2403	+1.5	NC	43/5.4	46/5.3	112	39%	Energy transduction, Mitochondrial
Ubiquinol-cytochrome c reductase core protein 1	2503	+1.4	NC	53/5.8	49/5.2	86	29%	Energy transduction, Mitochondrial
ATPase, H^+-transporting, V1 subunit A	2705	+2.4	+1.4	56/5.6	68/5.3	79	20%	Vesicular proton pump subunit
Isovaleryl coenzyme A dehydrogenase	4404	+1.5	NC	46/8.3	43/6.0	94	22%	Energy transduction, Mitochondrial
Glutamate dehydrogenase	6605	+1.4	NC	61/8.1	55/6.7	86	24%	Glutamate turnover, glutamate breakdown
Glutamine synthetase	5401	+1.5	NC	42/6.6	45/6.0	64	16%	Glutamate turnover, inactivates glutamate
Beta tubulin	1501	-1.5	+1.4	50/4.8	54/4.8	142	32%	Structural protein
Beta actin	1402	+1.4	-1.6	39/5.8	45/5.0	105	33%	Structural protein
Heat shock protein 8 (Hsc70)	2702	+1.8	NC	71/5.2	70/5.1	126	26%	Molecular chaperone
	2704	-1.8	NC	71/5.2	69/5.1	235	41%	
Heat shock prtotein 60	2601	+1.4	NC	61/5.7	60/5.0	116	25%	Molecular chaperone
Heat shock protein 84	1802	-1.4	NC	83/5.0	94/4.9	91	21%	Molecular chaperone
Glucose-regulated protein 58 (GRP58)	3605	+2.3	NC	57/5.8	59/5.8	107	28%	Molecular chaperone
No Pb^{2+} vs. High Pb^{2+}								
ATPase, H^+-transporting, V1 subunit A	2705	+4.0	+1.5	56/5.6	68/5.3	79	20%	Vesicular proton pump subunit
Creatine Kinase B	2403	+1.5	NC	43/5.4	46/5.3	112	39%	Maintains cellular energy homeostasis
Glutamine synthetase	5401	+1.4	NC	42/6.6	45/6.0	64	16%	Glutamate turnover, inactivates glutamate
Heat shock protein 8 (Hsc70)	2704	-1.7	NC	71/5.2	69/5.1	235	41%	Molecular chaperone

Table 2: Membrane protein fold change in VBS and DBS following chronic Pb exposure during development. Protein fold change of ±1.4 or greater were considered to reflect a significant effect of Pb exposure on protein expression. Theoretical and calculated molecular weight and isoelectric point (Mr/pI) are shown for each protein. Mascot search scores (Mowse score) of greater than 62 are considered significant.

Protein Name	SSP#	VBS Protein (fold change)	DBS Protein (fold change)	Mr/pI Theoretical	Mr/pI Calculated	Mascot Score	Sequence Coverage	Function
No Pb^{2+} vs. Low Pb^{2+}								
Neurofilament light polypeptide	503	+1.4	NC	61/4.6	65/4.6	182	37%	Structural protein
	2604	+1.6	NC	61/4.6	66/5.1	117	24%	
	3601	+1.5	NC	61/4.6	67/5.2	153	27%	
Neurofilament medium polypeptide	704	+2.0	NC	96/4.8	97/4.7	164	28%	Structural protein
	803	-1.7	+2.0	96/4.8	98/4.6	206	38%	
	3801	+2.5	+1.8	96/4.8	99/5.3	106	27%	
Neurofilament High polypeptide	2806	+2.5	NC	115/5.7	110/5.2	98	15%	Structural protein
Neurofilament 3, medium	3403	+1.5	+2.0	64/4.8	56/5.3	82	25%	Structural protein
Guanine nucleotide binding protein G(o) subunit alpha 1	2102	+1.5	NC	40/5.3	39/5.1	73	28%	Neurotransmitter release
NADH dehydrogenase (Ubiquinone) Fe-S protein 1	2605	+1.5	NC	80/5.5	75/5.2	104	24%	Energy transduction, Mitochondrial
Voltage dependent anion channel 1	9101	-2.1	NC	31/7.7	33/9.5	122	50%	Energy transduction, Mitochondrial
Cyclic nucleotide phosphodiesterase	9301	-1.4	-1.6	45/8.7	47/9.5	107	28%	Synaptic plasticity
No Pb^{2+} vs. High Pb^{2+}								
Neurofilament light polypeptide	2604	+1.9	NC	61/4.6	66/5.1	117	24%	Structural protein
NADH dehydrogenase (Ubiquinone) Fe-S protein 1	2605	+1.4	NC	80/5.5	75/5.2	104	24%	Energy transduction, Mitochondrial
Heat shock protein 8	2607	-1.5	NC	71/5.2	69/5.2	112	25%	Molecular chaperone

Table 3: Cytoskeletal protein fold change in VBS and DBS following chronic Pb exposure during development. Protein fold change of ±1.4 or greater were considered to reflect a significant effect of Pb exposure on protein expression. Theoretical and calculated molecular weight and isoelectric point (Mr/pI) are shown for each protein. Mascot search scores (Mowse score) of greater than 62 are considered significant.

We found that the majority of the proteins that changed expression following Pb exposure were specific to the VBS fraction and did not change within the DBS fraction. These proteins were organized into four major categories- energy metabolism proteins, molecular chaperones, synaptic proteins, and cytoskeletal proteins. As we predicted, chronic low-level Pb exposure has the greatest effect on proteins involved in energy metabolism (Figure 12) and the remainder of our analysis focuses on this group of proteins.

One of the largest changes in protein expression following low-level Pb exposure occurred in a protein spot identified as the voltage dependent anion channel 1 (VDAC). This protein spot is decreased by 2.1 fold in the VBS cytoskeletal fraction of low Pb animals (Table 3) and is one of the largest decreases in expression that we observe following Pb exposure. The decrease in VDAC expression does not appear to be a general response of the brain to Pb, because the DBS fraction shows no change in VDAC following Pb exposure. VDAC forms a large voltage gated pore and is located in the outer mitochondrial membrane, where it controls the flow of metabolites and ions through the outer membrane by passive diffusion (De Pinto *et al.*, 1985). Decreased VDAC expression is particularly interesting in terms of cellular energy metabolism since VDAC controls the transport of ATP and ADP between the cytosol and the mitochondria. Studies have shown that decreased VDAC expression results in decreased ATP synthesis and reduced cytosolic ADP and ATP levels (Abu-Hamad *et al.*, 2006).

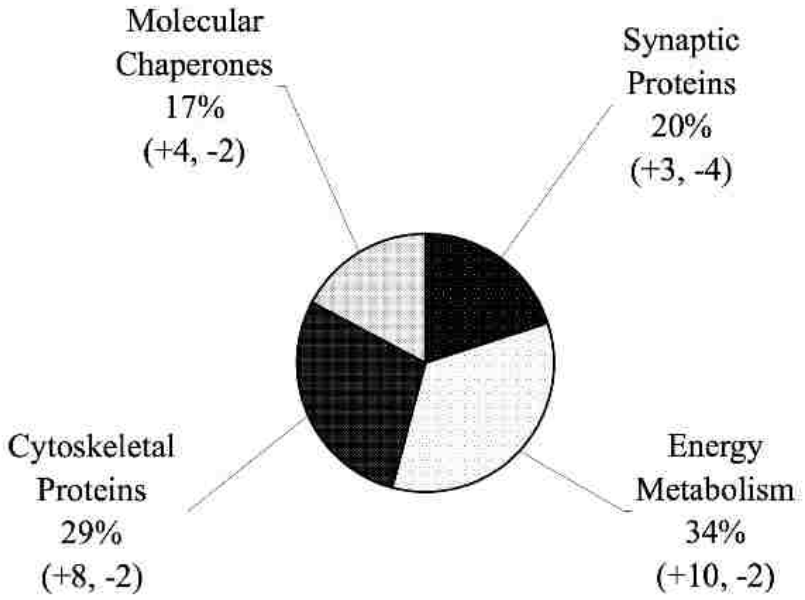

Figure 12: VBS protein groups regulated by low-level Pb exposure. Pie chart shows upregulated and down-regulated proteins (+ and -, respectively), following chronic low-level Pb exposure during development. The modified proteins are organized into four main categories- proteins involved in energy metabolism, molecular chaperones, synaptic proteins, and cytoskeletal proteins. Most of the proteins that changed expression following Pb exposure are specific to the VBS fraction and did not change within the DBS fraction, suggesting that Pb has a greater effect on the auditory region of the brainstem. It is important to note that the majority of proteins that are up-regulated following Pb exposure are involved in energy metabolism, and the majority of down-regulated proteins are those involved in synaptic structure and function.

Mice have three VDAC isoforms (VDAC-1, VDAC-2, and VDAC-3), and our 2-D gel analysis revealed that the spot identified as VDAC-1 decreases by 2.1 fold as a result of low-lead exposure. In order to further verify the results of the 2-D gel analysis and determine the effect of Pb on total VDAC, we performed a western blot analysis on individual Pb-exposed mice using a VDAC antibody that labels all three isoforms. Western blot analysis of the VBS fraction demonstrates that total VDAC is significantly decreased by 19%, which further confirms the direction of change for VDAC expression in the 2-D gel analysis (Figure 13A). It should be noted that the western data shows a smaller decrease for total VDAC (19%) compared to the 2-D gel data (2.1 fold decrease for VDAC 1) following Pb exposure. This is appropriate because the antibody used for the Western analysis is directed towards total VDAC, not specific VDAC isoforms such as VDAC-1, and it may be that only VDAC-1 expression is decreased by Pb exposure.

If decreased VDAC expression leads to the decreased production of mitochondrial ATP in the auditory brainstem, then an increase in expression for other proteins involved in energy metabolism may be expected in order to compensate for decreased ATP levels (Gellerich *et al.*, 2004). Brain type creatine kinase (CKB) is a cytosolic enzyme that plays an important role in the energy homeostasis of cells with high-energy requirements (Wallimann and Hemmer, 1994). CKB is part of a cellular energy buffering system, catalyzing the transfer of intracellular energy between ATP consuming and ATP generating sites in the cell, which is essential for maintaining ATP levels during high synaptic activity (Dzeja and Terzic, 2003). Its function is to reversibly catalyze the conversion of creatine phosphate to creatine, regenerating ATP from ADP (Wallimann *et al.*, 1992). CKB is able

to replenish ATP levels in areas of high demand at a faster rate than glycolysis or oxidative phosphorylation in mitochondria (Wallimann *et al.*, 1992). If decreased VDAC expression results in decreased cellular ATP levels, the expression of CKB could be expected to increase in order to compensate for decreases in mitochondrial ATP production (Rafalowska *et al.*, 1996; Bessman and Carpenter, 1985). Our 2-D gel analysis identified several spots as CKB and one of these spots was shown to increase 1.5 fold as a result of low-Pb exposure in the VBS membrane fraction. Additionally, western blots were used to confirm the direction of change for CKB in the auditory brainstem. We found that total CKB is significantly increased by 20% in the VBS fraction, which agreed with the direction of change observed for CKB in the 2-D gels (Figure 13B). These results support the idea that Pb exposure leads to reduced levels of mitochondrial ATP synthesis in the auditory brainstem, since an increase in CKB could compensate for reduced ATP levels in auditory neurons where ATP consumption is particularly high.

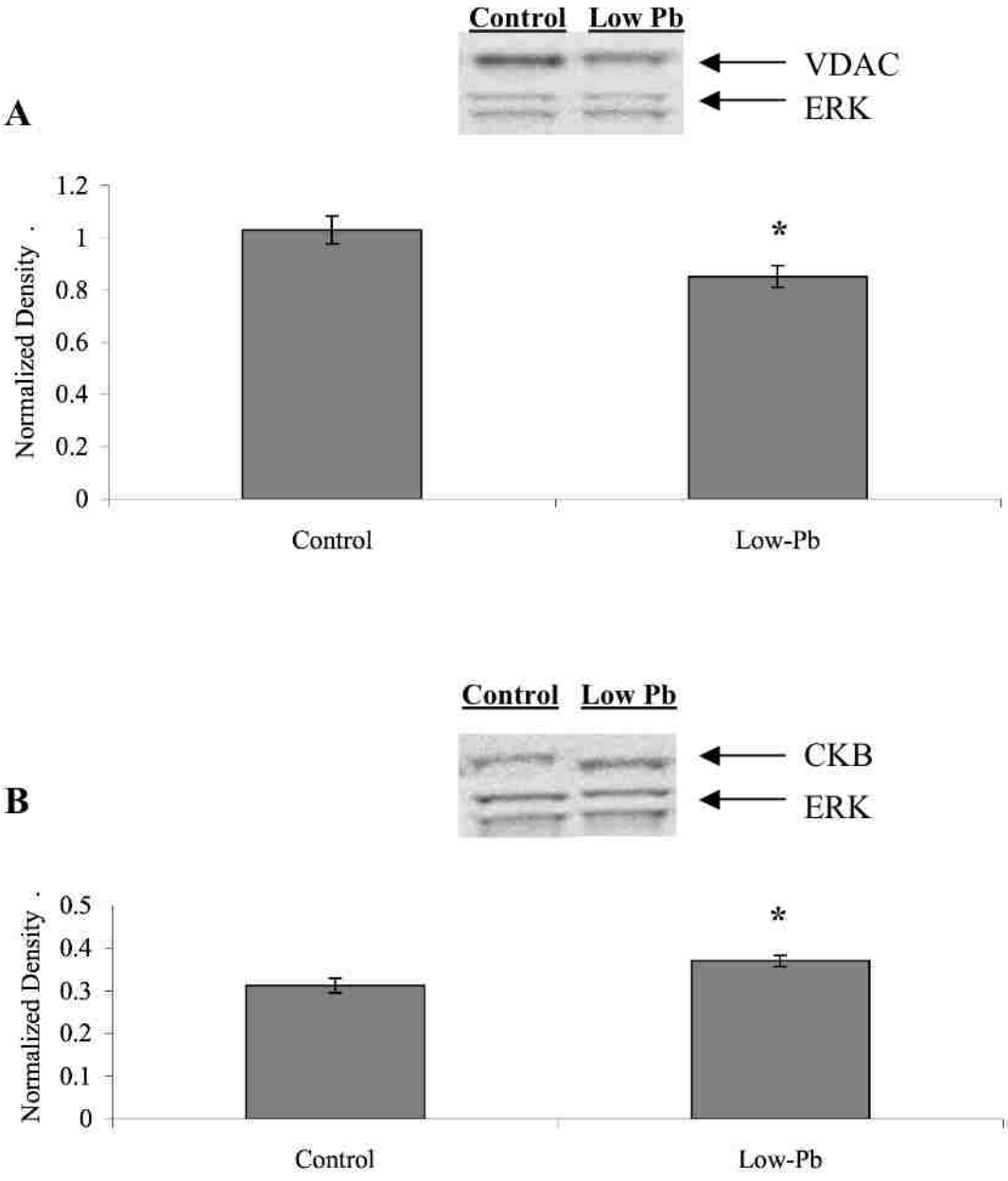

Figure 13: Western blots of VBS fractions from individual mice. Pb induced changes in protein expression obtained from the 2-D PAGE analysis of VDAC and CKBB in the VBS fraction. A) Total VDAC significantly decreases by 19% (n=4 mice). B) CKBB significantly increases by 19% (n=3 mice). Results are displayed as percentages of No Pb control. Data are expressed as the mean ±SEM. * t-test, $P<0.05$).

Brainstem auditory neurons show decreased VDAC expression

In order to determine whether the Pb induced decrease in VDAC expression occurs in auditory neurons, brainstem sections containing the superior olivary complex (SOC) were immunolabeled for VDAC and the expression quantified. Binaural auditory signals from the two ears converge in the SOC and sound localization within the brainstem occurs within this complex (Nothwang *et al.*, 2006). The SOC consists of three principal nuclei, the Medial Superior Olive (MSO), the Lateral Superior Olive (LSO), and the Medial Nucleus of the Trapezoid Body (MNTB). The MSO is associated with processing of interaural time differences, and the LSO and MNTB are associated with the processing of interaural intensity differences (Schneggenburger and Forsythe, 2006; Nothwang *et al.*, 2006).

VDAC expression is significantly decreased in neurons of the MNTB and LSO of very low and low-Pb mice as illustrated in Figures 14 and 15. We also examined VDAC immunostaining in neurons of the motor trigeminal nucleus. The motor trigeminal nuclei are non-auditory brainstem nuclei consisting almost entirely of motor neurons located within the VBS fraction. Interestingly, motor trigeminal neurons also demonstrate a significant decrease in VDAC expression (Figure 16), indicating that Pb induces a decrease in VDAC expression in VBS brainstem neurons. It is important to note that the very low Pb exposure also results in significant decreases in VDAC expression in brainstem neurons. The blood Pb levels of the very low Pb mice (8 μg/dL) is less than 10 μg/dL, the level at which cognitive impairments have been found in children. The fact that Pb exposure results in auditory temporal processing deficits suggests that because of their high energy

requirements, auditory brainstem neurons are particularly vulnerable to the Pb-induced decrease in VDAC.

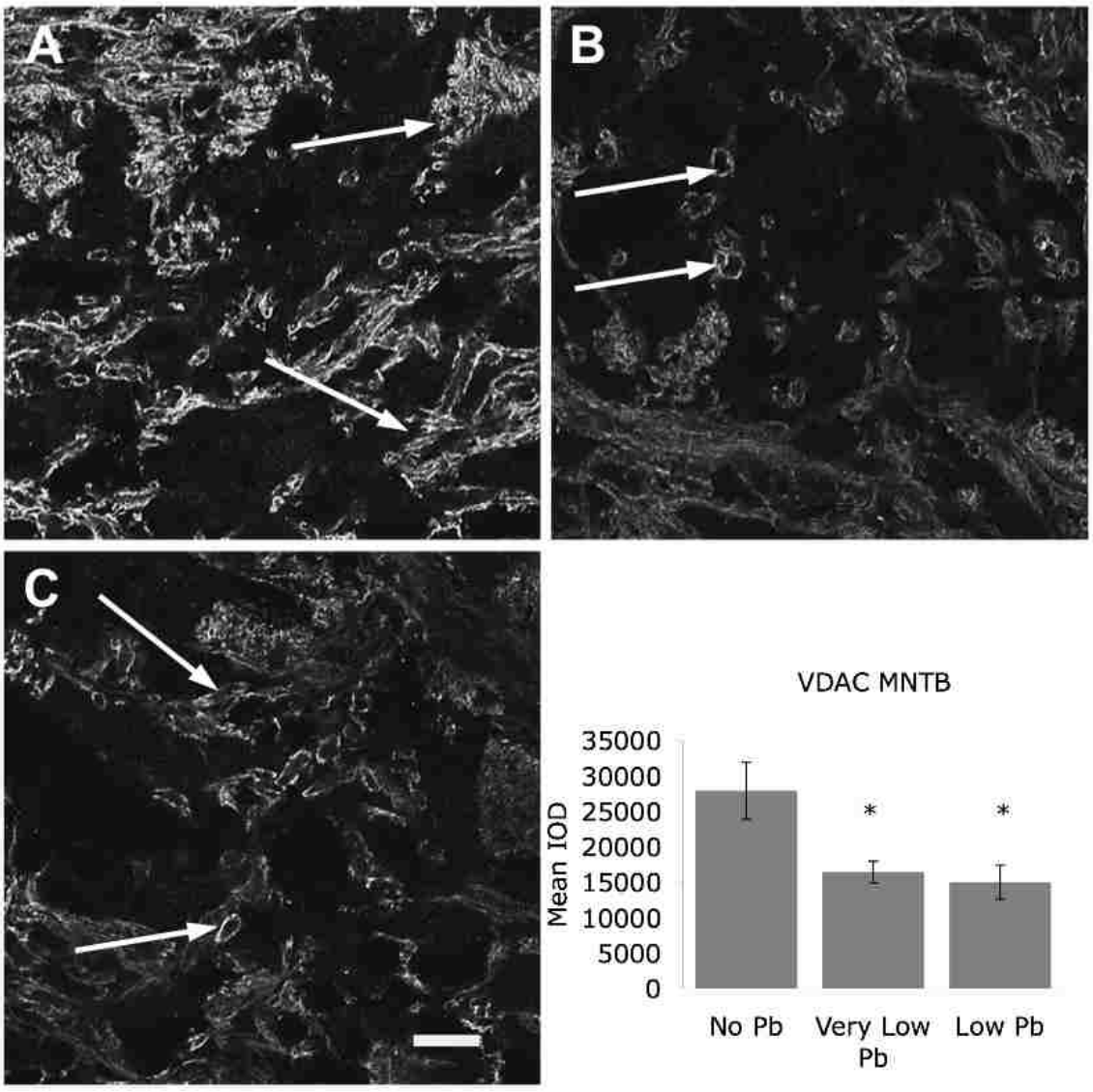

Figure 14: Pb treatment decreases VDAC expresssion in MNTB neurons. (A-C) Representative micrographs of immunofluorescent staining for VDAC in the MNTB in No (A), very Low (B) and Low (C) Pb mice reveal a decrease in immunoreactivity with Pb treatment (arrows). Quantification of staining for VDAC in the MNTB reveals that this decrease is statistically significant (D). Graphs illustrate mean + the standard error of the mean (SEM). (n=4 for No Pb, n = 3 for Low Pb group) *$p < 0.05$, One-way ANOVA with a Dunnett's post-hoc test. Bar = 10 μm for panels A-B.

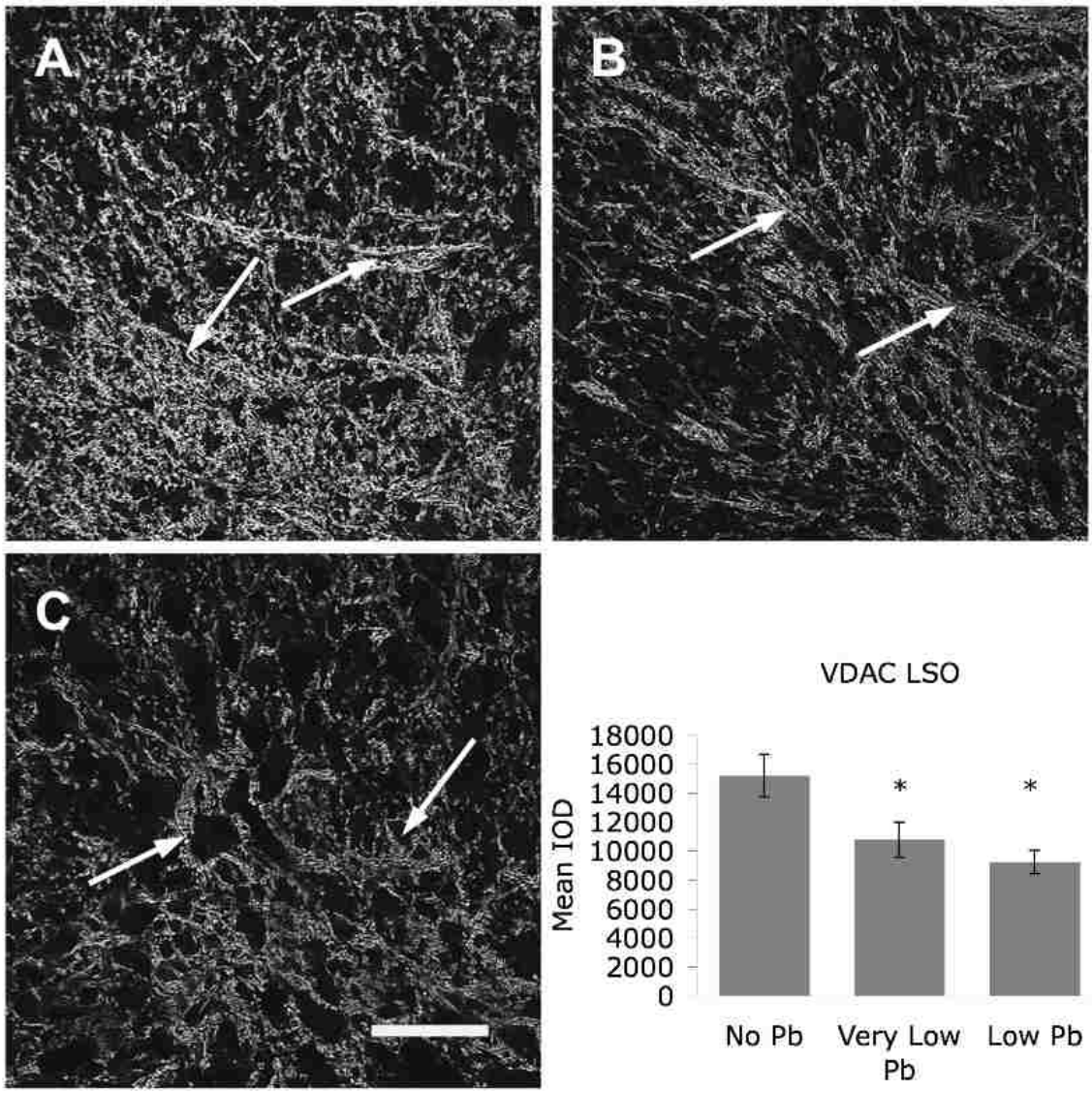

Figure 15: VDAC expression in LSO neurons decreases following Pb exposure. (A-C) Representative micrographs of immunofluorescent staining for VDAC in the LSO in No (A), very Low (B), and Low (C) Pb mice shows a decrease in immunoreactivity with Pb treatment (arrows). Quantification of staining for VDAC in the LSO demonstrates that this decrease is statistically significant (D). Graphs illustrate mean + the standard error of the mean (SEM). (n=4 for No Pb, n = 3 for Low Pb group) *$p < 0.05$, One-way ANOVA with a Dunnett's post-hoc test. Bar = 10 μm for panels A-B.

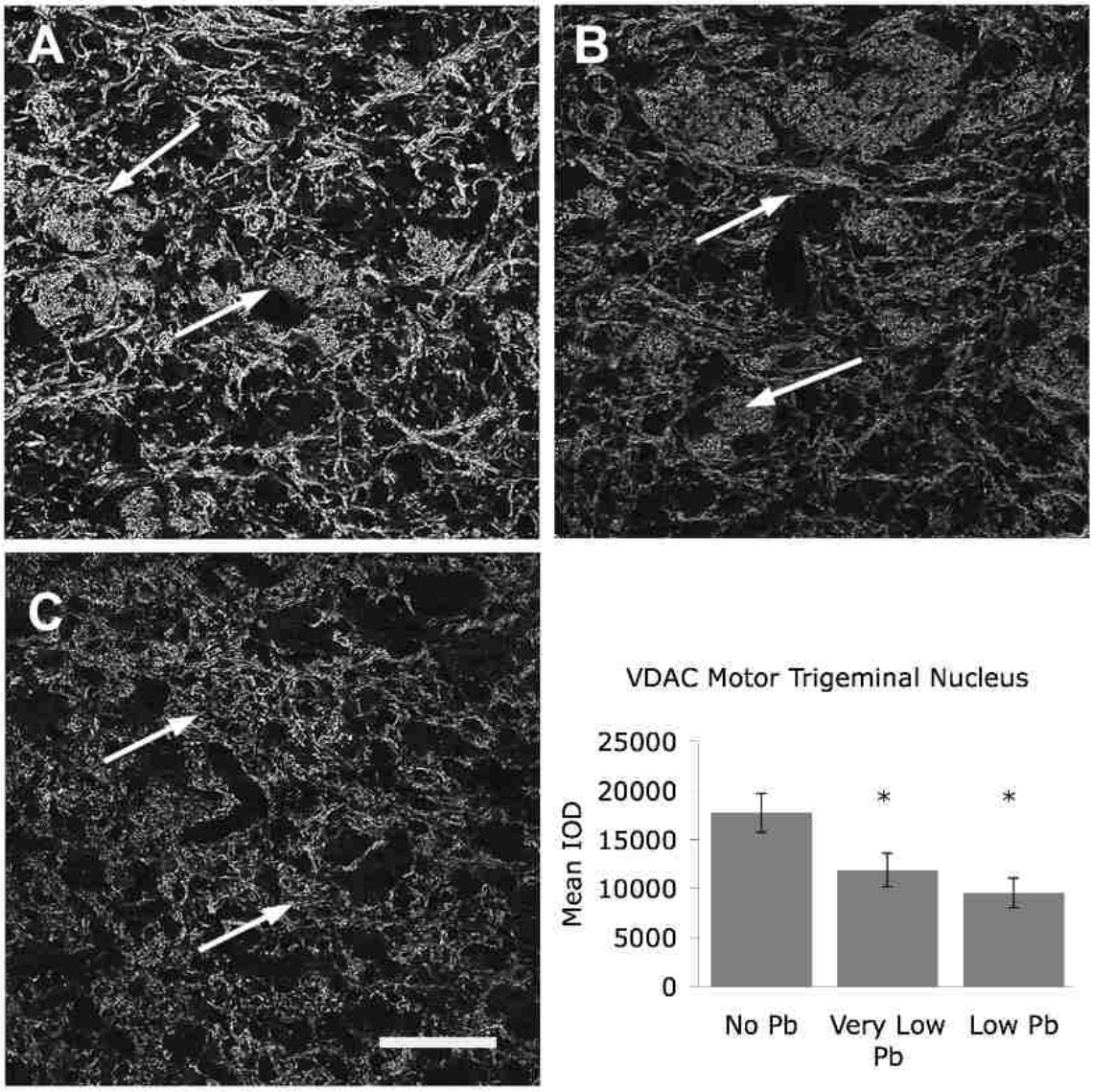

Figure 16: Pb exposure decreases VDAC expression in the motor trigeminal nucleus (Mo5). (A-C) Representative micrographs of immunofluorescent staining for VDAC in the Mo5 in No (A), very Low (B), and Low (C) Pb mice shows decreased immunoreactivity with Pb treatment (arrows). Quantification of staining for VDAC in the Mo5 demonstrates that this decrease is statistically significant (D). Graphs illustrate mean + the standard error of the mean (SEM). (n=4 for No Pb, n = 3 for Low Pb group) *$p < 0.05$, One-way ANOVA with a Dunnett's post-hoc test. Bar = 10 μm for panels A-B.

Discussion

The current study was undertaken to determine if developmental Pb exposure preferentially alters proteins involved in energy metabolism in central auditory neurons using a proteomic approach. Our proteomic analysis revealed that low-level Pb exposure results in the differential expression of several proteins involved in various cellular energy homeostasis and metabolizing pathways in the VBS, including the phosphocreatine circuit (VDAC 1 and CKB) (Wallimann *et al.*, 1992), glycolysis (Aldolase, ∝-enolase, and GAPDH), and oxidative phosphorylation (Ubiquinol-cytochrome c reductase core protein 1, isovaleryl coenzyme A dehydrogenase, NADH dehydrogenase (Ubiquinone) Fe-S protein 1).

Developmental Pb exposure results in decreased VDAC expression in the brainstem

One of the largest protein changes induced by developmental Pb exposure that we identified through the proteomic analysis is the large, 2.1 fold decrease in VDAC 1 expression. Western blot analysis of the VBS fraction confirmed this decrease in brainstem fractions and our immunohistochemistry analysis revealed that this decreased expression was specific to brainstem auditory neurons. The decrease in VDAC expression is particularly notable since the protein plays a central role in regulating cellular energy metabolism. VDAC is an ion channel involved in the regulation of mitochondrial physiology. VDAC is primarily located in the mitochondrial outer membrane and regulates mitochondrial permeability to anions, cations, creatine phosphate, Pi, ATP, ADP, and other metabolites into and out of the mitochondria (Shoshan-Barmatz and Israelson, 2005).

Disrupted VDAC function has been shown to compromise energy metabolism as well as Ca^{2+} homeostasis within the cell (Lemasters and Holmuhamedov, 2006; Shoshan-Barmatz and Gincel, 2003). In addition, it has been suggested that VDAC controls the production of cellular energy beginning with the control of the Ca^{2+} dependent enzymes pyruvate dehydrogenase and iso-citrate dehydrogenase in the mitochondria (Shoshan-Barmatz and Israelson, 2005). Downregulation of VDAC expression could result in the suppression of mitochondrial uptake of ADP and Pi for synthesis and release of ATP, thereby decreasing levels of cytosolic ATP, stimulating glycolysis and possibly the phosphocreatine circuit (Shoshan-Barmatz and Israelson, 2005; Lemasters and Holmuhamedov, 2006).

Pb exposure increases Creatine Kinase B expression in the brainstem

If decreased VDAC expression results in the decreased production of mitochondrial ATP in the auditory brainstem, then an observed increase in expression for other key energy metabolism proteins might be expected as a compensatory mechanism (Gellerich *et al.*, 2004). Numerous studies have described the ability of cellular systems to compensate for deficits in mitochondrial energy production by upregulating other energy producing processes which allows neurons to survive and function under adverse conditions (Hansson *et al.*, 2004; Silver *et al.*, 1997; Tachikawa *et al.*, 2004; Schurr and Rigor, 1998; Rafalowska *et al.*, 1996; Lutz and Nilsson, 1997). Although neuronal function is maintained to some extent, it is limited compared to normal physiological conditions (Lutz and Nilsson, 1997; Keating, 2008; Guo *et al.*, 2005; Verstreken *et al.*, 2005).

In order to explore this concept, we focused our attention on CKB, a key member of the

phosphocreatine circuit. The phosphocreatine circuit ensures that the ATP/ADP ratio remains high at subcellular regions with high energy requirements by acting as an intracellular energy buffering system, transporting ATP, via creatine/phosphocreatine, from where it is generated (mitochondria and glycolysis) to areas of high energy demand (Dzeja and Terzic, 2003; Wallimann *et al.*, 1992). Therefore, we expected CKB expression to increase in order to compensate for the decreased mitochondrial ATP synthesis that would result from decreased VDAC expression. As we predicted, Western blot analysis verified that VDAC expression decreased and CKB expression increased as a result of Pb exposure.

If Pb exposure does indeed lead to a reduction in cellular ATP levels due to a decrease in VDAC, then the expression levels of enzymes of the mitochondrial electron transport chain and glycolysis should be increased following low-level Pb exposure, and this turned out to be the case (Tables 1-3). Previous studies have shown a tight correlation between ATP levels and mitochondrial RNA synthesis (DasGupta *et al.*, 2001) and the increased expression of mitochondrial enzymes following Pb exposure may represent a response to decreases in cellular ATP. It is important to note that these increases in protein expression were observed in the VBS fraction only (containing auditory nuclei), but not the DBS fraction. In addition to Pb-induced expression increases in mitochondrial enzymes, several key glycolytic enzymes also show increased expression with low Pb exposure within the VBS but not the DBS fraction (Tables 1-3), suggesting that upregulation of these proteins is not a global effect of Pb and appears to be specific for the auditory areas of the brainstem. The increased expression of glycolytic enzymes may represent an increase in glycolysis in an attempt to maintain the high ATP levels required by auditory neurons.

Future studies will determine if Pb exposure results in increased glycolytic activity, and if this upregulation occurs in response to a decrease in cellular ATP levels.

VDAC expression decreases in brainstem auditory neurons

Immunohistochemistry confirmed that VDAC expression decreased by approximately 45% in brainstem auditory neurons following Pb exposure. These findings suggest that VDAC may represent a potential target for Pb in this area of the brain. Although further studies are needed to elucidate the mechanism by which Pb decreases VDAC expression, the decreased expression does not appear to be a result of a general stress response because our proteomic analysis demonstrated that VDAC did not decrease in the DBS fraction. However, within the VBS fraction, VDAC expression decreased in both the LSO and MNTB (auditory) and the motor trigeminal nucleus (non-auditory). The motor trigeminal nucleus controls the masseter reflex, and while this reflex has been shown to be altered by trichloroethene in printing workers (Ruijten *et al.*, 1991), a thorough search of the literature did not reveal any studies documenting an effect on the masseter reflex following Pb exposure. Thus, even though Pb exposure resulted in decreased VDAC expression in auditory and trigeminal motor neurons, the auditory neurons appear to be more vulnerable to the effects of the Pb-induced decrease in VDAC since Pb exposure produces auditory temporal processing deficits and does not appear to produce any changes in the masseter reflex. Central auditory neurons may be more vulnerable to the effects of Pb because of their high energy demand and even modest disruptions in energy production could alter the normal function of auditory neurons and disrupt the normal processing of auditory

information.

Pb exposure and energy metabolism

Disrupted energy metabolism has been proposed as a possible cause of behavioral abnormalities and brain dysfunction in animals exposed to Pb (Sterling *et al.*, 1982; Jonas, 2004). While the current study is the first to demonstrate that Pb exposure results in the decreased expression of VDAC, several studies have found that low levels of Pb can interfere with mitochondrial energy metabolism, resulting in decreased levels of ATP (Verity, 1990; Holtzman *et al.*, 1978; Gmerek *et al.*, 1981). Rafalowska et al., found that exposing rat brain synaptosomes to low levels of Pb resulted in decreased cytosolic ATP levels, increased creatine kinase activity, and increased concentrations of creatine phosphate, suggesting that the creatine phosphate system is is upregulated as a compensatory mechanism for decreased ATP levels (Rafalowska *et al.*, 1996). Because the synthesis and movements of ATP within cells of the CNS is a highly regulated and organized process, even small interruptions in cellular ATP producing processes could compromise neuronal activity in the CNS and interfere with normal brain function (Ames, 2000). This is particularly true for the auditory system, where auditory neurons have very high rates of activity.

Summary and Conclusions

The current study confirms that developmental Pb exposure results in decreased expression of proteins involved in energy metabolism in auditory areas of the brainstem.

The decrease in VDAC expression observed in auditory neurons is intriguing, and the possibility that the mitochondrial voltage dependent anion channel is a target for Pb is exciting, because VDAC plays such an important role in energy metabolism. The physiological consequences resulting from disrupted energy metabolism may be decidedly more pronounced in the auditory system, since tightly regulated and efficient energy production is crucial for auditory neurons to correctly perform the complicated processes involved in auditory processing. Therefore, decreased VDAC expression may severely compromise mitochondrial function in these neurons, disrupting normal rates of energy production and producing impairments in the processing of auditory information.

This study also provides insight into the mechanisms of Pb neurotoxicity by providing comparative data on the effects of low-level Pb exposure between the auditory and non-auditory brainstem. Changes in protein expression are only one facet of the multiple mechanisms by which Pb may alter the structure and function of auditory neurons, and further studies are needed to fully elucidate the cellular effects of Pb on central auditory processing.

General Proteomic Discussion

One of the techniques used in this study to confirm our hypothesis that Pb exposure impairs energy metabolism in auditory neurons was a proteomic approach. Specifically, we identified a large number of protein expression changes specific to the auditory brainstem following chronic low-level Pb exposure during development. Full characterization of all the proteins identified in the proteomic analysis is beyond the scope of this study, however many of the proteins that show expression changes following chronic low-level Pb exposure could affect the flow of auditory information through the CNS and warrant further discussion. The majority of the proteins that changed expression following Pb exposure were specific to the VBS fraction and did not change within the DBS fraction, and therefore were specific to the auditory brainstem region. These proteins were organized into four main categories- proteins involved in energy metabolism, molecular chaperones, synaptic proteins, and cytoskeletal proteins. The majority of proteins that are upregulated following Pb exposure, are proteins involved in energy metabolism, and the majority of down-regulated proteins are those involved in synaptic structure and function. Proteins involved in cellular energy metabolism were discussed previously therefore we will limit the discussion to the remaining protein groups in this section.

Chaperones

Molecular chaperones assist a new protein to fold into a full functional conformation, then helps with the delivery of that protein to its site of action within the cell. Molecular chaperones also function to combat oxidative stress, apoptosis, and to facilitate synaptic

activity (Ohtsuka and Suzuki, 2000). Therefore, alterations in normal molecular chaperone protein levels would be expected to have consequences on normal neuronal function (Miller *et al.*, 2003). We found that chronic low-level Pb exposure results in the differential expression of a variety of molecular chaperones, i.e. HSP8, HSP60, HSP84, and GRP 58. Heat shock proteins are normally transcribed at low levels in the absence of stress, but expression is increased in response to stressors, such as exposure to heavy metals or heat stress (Ohtsuka and Suzuki, 2000). We found increased expression of HSP60 in the VBS following Pb exposure, perhaps in response to the mitochondrial dysfunction induced by Pb as described previously. HSP60, a 60 kDa heat shock protein, is located in both the mitochondria and cytosol and this protein is thought to participate in maintaining normal mitochondrial function during stress (Chen *et al.*, 2006; Shan *et al.*, 2003). We also observed a decrease in protein expression of HSP84 (HSP90), a protein thought to play a role in signal transduction through its interaction with various kinases (Sreedhar *et al.*, 2004) and its regulation of Rab3A recycling following vesicle fusion (Sakisaka *et al.*, 2002; Pfeffer *et al.*, 1995). Interestingly, HSP90 plays a role in Ca^{2+} mediated exocytosis by interacting with GDI, a protein that also decreased following low-level Pb exposure in our studies (Sakisaka *et al.*, 2002; Pfeffer *et al.*, 1995). In addition, HSP90 is thought to play a role in regulating neurotransmitter release via a co-chaperone complex, present in presynaptic neurotransmitter vesicles, composed of Hsc70, HSP90, and cysteine string protein (Gerges *et al.*, 2004). The expression of Hsc70 (also known at HSP8) is altered by Pb in our studies, as was GRP58. Taken together, our proteomic analysis suggests that Pb may alter vesicle recycling and synaptic release in central auditory areas through its effect

on molecular chaperones and heat shock proteins.

Synaptic Proteins

The expression of two subunits of H^+-transporting vacuolar-ATPase (V-ATPase A and V-ATPase E) increased following low-level Pb exposure. V-ATPase is an ATP driven pump that transports H^+ across diverse biological membranes, including synaptic vesicles, creating a proton gradient that can be used to drive a variety of transport systems (Beyenbach and Wieczorek, 2006). Synaptic vesicles contain V-type H^+ ATPases and are located adjacent to neurotransmitter transporters, which use the H^+- gradient to transport neurotransmitters into synaptic vesicles (Beyenbach and Wieczorek, 2006). It is not clear what role this increased expression of V-ATPase has on the Pb exposed brain, but increased protein levels could impact the loading of neurotransmitter into synaptic vesicles.

We also found that low Pb exposure changed the expression of several proteins involved in synaptic release including 14-3-3 zeta protein, GDI, and guanine nucleotide binding protein G(o) subunit alpha 1 within the VBS. These proteins modulate synaptic function and release and could affect neurotransmitter release within auditory neurons. Finally, the expression of glutamate dehydrogenase and glutamine synthetase, increased specifically in the VBS following Pb exposure. These proteins participate in glutamate-glutamine cycling between astrocytes and neurons and are important for the proper functioning of the superior olivary complex (Nothwang *et al.*, 2006). Interestingly, we have found no change in expression of the vesicular glutamate transporter within the SOC (unpublished data) and further studies are needed to define the effect of increased expression of these glutaminergic

enzymes on brainstem auditory neurons.

Cytoskeletal proteins

The cytoskeleton is a dynamic system of protein filaments that provides structural integrity to the cell and regulates many biological process including, cell division, cell motility, intracellular trafficking of organelles, formation of synapses, and axon and dendrite formation. Three main types of protein filaments make up the cytoskeletal network: actins, microtubules, and intermediate filaments (i.e. neurofilament) (Arimura *et al.*, 2004). Previous immunocytochemical studies in our laboratory have found that Pb exposure increases neurofilament phosphorylation in brainstem auditory axons (Jones *et al.*, 2008). The present study confirms our previous studies. The majority of the protein spots for neurofilament increased in the VBS following Pb exposure, and were located in the lower pI range of the gel confirming a posttranslational modification such as increased phosphorylation. Several other cytoskeletal proteins changed expression following low Pb exposure within the VBS fraction including α-tubulin (decreased in VBS fraction and increased in DBS fraction) and β-actin (increased in the VBS fraction and decreased in the DBS fraction). In addition, we also identified several cytoskeletal associated proteins that changed expression following low level Pb exposure. For example, cyclic nucleotide phosphodiesterase was decreased following low-level Pb exposure. This protein has been shown to be associated with tubulin and is thought to play a role in promoting microtubule assembly (Bertoni and Sprenkle, 1988).

We also found increased expression of dihydropyrimidinase-related protein 2 (DRP 2).

DRP-2, also known as collapsing response mediator protein 2, is involved in neuronal polarity and axon specification and elongation (Kimura *et al.*, 2005). It has been suggested that DRP-2 acts as an adaptor protein linking microtubules to kinesin-1 motors (Bifulco *et al.*, 2002). All of these cytoskeletal changes could modify axonal structure, thereby altering the conduction of action potentials along auditory axons. Disrupted cytoskeletal organization, could potentially affect the structure of axons and influence the conduction of action potentials down the axon (Dillon and Goda, 2005).

Overall Summary and Conclusions

In this study, we investigated the effects of Pb exposure on the expression of VDAC and found that low-level Pb exposure resulted in the decreased expression of VDAC both in vitro and in vivo. For our in vitro model, we used PC-12 and SH-SY5Y cells since they differentiate to resemble primary neuronal cells. We found that VDAC expression levels were significantly decreased 48 h after exposure to Pb in both cell lines. In contrast, exposure to 24 h of hypoxia failed to produce a decrease in VDAC, suggesting that decreased VDAC expression is not a general cellular stress response, but is a specific result of Pb exposure. This decreased VDAC expression was also correlated with a corresponding decrease in cellular ATP levels. Real-time RT-PCR demonstrated a significant decrease in mRNA levels for the VDAC-1 isoform, indicating that Pb reduces transcription of VDAC-1. These results demonstrate that exposure to low-levels of Pb reduce VDAC transcription and expression and is associated with reduced cellular ATP levels.

The results from our real time RT-PCR analysis suggest that Pb is interfering with gene expression for VDAC-1 and possibly VDAC-2. Although it is not known how Pb may be influencing VDAC gene expression, Pb has been shown to interfere with gene expression by competing for Zn^{2+}-binding sites of transcription factors, such as zinc-finger proteins (Zawia, 2003; Basha *et al.*, 2003). The zinc finger transcription factor Sp1 may represent a potential target, since numerous studies have reported that Pb exposure interferes with the DNA binding both in vivo and in vitro (Crumpton *et al.*, 2001; Zawia *et al.*, 1998; Atkins *et al.*, 2003; Basha *et al.*, 2003; Hanas *et al.*, 1999). In addition, all three VDAC isoforms

contain Sp1 binding sites (Sampson *et al.*, 1997), although a relationship between Sp1 DNA binding and VDAC gene expression remains to be established. Future experiments will be needed in order to determine whether Pb exposure decreases VDAC transcription by altering Sp1 binding. Finally, a study using VDAC knock-out mice found that deficiencies in VDAC-1 and VDAC-2 resulted in reductions of mitochondrial respiratory capacity (Wu *et al.*, 1999), which demonstrates the importance of these proteins in maintaining cellular energy levels. Therefore, decreases in VDAC expression may be particularly detrimental to cells with high-energy requirements, like those found in the auditory brainstem.

Maintenance of high rates of neurotransmission is extremely important in order to maintain the pattern and timing of the incoming auditory signals and this high rate of neurotransmission requires high levels of energy production. It has been suggested that VDAC controls the production of cellular energy beginning with the control of the Ca^{2+} dependent enzymes pyruvate dehydrogenase and iso-citrate dehydrogenase in the mitochondria (Shoshan-Barmatz and Israelson, 2005). Impaired VDAC function or downregulation of VDAC expression would suppress mitochondrial uptake of ADP and Pi for synthesis and release of ATP, thereby decreasing levels of cytosolic ATP, and stimulating glycolysis and possibly the phosphocreatine circuit (Shoshan-Barmatz and Israelson, 2005; Lemasters and Holmuhamedov, 2006). Our proteomic analysis demonstrated that low-levels of Pb exposure resulted in the differential expression of several proteins involved in various cellular energy homeostasis and metabolizing pathways in the VBS, including glycolysis (Aldolase, ∝-enolase, and GAPDH), oxidative

phosphorylation (Ubiquinol-cytochrome c reductase core protein 1, Isovaleryl coenzyme A dehydrogenase, NADH dehydrogenase (Ubiquinone) Fe-S protein 1), and the phosphocreatine circuit (CKB and VDAC-1) (Wallimann *et al.*, 1992). The expression level for the majority of these proteins is increased, with the exception of VDAC-1 and one spot identified as Aldolase C in the cytosolic fraction, where expression levels decreased. Upregulation of these proteins would be expected if Pb decreases VDAC and inhibits mitochondrial ATP synthesis (Hansson *et al.*, 2004).

The downregulation of VDAC-1 in-vivo is particularly notable since it agrees with our in-vitro data and may represent a potential target for Pb in-vivo. These results demonstrate an upregulation of other cellular energy producing systems in response to decreases in VDAC and supports our hypothesis that Pb exposure is disrupting cellular energy metabolism in the auditory brainstem. Immunohistochemistry confirms that Pb exposure results in decreased expression of VDAC in auditory nuclei. Further, very low levels of Pb induce a similar decrease in VDAC expression in auditory neurons, confirming that low-level Pb exposure has a significant impact on auditory neurons. Thus, the Pb-induced decrease in VDAC could have a major effect on the function of auditory neurons, contributing to the deficits in auditory temporal processing that are observed with Pb exposure.

Immunohistochemistry confirmed that VDAC expression in brainstem auditory neurons following Pb exposure and suggest that VDAC may represent a potential target for Pb in this area of the brain. VDAC expression decreased in both the LSO and MNTB (auditory) as well as the motor trigeminal nucleus (non-auditory). Even though Pb exposure resulted

in decreased VDAC expression in auditory and trigeminal motor neurons, the auditory neurons appear to be more vulnerable to the effects of the Pb-induced decrease in VDAC. It is important to note that Pb exposure produces auditory temporal processing deficits, whereas no effect on the masseter reflex (mediated by the motor trigeminal nucleus that also showed decreased VDAC expression) following Pb exposure has been reported in the literature. Further studies will be needed to fully define the mechanism by which Pb decreases VDAC expression, but the decreased expression does not appear to be a general global response because our proteomic analysis demonstrated that VDAC did not decrease in the DBS fraction. Central auditory neurons may be more vulnerable to the effects of Pb because of their high energy demand and even modest disruptions in energy production could alter the normal function of auditory neurons and disrupt the normal processing of auditory information.

While the current study identified many proteins that changed expression following low-level Pb exposure, there is still much work to be done in determining which of these proteins are crucial for normal central auditory function. A recent study comparing the gene expression profile in the SOC with that of the striatum and hippocampus identified genes that were upregulated in the SOC and thought to be important for the specific function of auditory neurons (Nothwang *et al.*, 2006). Interestingly, we found that chronic low-level Pb exposure resulted in the differential expression of several of these proteins, including alpha tubulin, HSP8, aldolase C, glutamine synthetase 1, neurofilament 3 (medium), and glutamate dehydrogenase 1. Further studies are needed to elucidate the role of these proteins in central auditory neurons. We do know from our in vitro and in vivo

studies that Pb can interfere with cellular energy metabolism. Pb does not appear to be acting as a general cellular stressor, since hypoxia failed to produce a decrease in VDAC expression and many of the protein expression changes that we observed in vivo were restricted to the VBS region. Therefore the high rate of activity of auditory neurons appears to make them vulnerable to the effects of Pb exposure. The current study provides insight into the mechanisms of Pb neurotoxicity by providing some comparative data on the effects of low-level Pb exposure between the auditory and non-auditory brainstem. Changes in protein expression, including VDAC, are only one facet of the multiple mechanisms by which Pb affects auditory neurons, and further studies are needed to fully elucidate the cellular effects of Pb on central auditory processing.

References

Abu-Hamad, S., Sivan, S., and Shoshan-Barmatz, V. (2006). The expression level of the voltage-dependent anion channel controls life and death of the cell. *Proc Natl Acad Sci U S A* **103**, 5787-5792.

Aebersold, R., and Goodlett, D. R. (2001). Mass spectrometry in proteomics. *Chem Rev* **101**, 269-295.

Ames, A., 3rd (2000). CNS energy metabolism as related to function. *Brain Res Brain Res Rev* **34**, 42-68.

Arimura, N., Menager, C., Fukata, Y., and Kaibuchi, K. (2004). Role of CRMP-2 in neuronal polarity. *J Neurobiol* **58**, 34-47.

Atkins, D. S., Basha, M. R., and Zawia, N. H. (2003). Intracellular signaling pathways involved in mediating the effects of lead on the transcription factor Sp1. *Int J Dev Neurosci* **21**, 235-244.

Baines, C. P., Kaiser, R. A., Sheiko, T., Craigen, W. J., and Molkentin, J. D. (2007). Voltage-dependent anion channels are dispensable for mitochondrial-dependent cell death. *Nat Cell Biol* **9**, 550-555.

Basha, M. R., Wei, W., Brydie, M., Razmiafshari, M., and Zawia, N. H. (2003). Lead-induced developmental perturbations in hippocampal Sp1 DNA-binding are prevented by zinc supplementation: in vivo evidence for Pb and Zn competition. *Int J Dev Neurosci* **21**, 1-12.

Bellinger, D., and Dietrich, K. N. (1994). Low-level lead exposure and cognitive function in children. *Pediatr Ann* **23**, 600-605.

Bellinger, D. C. (2004). Lead. *Pediatrics* **113**, 1016-1022.

Bellinger, D. C. (2008). Very low lead exposures and children's neurodevelopment. *Curr Opin Pediatr* **20**, 172-177.

Bertoni, J. M., and Sprenkle, P. M. (1988). Lead acutely reduces glucose utilization in the rat brain especially in higher auditory centers. *Neurotoxicology* **9**, 235-242.

Bessman, S. P., and Carpenter, C. L. (1985). The creatine-creatine phosphate energy shuttle. *Annu Rev Biochem* **54**, 831-862.

Beyenbach, K. W., and Wieczorek, H. (2006). The V-type H+ ATPase: molecular

structure and function, physiological roles and regulation. *J Exp Biol* **209**, 577-589.

Bifulco, M., Laezza, C., Stingo, S., and Wolff, J. (2002). 2',3'-Cyclic nucleotide 3'-phosphodiesterase: a membrane-bound, microtubule-associated protein and membrane anchor for tubulin. *Proc Natl Acad Sci U S A* **99**, 1807-1812.

Blachly-Dyson, E., and Forte, M. (2001). VDAC channels. *IUBMB Life* **52**, 113-118.

Braun, J. M., Kahn, R. S., Froehlich, T., Auinger, P., and Lanphear, B. P. (2006). Exposures to environmental toxicants and attention deficit hyperactivity disorder in U.S. children. *Environ Health Perspect* **114**, 1904-1909.

Breier, J. I., Fletcher, J. M., Foorman, B. R., Klaas, P., and Gray, L. C. (2003). Auditory temporal processing in children with specific reading disability with and without attention deficit/hyperactivity disorder. *J Speech Lang Hear Res* **46**, 31-42.

Canfield, R. L., Henderson, C. R., Jr., Cory-Slechta, D. A., Cox, C., Jusko, T. A., and Lanphear, B. P. (2003). Intellectual impairment in children with blood lead concentrations below 10 microg per deciliter. *N Engl J Med* **348**, 1517-1526.

Chen, H. B., Chan, Y. T., Hung, A. C., Tsai, Y. C., and Sun, S. H. (2006). Elucidation of ATP-stimulated stress protein expression of RBA-2 type-2 astrocytes: ATP potentiate HSP60 and Cu/Zn SOD expression and stimulates pI shift of peroxiredoxin II. *J Cell Biochem* **97**, 314-326.

Chiodo, L. M., Jacobson, S. W., and Jacobson, J. L. (2004). Neurodevelopmental effects of postnatal lead exposure at very low levels. *Neurotoxicol Teratol* **26**, 359-371.

Cordova, F. M., Rodrigues, A. L., Giacomelli, M. B., Oliveira, C. S., Posser, T., Dunkley, P. R., and Leal, R. B. (2004). Lead stimulates ERK1/2 and p38MAPK phosphorylation in the hippocampus of immature rats. *Brain Res* **998**, 65-72.

Costa, L. G., Aschner, M., Vitalone, A., Syversen, T., and Soldin, O. P. (2004). Developmental neuropathology of environmental agents. *Annu Rev Pharmacol Toxicol* **44**, 87-110.

Crumpton, T., Atkins, D. S., Zawia, N. H., and Barone, S., Jr. (2001). Lead exposure in pheochromocytoma (PC12) cells alters neural differentiation and Sp1 DNA-binding. *Neurotoxicology* **22**, 49-62.

DasGupta, S. F., Rapoport, S. I., Gerschenson, M., Murphy, E., Fiskum, G., Russell, S. J., and Chandrasekaran, K. (2001). ATP synthesis is coupled to rat liver mitochondrial RNA synthesis. *Mol Cell Biochem* **221**, 3-10.

De Pinto, V., Tommasino, M., Benz, R., and Palmieri, F. (1985). The 35 kDa DCCD-binding protein from pig heart mitochondria is the mitochondrial porin. *Biochim Biophys Acta* **813**, 230-242.

Dillon, C., and Goda, Y. (2005). The actin cytoskeleton: integrating form and function at the synapse. *Annu Rev Neurosci* **28**, 25-55.

Drabik, A., Bierczynska-Krzysik, A., Bodzon-Kulakowska, A., Suder, P., Kotlinska, J., and Silberring, J. (2007). Proteomics in neurosciences. *Mass Spectrom Rev* **26**, 432-450.

Dzeja, P. P., and Terzic, A. (2003). Phosphotransfer networks and cellular energetics. *J Exp Biol* **206**, 2039-2047.

Finkelstein, Y., Markowitz, M. E., and Rosen, J. F. (1998). Low-level lead-induced neurotoxicity in children: an update on central nervous system effects. *Brain Res Brain Res Rev* **27**, 168-176.

Freeman, W. M., and Hemby, S. E. (2004). Proteomics for protein expression profiling in neuroscience. *Neurochem Res* **29**, 1065-1081.

Frisina, R. D. (2001). Subcortical neural coding mechanisms for auditory temporal processing. *Hear Res* **158**, 1-27.

Garza, A., Vega, R., and Soto, E. (2006). Cellular mechanisms of lead neurotoxicity. *Med Sci Monit* **12**, RA57-65.

Gellerich, F. N., Trumbeckaite, S., Muller, T., Deschauer, M., Chen, Y., Gizatullina, Z., and Zierz, S. (2004). Energetic depression caused by mitochondrial dysfunction. *Mol Cell Biochem* **256-257**, 391-405.

Gerges, N. Z., Tran, I. C., Backos, D. S., Harrell, J. M., Chinkers, M., Pratt, W. B., and Esteban, J. A. (2004). Independent functions of hsp90 in neurotransmitter release and in the continuous synaptic cycling of AMPA receptors. *J Neurosci* **24**, 4758-4766.

Gidlow, D. A. (2004). Lead toxicity. *Occup Med (Lond)* **54**, 76-81.

Gilbert, S. G., and Weiss, B. (2006). A rationale for lowering the blood lead action level from 10 to 2 microg/dL. *Neurotoxicology* **27**, 693-701.

Gincel, D., Zaid, H., and Shoshan-Barmatz, V. (2001). Calcium binding and translocation

by the voltage-dependent anion channel: a possible regulatory mechanism in mitochondrial function. *Biochem J* **358**, 147-155.

Gmerek, D. E., McCafferty, M. R., O'Neill, K. J., Melamed, B. R., and O'Neill, J. J. (1981). Effect of inorganic lead on rat brain mitochondrial respiration and energy production. *J Neurochem* **36**, 1109-1113.

Goldstein, G. W. (1992). Neurologic concepts of lead poisoning in children. *Pediatr Ann* **21**, 384-388.

Gong, P., Ogra, Y., and Koizumi, S. (2000). Inhibitory effects of heavy metals on transcription factor Sp1. *Ind Health* **38**, 224-227.

Grant, S. G., and Blackstock, W. P. (2001). Proteomics in neuroscience: from protein to network. *J Neurosci* **21**, 8315-8318.

Gray, L. a. H., A. (1999). Early lead exposure affects auditory temporal processing in chicks. *Journal of Environmental Medicine* **1**, 87-93.

Greene, L. A., and Tischler, A. S. (1976). Establishment of a noradrenergic clonal line of rat adrenal pheochromocytoma cells which respond to nerve growth factor. *Proc Natl Acad Sci U S A* **73**, 2424-2428.

Guo, X., Macleod, G. T., Wellington, A., Hu, F., Panchumarthi, S., Schoenfield, M., Marin, L., Charlton, M. P., Atwood, H. L., and Zinsmaier, K. E. (2005). The GTPase dMiro is required for axonal transport of mitochondria to Drosophila synapses. *Neuron* **47**, 379-393.

Hanas, J. S., Rodgers, J. S., Bantle, J. A., and Cheng, Y. G. (1999). Lead inhibition of DNA-binding mechanism of Cys(2)His(2) zinc finger proteins. *Mol Pharmacol* **56**, 982-988.

Hansson, A., Hance, N., Dufour, E., Rantanen, A., Hultenby, K., Clayton, D. A., Wibom, R., and Larsson, N. G. (2004). A switch in metabolism precedes increased mitochondrial biogenesis in respiratory chain-deficient mouse hearts. *Proc Natl Acad Sci U S A* **101**, 3136-3141.

Holdstein, Y., Pratt, H., Goldsher, M., Rosen, G., Shenhav, R., Linn, S., Mor, A., and Barkai, A. (1986). Auditory brainstem evoked potentials in asymptomatic lead-exposed subjects. *J Laryngol Otol* **100**, 1031-1036.

Holtzman, D., Shen Hsu, J., and Mortell, P. (1978). In vitro effects of inorganic lead on isolated rat brain mitochondrial respiration. *Neurochem Res* **3**, 195-206.

Israelson, A., Abu-Hamad, S., Zaid, H., Nahon, E., and Shoshan-Barmatz, V. (2007). Localization of the voltage-dependent anion channel-1 Ca2+-binding sites. *Cell Calcium* **41**, 235-244.

Johnson, K. L., Nicol, T. G., Zecker, S. G., and Kraus, N. (2007). Auditory brainstem correlates of perceptual timing deficits. *J Cogn Neurosci* **19**, 376-385.

Johnson, M. D., Yu, L. R., Conrads, T. P., Kinoshita, Y., Uo, T., McBee, J. K., Veenstra, T. D., and Morrison, R. S. (2005). The proteomics of neurodegeneration. *Am J Pharmacogenomics* **5**, 259-270.

Jonas, E. (2004). Regulation of synaptic transmission by mitochondrial ion channels. *J Bioenerg Biomembr* **36**, 357-361.

Jones, L. G., Prins, J., Park, S., Walton, J. P., Luebke, A. E., and Lurie, D. I. (2008). Lead exposure during development results in increased neurofilament phosphorylation, neuritic beading, and temporal processing deficits within the murine auditory brainstem. *J Comp Neurol* **506**, 1003-1017.

Kann, O., and Kovacs, R. (2007). Mitochondria and neuronal activity. *Am J Physiol Cell Physiol* **292**, C641-657.

Keating, D. J. (2008). Mitochondrial dysfunction, oxidative stress, regulation of exocytosis and their relevance to neurodegenerative diseases. *J Neurochem* **104**, 298-305.

Kim, S. I., Voshol, H., van Oostrum, J., Hastings, T. G., Cascio, M., and Glucksman, M. J. (2004). Neuroproteomics: expression profiling of the brain's proteomes in health and disease. *Neurochem Res* **29**, 1317-1331.

Kimura, T., Watanabe, H., Iwamatsu, A., and Kaibuchi, K. (2005). Tubulin and CRMP-2 complex is transported via Kinesin-1. *J Neurochem* **93**, 1371-1382.

Lanphear, B. P., Dietrich, K., Auinger, P., and Cox, C. (2000). Cognitive deficits associated with blood lead concentrations <10 microg/dL in US children and adolescents. *Public Health Rep* **115**, 521-529.

Lasley, S. M., and Gilbert, M. E. (2000). Glutamatergic components underlying lead-induced impairments in hippocampal synaptic plasticity. *Neurotoxicology* **21**, 1057-1068.

Leal, R. B., Cordova, F. M., Herd, L., Bobrovskaya, L., and Dunkley, P. R. (2002). Lead-

stimulated p38MAPK-dependent Hsp27 phosphorylation. *Toxicol Appl Pharmacol* **178**, 44-51.

Lemasters, J. J., and Holmuhamedov, E. (2006). Voltage-dependent anion channel (VDAC) as mitochondrial governator--thinking outside the box. *Biochim Biophys Acta* **1762**, 181-190.

Lidsky, T. I., and Schneider, J. S. (2003). Lead neurotoxicity in children: basic mechanisms and clinical correlates. *Brain* **126**, 5-19.

Livak, K. J., and Schmittgen, T. D. (2001). Analysis of relative gene expression data using real-time quantitative PCR and the 2(-Delta Delta C(T)) Method. *Methods* **25**, 402-408.

Lurie, D. I., Brooks, D. M., and Gray, L. C. (2006). The effect of lead on the avian auditory brainstem. *Neurotoxicology* **27**, 108-117.

Lurie, D. I., Solca, F., Fischer, E. H., and Rubel, E. W. (2000). Tyrosine phosphatase SHP-1 immunoreactivity increases in a subset of astrocytes following deafferentation of the chicken auditory brainstem. *J Comp Neurol* **421**, 199-214.

Lutz, P. L., and Nilsson, G. E. (1997). Contrasting strategies for anoxic brain survival--glycolysis up or down. *J Exp Biol* **200**, 411-419.

Miller, L. C., Swayne, L. A., Chen, L., Feng, Z. P., Wacker, J. L., Muchowski, P. J., Zamponi, G. W., and Braun, J. E. (2003). Cysteine string protein (CSP) inhibition of N-type calcium channels is blocked by mutant huntingtin. *J Biol Chem* **278**, 53072-53081.

Montgomery, C. R., Morris, R. D., Sevcik, R. A., and Clarkson, M. G. (2005). Auditory backward masking deficits in children with reading disabilities. *Brain Lang* **95**, 450-456.

Moore, J. K. (2000). Organization of the human superior olivary complex. *Microsc Res Tech* **51**, 403-412.

Mulders, W. H., and Robertson, D. (2004). Dopaminergic olivocochlear neurons originate in the high frequency region of the lateral superior olive of guinea pigs. *Hear Res* **187**, 122-130.

Needleman, H. L., and Bellinger, D. (1991). The health effects of low level exposure to lead. *Annu Rev Public Health* **12**, 111-140.

Nothwang, H. G., Koehl, A., and Friauf, E. (2006). Comparative gene expression analysis reveals a characteristic molecular profile of the superior olivary complex. *Anat Rec A Discov Mol Cell Evol Biol* **288**, 409-423.

Oertel, D. (1999). The role of timing in the brain stem auditory nuclei of vertebrates. *Annu Rev Physiol* **61**, 497-519.

Ohtsuka, K., and Suzuki, T. (2000). Roles of molecular chaperones in the nervous system. *Brain Res Bull* **53**, 141-146.

Otto, D. A., and Fox, D. A. (1993). Auditory and visual dysfunction following lead exposure. *Neurotoxicology* **14**, 191-207.

Pfeffer, S. R., Dirac-Svejstrup, A. B., and Soldati, T. (1995). Rab GDP dissociation inhibitor: putting rab GTPases in the right place. *J Biol Chem* **270**, 17057-17059.

Rafalowska, U., Struzynska, L., Dabrowska-Bouta, B., and Lenkiewicz, A. (1996). Is lead toxicosis a reflection of altered energy metabolism in brain synaptosomes? *Acta Neurobiol Exp (Wars)* **56**, 611-617.

Robson, J. A., and Sidell, N. (1985). Ultrastructural features of a human neuroblastoma cell line treated with retinoic acid. *Neuroscience* **14**, 1149-1162.

Rowland, K. C., Irby, N. K., and Spirou, G. A. (2000). Specialized synapse-associated structures within the calyx of Held. *J Neurosci* **20**, 9135-9144.

Ruijten, M. W., Verberk, M. M., and Salle, H. J. (1991). Nerve function in workers with long term exposure to trichloroethene. *Br J Ind Med* **48**, 87-92.

Sakisaka, T., Meerlo, T., Matteson, J., Plutner, H., and Balch, W. E. (2002). Rab-alphaGDI activity is regulated by a Hsp90 chaperone complex. *Embo J* **21**, 6125-6135.

Sampson, M. J., Decker, W. K., Beaudet, A. L., Ruitenbeek, W., Armstrong, D., Hicks, M. J., and Craigen, W. J. (2001). Immotile sperm and infertility in mice lacking mitochondrial voltage-dependent anion channel type 3. *J Biol Chem* **276**, 39206-39212.

Sampson, M. J., Lovell, R. S., and Craigen, W. J. (1997). The murine voltage-dependent anion channel gene family. Conserved structure and function. *J Biol Chem* **272**, 18966-18973.

Schneggenburger, R., and Forsythe, I. D. (2006). The calyx of Held. *Cell Tissue Res* **326**,

311-337.

Schurr, A., and Rigor, B. M. (1998). Brain anaerobic lactate production: a suicide note or a survival kit? *Dev Neurosci* **20**, 348-357.

Shan, Y. X., Liu, T. J., Su, H. F., Samsamshariat, A., Mestril, R., and Wang, P. H. (2003). Hsp10 and Hsp60 modulate Bcl-2 family and mitochondria apoptosis signaling induced by doxorubicin in cardiac muscle cells. *J Mol Cell Cardiol* **35**, 1135-1143.

Shoshan-Barmatz, V., and Gincel, D. (2003). The voltage-dependent anion channel: characterization, modulation, and role in mitochondrial function in cell life and death. *Cell Biochem Biophys* **39**, 279-292.

Shoshan-Barmatz, V., and Israelson, A. (2005). The voltage-dependent anion channel in endoplasmic/sarcoplasmic reticulum: characterization, modulation and possible function. *J Membr Biol* **204**, 57-66.

Shoshan-Barmatz, V., Israelson, A., Brdiczka, D., and Sheu, S. S. (2006). The voltage-dependent anion channel (VDAC): function in intracellular signalling, cell life and cell death. *Curr Pharm Des* **12**, 2249-2270.

Silver, I. A., Deas, J., and Erecinska, M. (1997). Ion homeostasis in brain cells: differences in intracellular ion responses to energy limitation between cultured neurons and glial cells. *Neuroscience* **78**, 589-601.

Squire, L. R., Roberts, J. L., Spitzer, N. C., Zigmond, M. J., McConnell, S. K., and Bloom, F. E. (2003). *Fundamental Neuroscience*. Academic Press, San Diego, Calif.

Sreedhar, A. S., Soti, C., and Csermely, P. (2004). Inhibition of Hsp90: a new strategy for inhibiting protein kinases. *Biochim Biophys Acta* **1697**, 233-242.

Sterling, G. H., O'Neill, K. J., McCafferty, M. R., and O'Neill, J. J. (1982). Effect of chronic lead ingestion by rats on glucose metabolism and acetylcholine synthesis in cerebral cortex slices. *J Neurochem* **39**, 592-596.

Tachikawa, M., Fukaya, M., Terasaki, T., Ohtsuki, S., and Watanabe, M. (2004). Distinct cellular expressions of creatine synthetic enzyme GAMT and creatine kinases uCK-Mi and CK-B suggest a novel neuron-glial relationship for brain energy homeostasis. *Eur J Neurosci* **20**, 144-160.

Toscano, C. D., and Guilarte, T. R. (2005). Lead neurotoxicity: from exposure to molecular effects. *Brain Res Brain Res Rev* **49**, 529-554.

Trussell, L. O. (1999). Synaptic mechanisms for coding timing in auditory neurons. *Annu Rev Physiol* **61**, 477-496.

Tsuchitani, C. (1997). Input from the medial nucleus of trapezoid body to an interaural level detector. *Hear Res* **105**, 211-224.

Verity, M. A. (1990). Comparative observations on inorganic and organic lead neurotoxicity. *Environ Health Perspect* **89**, 43-48.

Verstreken, P., Ly, C. V., Venken, K. J., Koh, T. W., Zhou, Y., and Bellen, H. J. (2005). Synaptic mitochondria are critical for mobilization of reserve pool vesicles at Drosophila neuromuscular junctions. *Neuron* **47**, 365-378.

Vignali, G., Niclas, J., Sprocati, M. T., Vale, R. D., Sirtori, C., and Navone, F. (1996). Differential expression of ubiquitous and neuronal kinesin heavy chains during differentiation of human neuroblastoma and PC12 cells. *Eur J Neurosci* **8**, 536-544.

von Gersdorff, H., and Borst, J. G. (2002). Short-term plasticity at the calyx of held. *Nat Rev Neurosci* **3**, 53-64.

Wallimann, T., and Hemmer, W. (1994). Creatine kinase in non-muscle tissues and cells. *Mol Cell Biochem* **133-134**, 193-220.

Wallimann, T., Wyss, M., Brdiczka, D., Nicolay, K., and Eppenberger, H. M. (1992). Intracellular compartmentation, structure and function of creatine kinase isoenzymes in tissues with high and fluctuating energy demands: the 'phosphocreatine circuit' for cellular energy homeostasis. *Biochem J* **281 (Pt 1)**, 21-40.

Weeber, E. J., Levy, M., Sampson, M. J., Anflous, K., Armstrong, D. L., Brown, S. E., Sweatt, J. D., and Craigen, W. J. (2002). The role of mitochondrial porins and the permeability transition pore in learning and synaptic plasticity. *J Biol Chem* **277**, 18891-18897.

Widzowski, D. V., and Cory-Slechta, D. A. (1994). Homogeneity of regional brain lead concentrations. *Neurotoxicology* **15**, 295-307.

Wishcamper, C. A., Coffin, J. D., and Lurie, D. I. (2001). Lack of the protein tyrosine phosphatase SHP-1 results in decreased numbers of glia within the motheaten (me/me) mouse brain. *J Comp Neurol* **441**, 118-133.

Wu, S., Sampson, M. J., Decker, W. K., and Craigen, W. J. (1999). Each mammalian mitochondrial outer membrane porin protein is dispensable: effects on cellular respiration. *Biochim Biophys Acta* **1452**, 68-78.

Zawia, N. H. (2003). Transcriptional involvement in neurotoxicity. *Toxicol Appl Pharmacol* **190**, 177-188.

Zawia, N. H., Sharan, R., Brydie, M., Oyama, T., and Crumpton, T. (1998). Sp1 as a target site for metal-induced perturbations of transcriptional regulation of developmental brain gene expression. *Brain Res Dev Brain Res* **107**, 291-298.

Zhao, Q., Slavkovich, V., and Zheng, W. (1998). Lead exposure promotes translocation of protein kinase C activities in rat choroid plexus in vitro, but not in vivo. *Toxicol Appl Pharmacol* **149**, 99-106.

Appendix A

Table 4: Complete list of cytosolic proteins identified in VBS and DBS

SSP#	*Match*	*Protein name*	*Mr/pI Theoretical*	*Mr/pI Calculated*	*Mascot Score*	*Sequence coverage*
202	BAA11751	14-3-3 zeta.	28/4.7	31/4.6	85	36%
306	AAH03716	Annexin A5	36/4.8	35/4.7	63	20%
502	RSSA_MOUSE	40S ribosomal protein SA (p40) (34/67 kDa laminin receptor).- Mus musculus (Mouse).	33/4.7	40/4.7	68	24%
801	AAA39814	Brain Neurofilament light polypeptide	61/4.6	68/4.6	91	20%
1101	PRDX2_MOUSE	Peroxiredoxin-2 (Thioredoxin peroxidase 1) (Thioredoxin-dependent peroxide reductase 1) (Thiol-specific antioxidant protein) (TSA).-	22/5.2	25/4.9	106	43%
1202	Q5M9P6_MOUSE	Rho GDP-dissociation inhibitor 1 (Rho GDI 1) (Rho-GDI alpha) (GDI-1)	23/5.1	28/5.0	108	44%
1203	BAB28976	Ubiquitin carboxy-terminal hydrolase L1	25/5.1	29/5.1	88	44%
1601	ENOG_MOUSE	Gamma enolase (2-phospho-D-glycerate hydro-lyase) (Neural enolase) (Neuron-specific enolase) (NSE) (Enolase 2).- Mus musculus (Mouse).	47/5.0	48/4.9	178	46%
703	Q7TMM9_MOUSE	Tubulin, beta 2	50/4.8	51/4.8	116	26%
1701	Q5XJF8_MOUSE	Tubulin, alpha 1.- Mus musculus (Mouse).	50/4.9	54/4.9	102	31%
1802	Q3TBI9_MOUSE	Guanosine diphosphate (GDP) dissociation inhibitor 1	51/5.0	59/4.9	125	42%
1811	HHMS84	Heat shock protein 84 - mouse	83/5.0	84/4.9	136	25%
2701	A42078	Creatine kinase B - mouse	43/5.4	49/5.2	92	32%
3602	A42078	Creatine kinase B - mouse	43/5.4	48/5.3	185	49%
2807	A45935	dnaK-type molecular chaperone hsc70 - mouse	71/5.4	69/5.2	79	20%
2806	S49985	Dihydropyrimidinase-related protein 2 [similarity] - rat	62/6.0	64/5.2	92	28%
2812	Q3U5W3_MOUSE	ATPase, H+ transporting, V1 subunit A, isoform 1	68/5.5	65/5.2	120	25%
4201	PRDX6_MOUSE	Peroxiredoxin 6 (Antioxidant protein 2) (1-Cys peroxiredoxin) (1-Cys PRX) (Acidic calcium-independent phospholipase A2) (aiPLA2)	25/5.7	28/5.6	116	45%
3406	LDHB_MOUSE	L-lactate dehydrogenase B chain (LDH-B)	36/5.7	37/5.4	118	35%
5102	Q9D412_MOUSE	Hypothetical Zinc finger C-x8-C-x5- C-x3-H type containing protein	37/6.2	26/6.5	67	18%
5304	LDHB_MOUSE	L-lactate dehydrogenase B chain (LDH-B) (LDH-H).	36/5.7	31/6.5	106	33%
5604	Q91VC6_MOUSE	Glutamine synthetase (Glutamate-ammonia ligase) (Glutamine synthase).	42/6.6	45/6.2	89	24%
5606	Q3TRK7_MOUSE	Glutamate-ammonia ligase (glutamine synthase)	42/6.6	45/6.5	112	24%
6201	PGAM1_MOUSE	Phosphoglycerate mutase 1 (Phosphoglycerate mutase isozyme B) (PGAM-B) (BPG-dependent PGAM 1)	29/6.8	31/6.5	162	58%
6501	ALDOA_MOUSE	Fructose-bisphosphate aldolase C (Brain-type aldolase) (Aldolase 3) (Zebrin II) (Scrapie-responsive protein 2).	39/6.8	41/6.6	107	47%
6403	BAC20217	Acyl-CoA hydrolase	43/8.9	39/6.6	76	30%
6801	KPYM_MOUSE	Pyruvate kinase isozyme M2	58/7.4	58/6.7	70	24%
7402	DEMSG	Glyceraldehyde-3-phosphate dehydrogenase (phosphorylating)	36/8.4	36/6.8	70	33%
8003	PPIA_MOUSE	Peptidyl-prolyl cis-trans isomerase A (PPIase A) (Rotamase A) (Cyclophilin A) (Cyclosporin A-binding protein) (SP18)	18/7.9	18/9.5	71	47%
7708	AAH58079	4-aminobutyrate aminotransferase	56/8.4	52/6.9	79	21%
9301	Q99LD0_MOUSE	ATPase, H+ transporting, V1 subunit E isoform 1.- Mus musculus (Mouse).	26/8.4	32/9.5	81	31%
302	S31975	14-3-3 protein epsilon	29/4.6	33/4.5	99	40%
303	Q8C7C3_MOUSE	Tropomyosin 3, gamma	29/4.7	34/4.6	148	38%
304	Q8BP43_MOUSE	Tropomyosin 1, alpha	33/4.7	33/4.6	66	24%
203	BAA11751	14-3-3 zeta protein	28/4.7	30/4.7	89	39%
308	AAH54410	Ubiquitin aldehyde binding 1	31/4.9	35/4.7	87	35%
702	Q3UWP8_MOUSE	Calreticulin	42/4.6	52/4.6	74	23%
106	VISL1_BOVIN	Visinin-like protein 1 (Neurocalcin alpha).-	22/5.0	23/4.8	102	50%
2502	Q3TVP6_MOUSE	Actin, beta, cytoplasmic	42/5.3	43/5.1	133	43%
2808	Q3KQP2_MOUSE	Heat shock protein, 60 kDa	61/5.7	61/5.2	81	15%
3401	LDHB_MOUSE	L-lactate dehydrogenase B chain (LDH-B) (LDH heart subunit) (LDH-H)	36/5.7	36/5.3	143	39%
3701	Q3UAW8_MOUSE	Tubulin, alpha 2	50/4.9	55/5.3	66	27%
4402	MDHC_MOUSE	Malate dehydrogenase, cytoplasmic (Cytosolic malate dehydrogenase).	36/6.2	36/5.7	124	39%
4702	S10246	Phosphopyruvate hydratase alpha	47/6.4	51/5.6	111	35%

Table 5: Complete list of membrane proteins identified in VBS and DBS.

SSP#	*Match*	*Protein name*	*Mr/pI Theoretical*	*Mr/pI Calculated*	*Mascot Score*	*Sequence coverage*
206	1433G_HUMAN	14-3-3 protein gamma (Protein kinase C inhibitor protein 1) (KCIP-1)	28/4.8	31/4.7	98	39%
602	Q3UDR2_MOUSE	Prolyl 4-hydroxylase, beta polypeptide	57/4.8	59/4.7	103	28%
1101	S34070	GTP-binding protein rab3A	25/4.9	28/4.8	79	38%
1105	Q58EV2_MOUSE	Apoa1 protein	23/7.0	29/5.1	90	45%
1104	Q8BPI0_MOUSE	RHOGDI-1	23/5.2	29/5.0	83	37%
1802	HHMS84	Heat shock protein 84	83/5.0	94/4.9	91	21%
1702	Q3UEM8_MOUSE	Heat shock 70kD protein 5 (glucose-regulated protein)	68/5.2	73/5.0	88	24%
2104	ATP5H_MOUSE	ATP synthase D chain, mitochondrial	19/5.5	25/5.3	64	45%
2306	BAB26679	Isocitrate dehydrogenase 3 (NAD+) alpha	40/6.3	38/5.3	64	21%
1402	CAA27396	Cytoplasmatic beta-actin	39/5.8	45/5.0	105	33%
2401	CAA27396	Cytoplasmatic beta-actin	39/5.8	44/5.1	155	42%
2403	A42078	Creatine kinase B	43/5.4	46/5.3	112	39%
2702	Q3U764_MOUSE	Heat shock protein 8	71/5.2	70/5.1	126	26%
2704	Q3TEK2_MOUSE	Heat shock protein 8	71/5.2	69/5.1	235	41%
2601	Q8C2C7_MOUSE	Heat shock protein, 60 kDa	61/5.7	60/5.0	116	25%
2706	Q3US31_MOUSE	ATPase, H+ transporting, V1 subunit A	56/5.6	68/5.3	79	20%
3502	ENOA_MOUSE	Alpha-enolase (2-phospho-D-glycerate hydro-lyase) (Non- neural enolase) (NNE) (Enolase 1)	47/6.4	49/5.6	71	24%
4501	S10246	Phosphopyruvate hydratase alpha (alpha enolase)	47/6.4	49/5.7	67	19%
3605	Q8C2F4_MOUSE	Glucose regulated protein, 58 kDa	57/5.8	59/5.8	107	28%
4301	MDHC_MOUSE	Malate dehydrogenase, cytoplasmic (Cytosolic malate dehydrogenase)	36/6.2	35/5.7	67	28%
5401	AAA17989	Glutamate-ammonia ligase	42/6.6	45/6.0	64	16%
5403	Q3TRK7_MOUSE	Glutamate-ammonia ligase (glutamine synthase)	42/6.6	44/6.3	82	20%
4503	ENOA_MOUSE	Alpha-enolase (2-phospho-D-glycerate hydro-lyase) (Non- neural enolase) (NNE) (Enolase 1)	47/6.4	49/5.9	96	30%
4504	AAH60959	Tu translation elongation factor, mitochondrial	47/7.7	48/5.9	73	26%
5101	TPIS_MOUSE	Triosephosphate isomerase (TIM) (Triose-phosphate isomerase)	27/7.1	29/6.5	64	25%
5202	PGAM1_MOUSE	Phosphoglycerate mutase 1 (Phosphoglycerate mutase isozyme B) (PGAM-B) (BPG-dependent PGAM 1)	29/6.8	31/6.4	68	37%
5303	ALDOC_MOUSE	Fructose-bisphosphate aldolase C (Brain-type aldolase) (Aldolase 3) (Zebrin II) (Scrapie-responsive protein 2)	39/6.8	41/6.5	73	29%
6304	ALDOC_MOUSE	Fructose-bisphosphate aldolase C (Brain-type aldolase) (Aldolase 3) (Zebrin II) (Scrapie-responsive protein 2)	39/6.8	40/6.7	77	33%
6403	AATC_MOUSE	Aspartate aminotransferase, cytoplasmic (Transaminase A) (Glutamate oxaloacetate transaminase 1)	46/6.8	42/6.7	72	21%
5604	S16239	Glutamate dehydrogenase [NAD(P)]	61/8.1	55/6.4	89	25%
6602	S16239	Glutamate dehydrogenase [NAD(P)]	61/8.1	55/6.6	107	26%
6604	S16239	Glutamate dehydrogenase [NAD(P)]	61/8.1	55/6.7	86	24%
7102	Q3UFR1_MOUSE	EDAR (ectodysplasin-A receptor)-associated death domain	24/5.0	26/6.9	67	25%
7405	S24612	Creatine kinase, mitochondrial	47/8.4	45/7.0	62	26%
7505	AAH58079	4-aminobutyrate aminotransferase	56/8.4	52/7.0	73	21%
7802	Q3UNH7_MOUSE	Aconitase 2, mitochondrial	85/8.1	85/6.8	70	15%
8002	PPIA_MOUSE	Peptidyl-prolyl cis-trans isomerase A (PPIase A) (Rotamase A) (Cyclophilin A) (Cyclosporin A-binding protein) (SP18)	18/7.9	19/7.4	86	36%
8403	Q91VA7_MOUSE	Isocitrate dehydrogenase 3, beta subunit	42/8.8	41/8.2	121	36%
8503	Q3UIA9_MOUSE	Fumarate hydratase 1	54/9.1	49/8.2	71	18%
8605	JC1473	H+-transporting two-sector ATPase alpha chain	60/9.2	54/9.5	177	38%
101	CALM_MOUSE	Calmodulin	17/4.1	21/4.0	77	35%
104	BAC37105	Synaptosomal-associated 25K protein	23/4.7	30/4.5	82	55%
2203	Q505N8_MOUSE	Pyruvate dehydrogenase (lipoamide) beta	39/6.4	35/5.3	70	25%
2503	Q3TV75_MOUSE	Ubiquinol-cytochrome C reductase core protein 1	53/5.8	49/5.2	86	29%
1505	ENOG_MOUSE	Gamma enolase (2-Phospho-D-glycerate hydrolase)	47/5.0	49/4.9	86	25%

Table 6: Complete list of cytoskeletal proteins identified in VBS and DBS.

SSP#	*Match*	*Protein name*	*Mr/pI Theoretical*	*Mr/pI Calculated*	*Mascot Score*	*Sequence coverage*
102	S31975	14-3-3 protein epsilon	29/4.6	32/4.5	70	29%
103	Q8C7C3_MOUSE	Tropomyosin 3, gamma	29/4.7	33/4.6	109	30%
301	GSTM1_MOUSE	Glutathione S-transferase Mu 1	26/8.1	48/4.0	69	35%
104	C34787	Tropomyosin 3 alpha, brain - rat	28/4.7	32/4.6	97	29%
4	1433G_HUMAN	14-3-3 protein gamma (Protein kinase C inhibitor protein 1)	28/4.8	31/4.7	70	26%
1103	Q8BLI2_MOUSE	Kinesin Superfamily Protein 20B	79/5.3	33/4.9	74	15%
1104	BAB27476	SWIPROSIN 1	25/5.0	33/4.9	66	32%
1303	Q3TFD7_MOUSE	ATP synthase, H+ transporting mitochondrial F1 complex, beta subunit	56/5.3	51/4.9	115	35%
503	NFL_MOUSE	Neurofilament triplet L protein (Neurofilament light polypeptide)	61/4.6	65/4.6	182	37%
803	Q3TNS4_MOUSE	Neurofilament triplet M protein - mouse	96/4.8	98/4.6	206	38%
601	NFL_MOUSE	Neurofilament triplet L protein (Neurofilament light polypeptide)	61/4.6	67/4.7	122	25%
1603	Q3U7T8_MOUSE	Heat shock 70kD protein 5 (glucose-regulated protein),	68/5.2	72/4.9	81	19%
2806	CAA83229	Neurofilament triplet H protein	115/5.7	110/5.2	98	15%
1404	I77428	Tubulin alpha chain isotype M-alpha-6 - mouse	50/5.0	55/4.9	121	41%
2102	GNAO1_MOUSE	Guanine nucleotide-binding protein G(o) subunit alpha 1.- Mus musculus (Mouse).	40/5.3	39/5.1	73	28%
2303	Q925K2_MOUSE	Glial fibrillary acidic protein	46/5.1	48/5.2	273	62%
2601	NFL_MOUSE	Neurofilament triplet L protein (Neurofilament light polypeptide)	61/4.6	68/5.1	117	24%
3501	AAH18383	Internexin neuronal intermediate filament protein, alpha	55/5.4	59/5.2	273	46%
2602	Q5SUH2_MOUSE	NADH dehydrogenase (Ubiquinone) Fe-S protein 1 (Ndufs1)	80/5.5	74/5.1	104	24%
2607	Q3U764_MOUSE	Heat shock protein 8	71/5.2	69/5.2	112	25%
3801	Q3TNS4_MOUSE	Neurofilament triplet M protein	96/4.8	99/5.3	106	27%
4808	Q8BQ20_MOUSE	Neurofilament protein M	96/4.8	99/5.6	138	24%
3003	A39682	Prohibitin	30/5.6	31/5.3	127	54%
3004	Q8BTZ3_MOUSE	NADH dehydrogenase (ubiquinone) Fe-S protein 3 (30kD)	30/6.7	30/5.3	140	34%
3303	A42078	Creatine kinase	43/5.4	47/5.3	67	25%
3601	NFL_MOUSE	Neurofilament triplet L protein (Neurofilament light polypeptide)	61/4.6	67/5.2	153	27%
3602	Q3UDS0_MOUSE	Heat shock protein 8	61/6.0	70/5.3	87	23%
3002	ATP5H_MOUSE	ATP synthase D chain, mitochondrial	19/5.5	25/5.3	66	53%
4305	Q3U5Y9_MOUSE	NADH dehydrogenase (ubiquinone) Fe-S protein 2	53/6.7	46/5.6	112	34%
3403	Q3TNS4_MOUSE	Neurofilament 3, medium	64/4.8	56/5.3	82	25%
4702	BAC29936	Inner membrane protein, mitochondrial	84/6.2	78/5.6	77	15%
5202	BAC32674	NADH dehydrogenase (ubiquinone) 1 alpha subcomplex 10	38/6.4	41/5.8	66	30%
7204	ALDOC_MOUSE	Fructose-bisphosphate aldolase C (EC 4.1.2.13) (Brain-type aldolase) (Aldolase 3) (Zebrin II)	39/6.8	40/6.6	108	43%
7202	S23506	Pyruvate dehydrogenase (lipoamide)	43/8.5	44/6.5	99	22%
7402	S16239	Glutamate dehydrogenase [NAD(P)]	61/8.1	54/6.5	98	27%
7403	S16239	Glutamate dehydrogenase [NAD(P)]	61/8.1	55/6.6	84	23%
7002	I57023	Superoxide dismutase (EC 1.15.1.1) (Mn) precursor	25/8.8	26/6.8	79	37%
8101	Q3THL7_MOUSE	Voltage-dependent anion channel 1	31/7.8	33/7.0	118	50%
8001	Q8BTZ3_MOUSE	NADH dehydrogenase (ubiquinone) Fe-S protein 3 (30kD)	30/6.7	31/7.4	150	34%
7103	S24612	Creatine kinase	43/5.4	35/6.8	90	22%
8201	S24612	Creatine kinase	47/8.4	44/7.0	137	31%
7205	Q9DBH1_MOUSE	Creatine kinase	47/8.4	44/6.8	85	21%
7305	Q3UIA9_MOUSE	Fumarate hydratase 1	54/9.1	49/6.9	64	18%
8401	JC1473	H+-transporting two-sector ATPase (EC 3.6.3.14) alpha chain - mouse	60/9.2	55/6.9	72	20%
8402	JC1473	H+-transporting two-sector ATPase (EC 3.6.3.14) alpha chain - mouse	60/9.2	55/7.3	86	23%
8404	JC1473	H+-transporting two-sector ATPase (EC 3.6.3.14) alpha chain - mouse	60/9.2	56/7.8	89	24%
8701	Q3UNH7_MOUSE	Aconitase 2, mitochondrial	85/8.1	79/7.0	71	16%
8801	Q3TNS4_MOUSE	Neurofilament triplet M protein - mouse	96/4.8	100/7.3	75	20%
9101	Q3THL7_MOUSE	Voltage-dependent anion channel 1	31/7.7	33/9.5	122	50%